UNIVERSIDAD DE SEVILLA

# Low Energy Nuclear Reaction Theory

## for basic science and applications

Gregory Potel Aguilar

XVII CPAN days, Valencia,
November 20, 2025

UNIVERSIDAD DE SEVILLA
1505

Escuela Técnica Superior de
INGENIERÍA DE SEVILLA

# 1

# Introduction and Motivation

# Nuclear reactions: why do we care? Nuclear reactions for applications

inertial confinement fusion

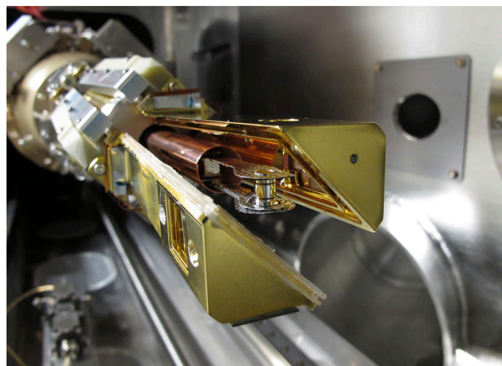

waste management


nuclear reactors

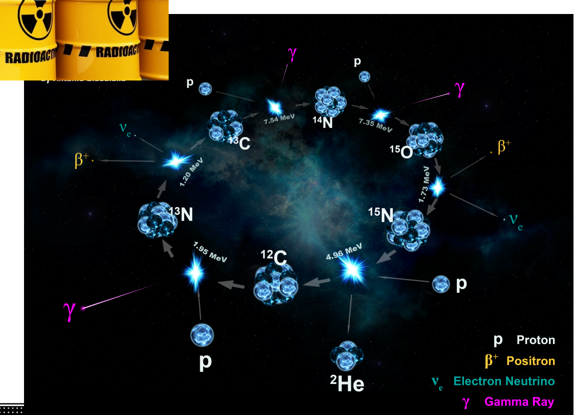


reactions of astrophysical interest

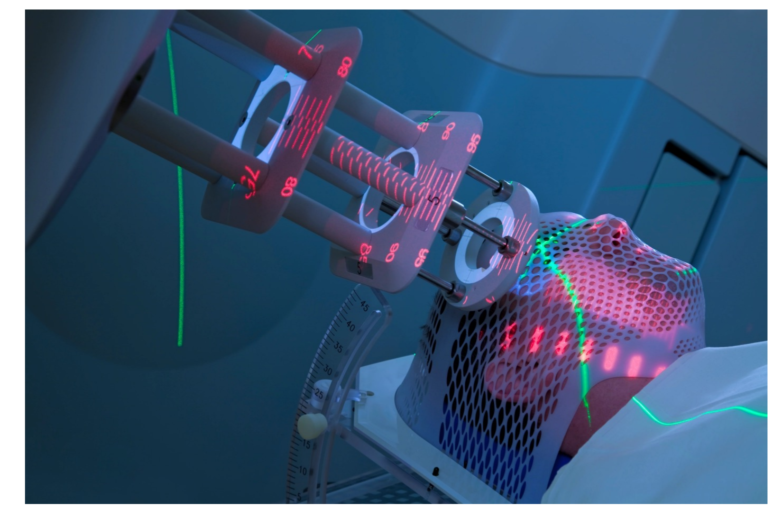

nuclear medicine

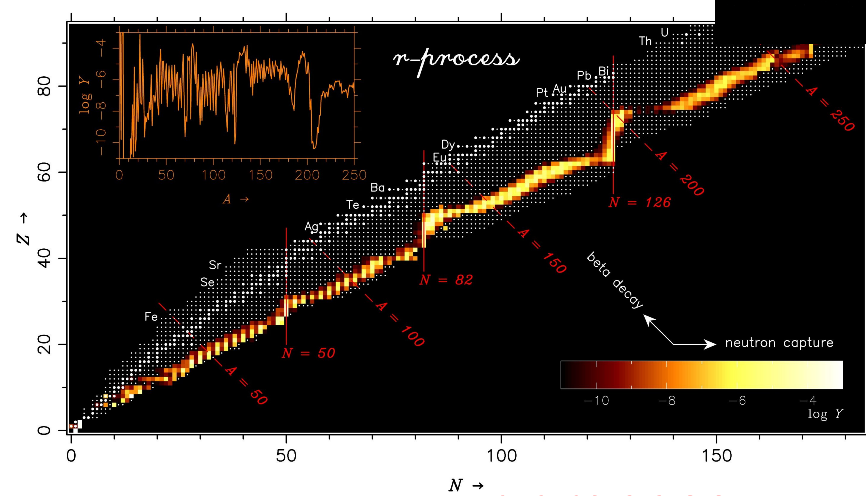


r-process

# Nuclear reactions: why do we care? Nuclear reactions as an experimental tool

- transfer reactions probe nuclear response to the addition of a nucleon
- a variety of observables provide rich information about nuclear structure:
  - angular differential cross section
  - absolute value
  - position
  - width (when in the continuum)

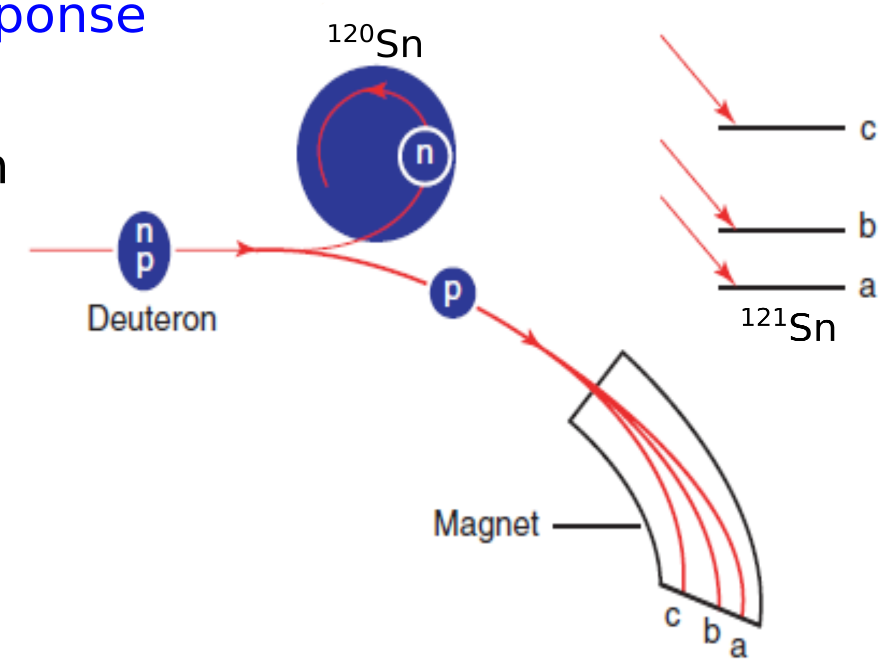


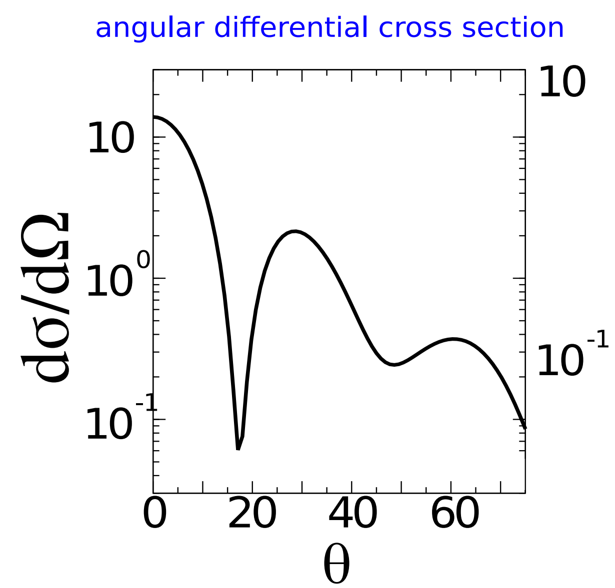


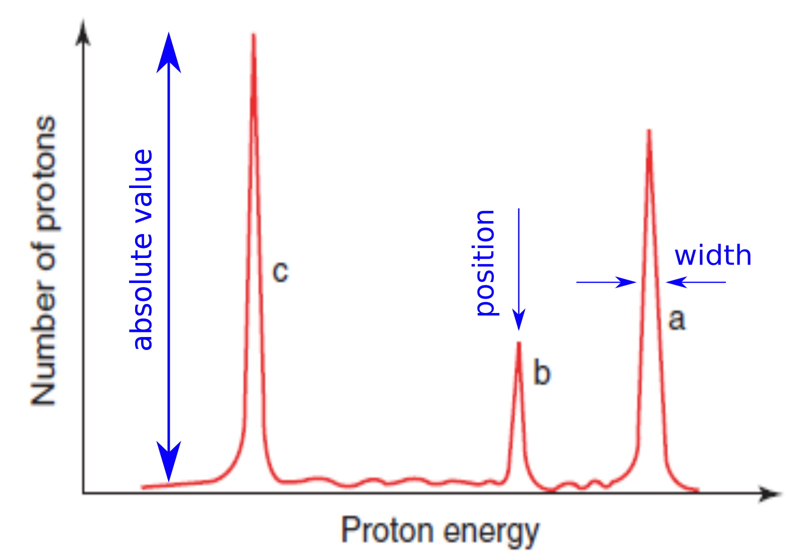

# 1a

## A theory challenge

# Features of nuclear spectra probed by nuclear reactions

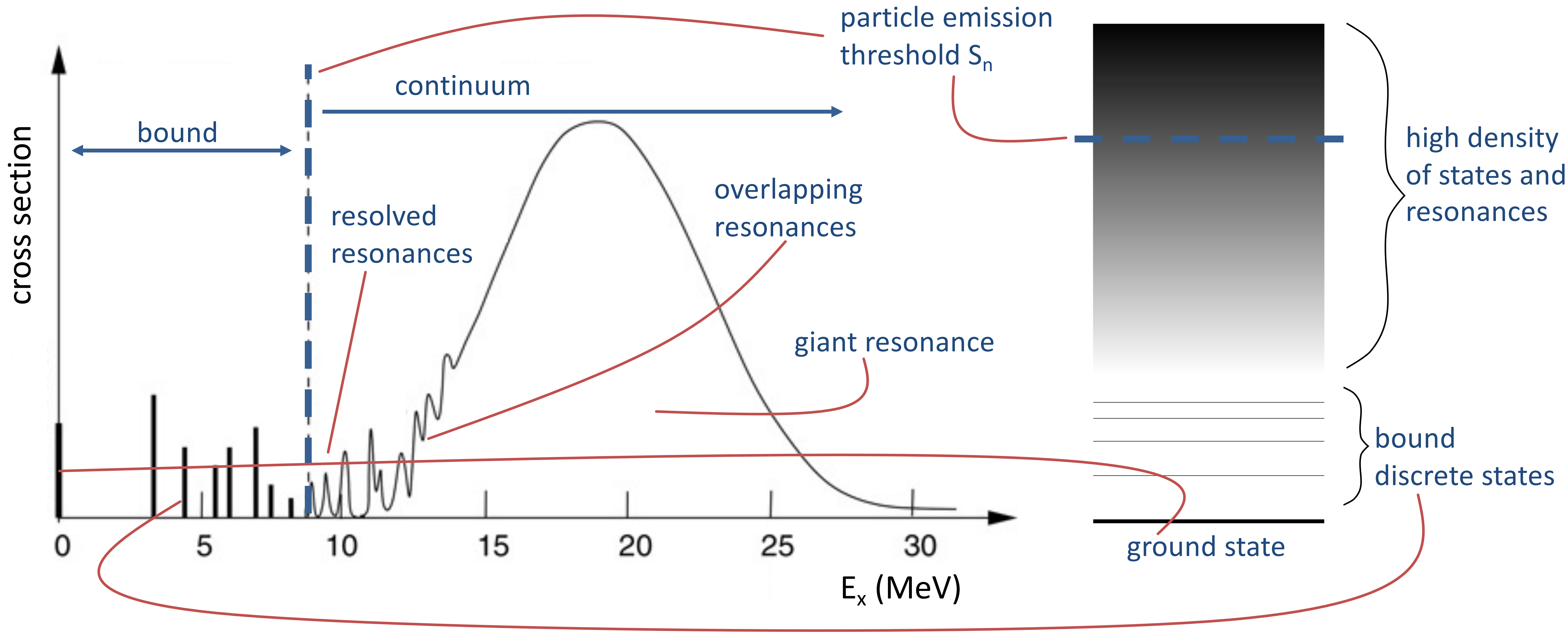

# Which reaction theories, and where?

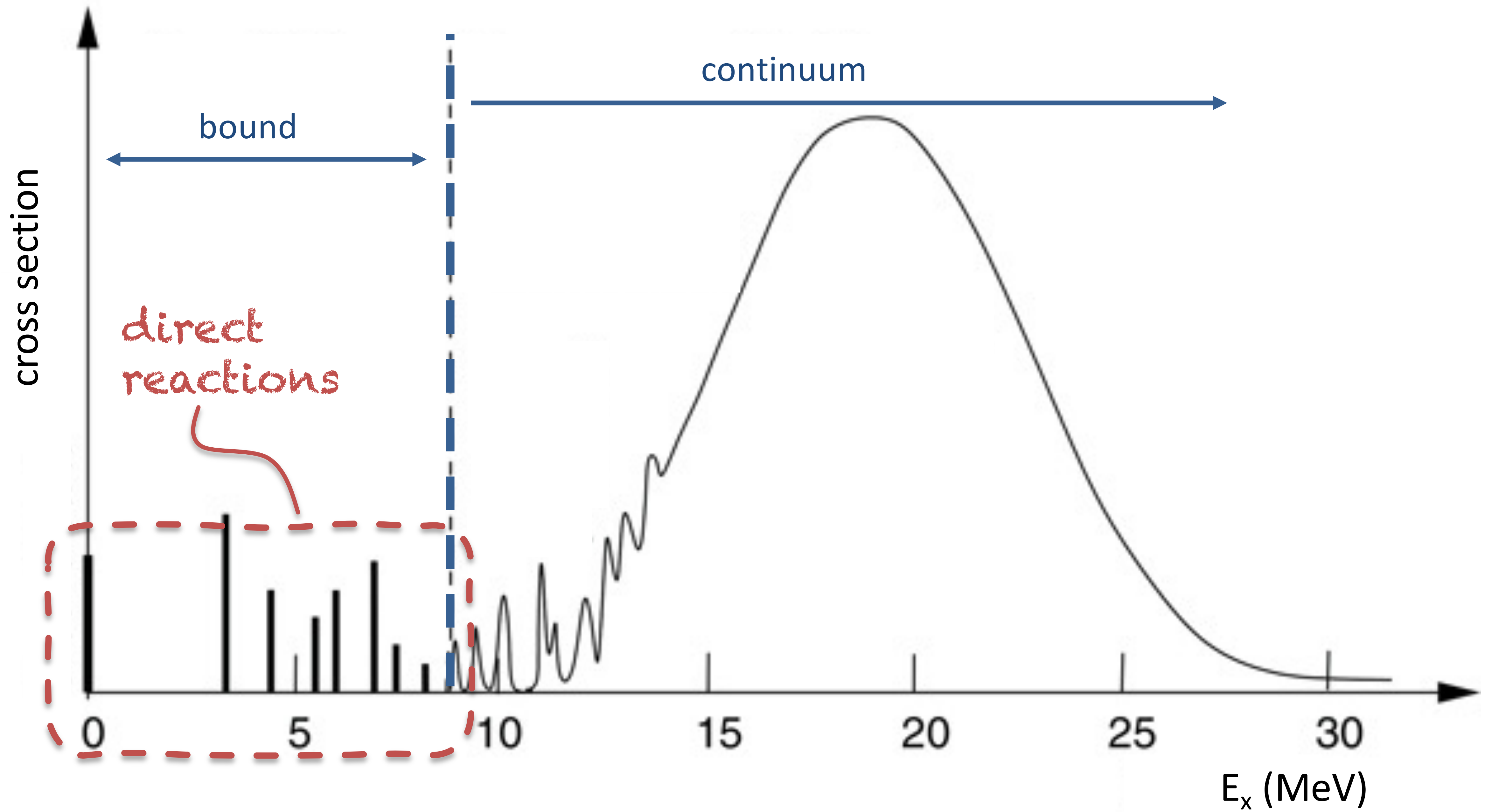

# Which reaction theories, and where?

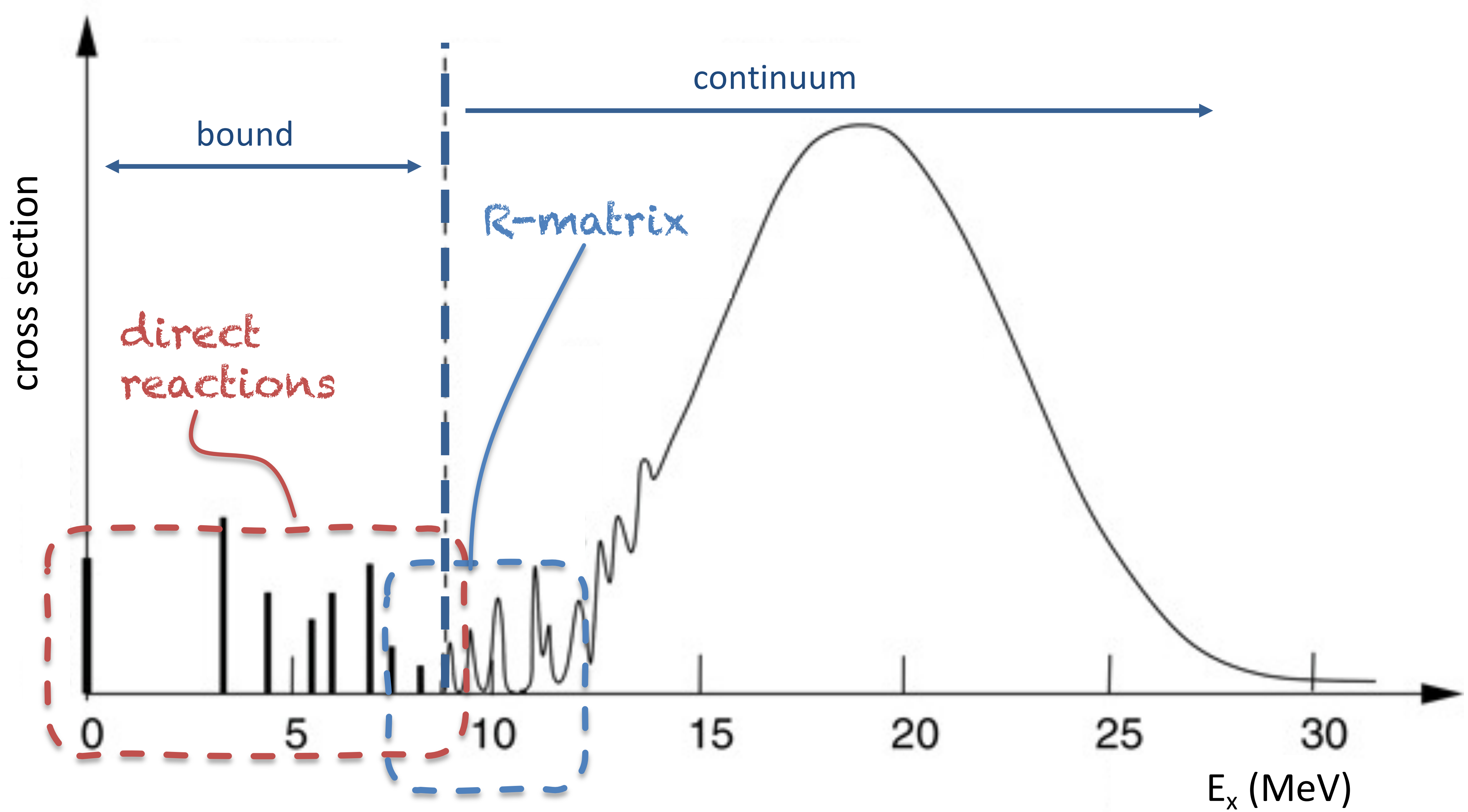

# Which reaction theories, and where?

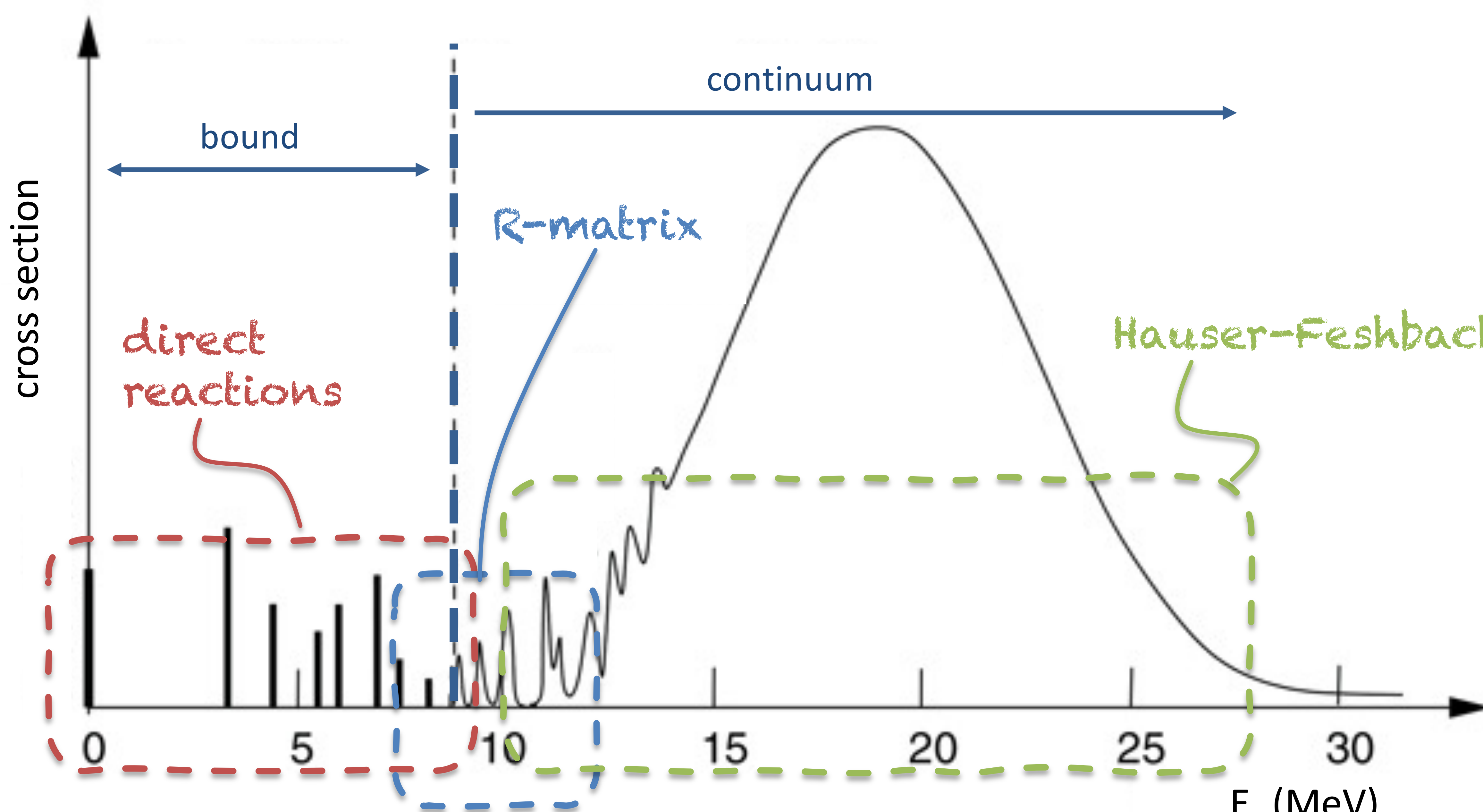

# **Challenge**: Can we treat everything on the same footing?


We want to address some ideas towards a consistent treatment of

- bound states and continuum
- direct and compound reactions
- structure and reactions

## **Challenge**: Can we treat everything on the same footing?


We want to address some ideas towards a consistent treatment of

- bound states and continuum
- direct and compound reactions
- structure and reactions

UQ

# 1b

## An experimental challenge

# Measuring cross sections and rates: problems (charged particles)

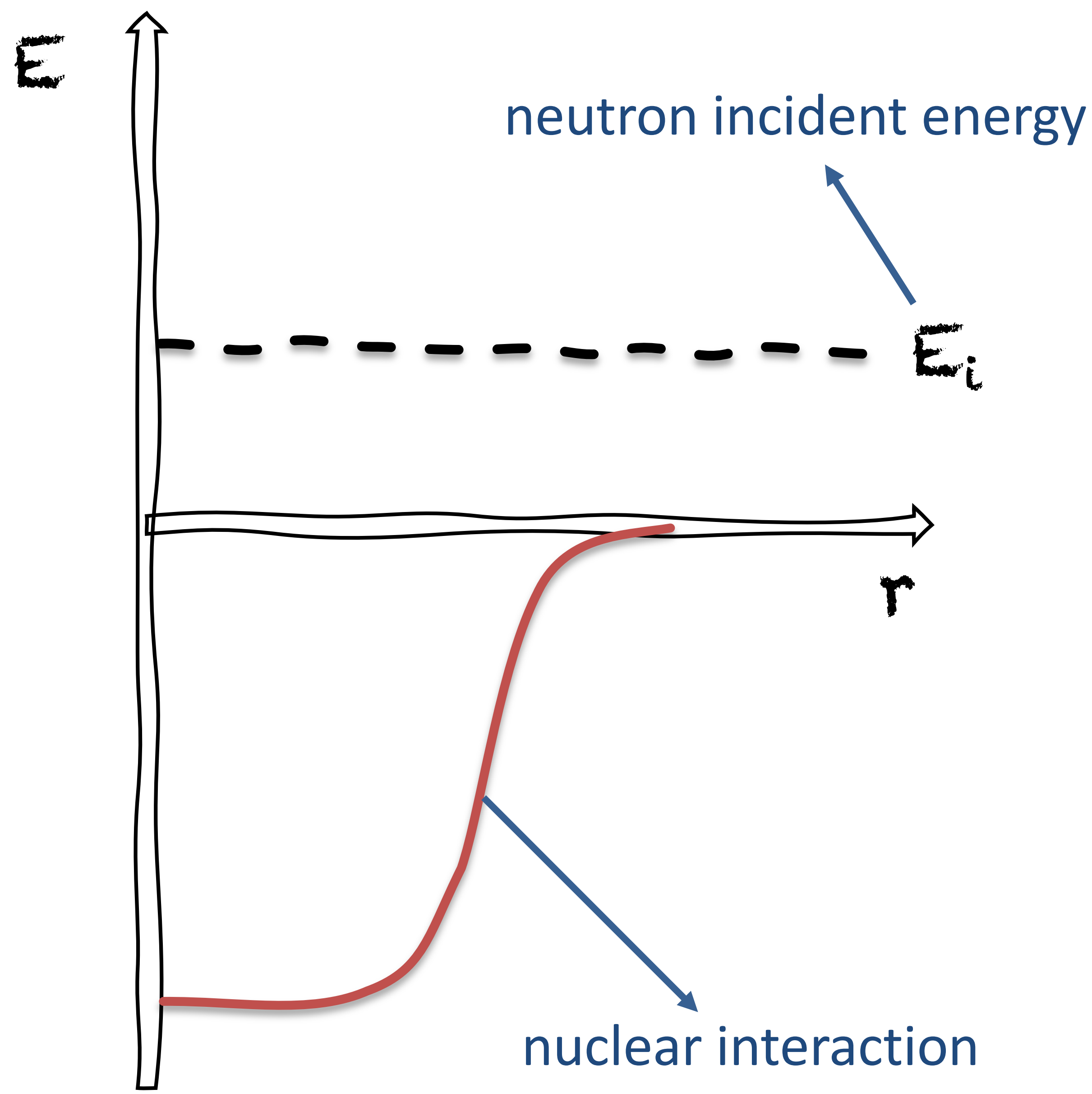

# Measuring cross sections and rates: problems (charged particles)

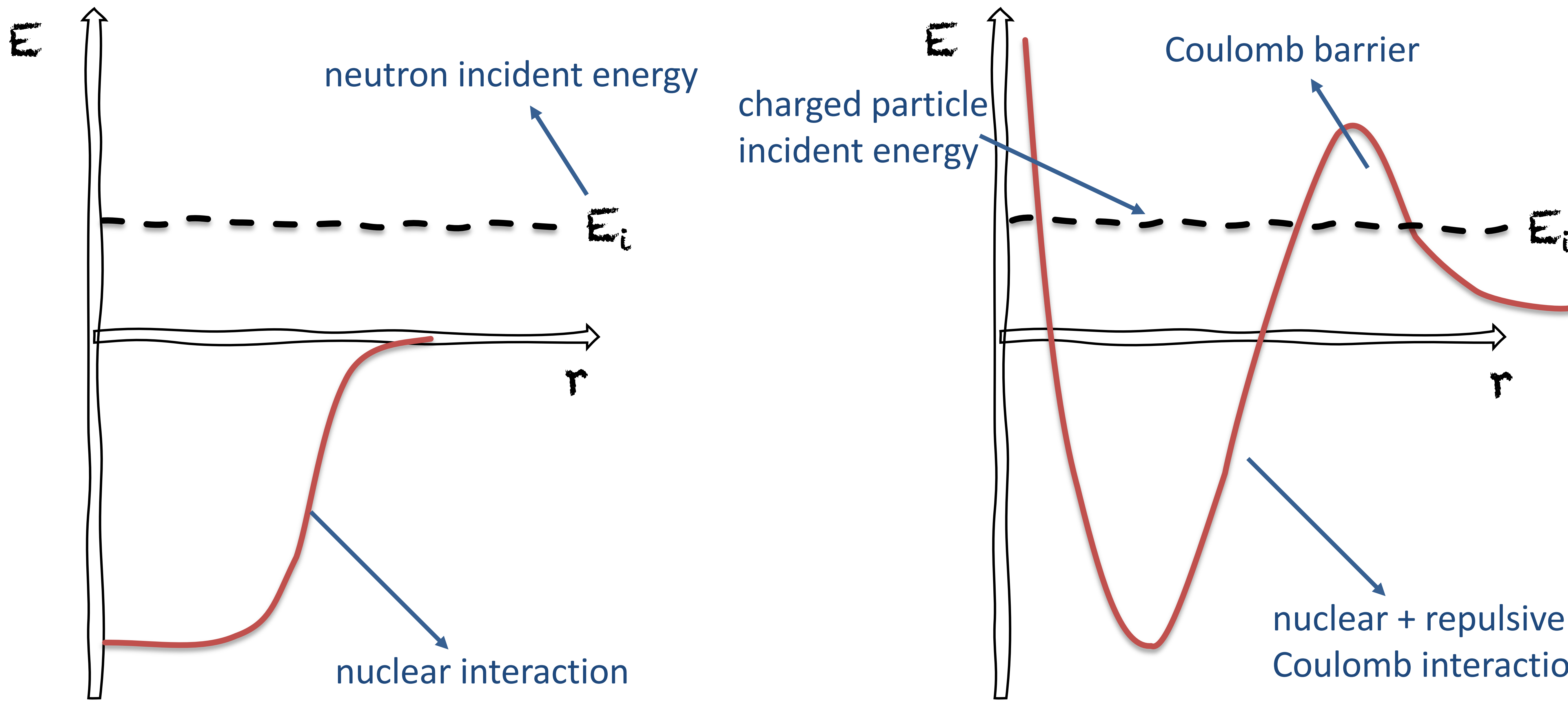

# Measuring cross sections and rates: problems (charged particles)

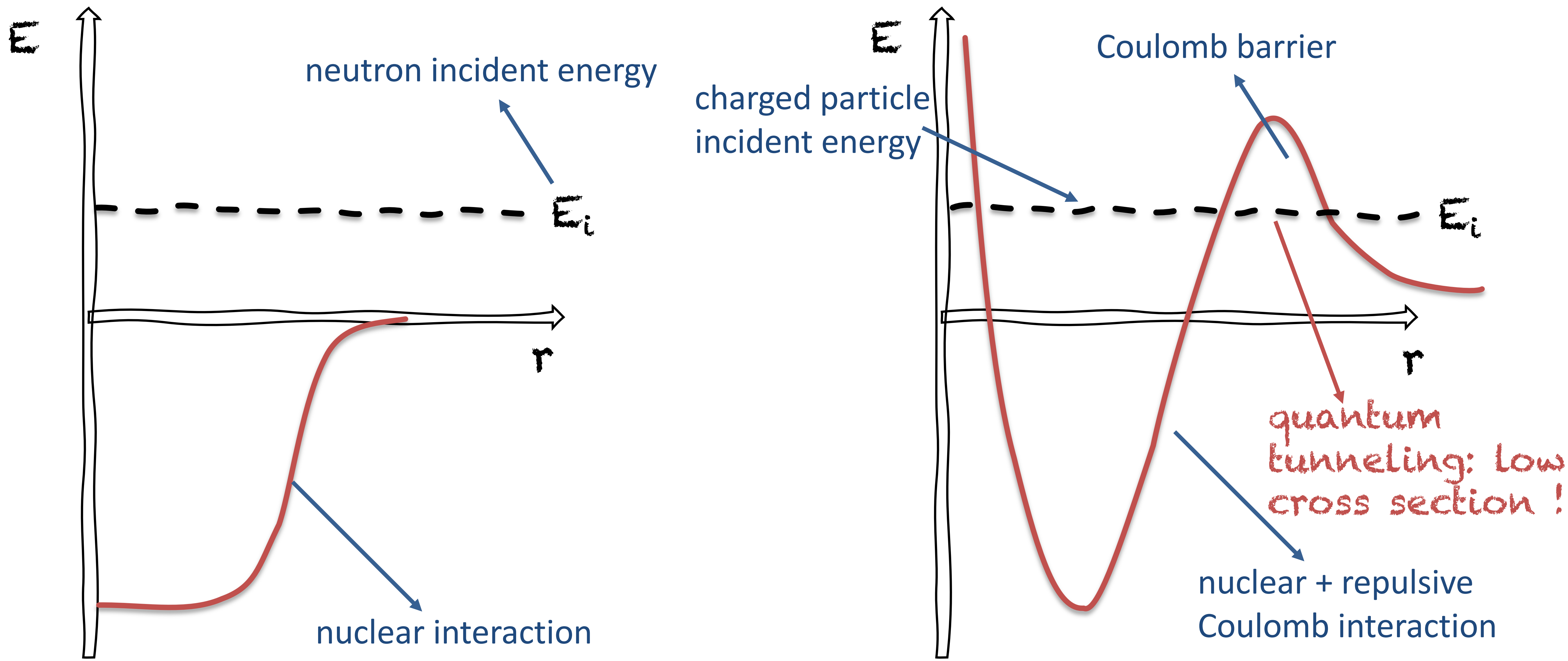

# Measuring cross sections and rates: problems (neutron-induced)

direct measurement: the stable nucleus is arranged in a target at a neutron beam facility

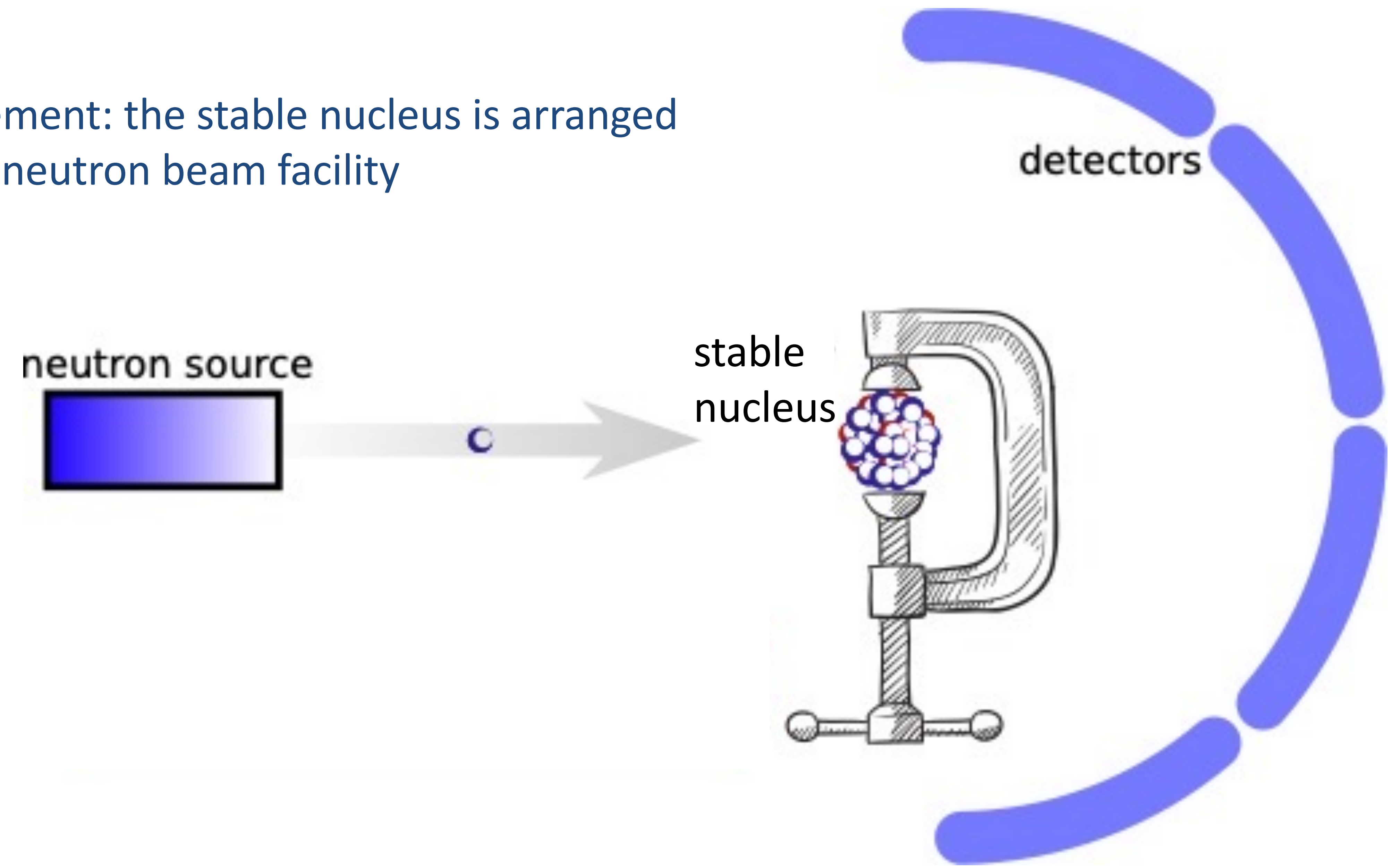

# Measuring cross sections and rates: problems (neutron-induced)

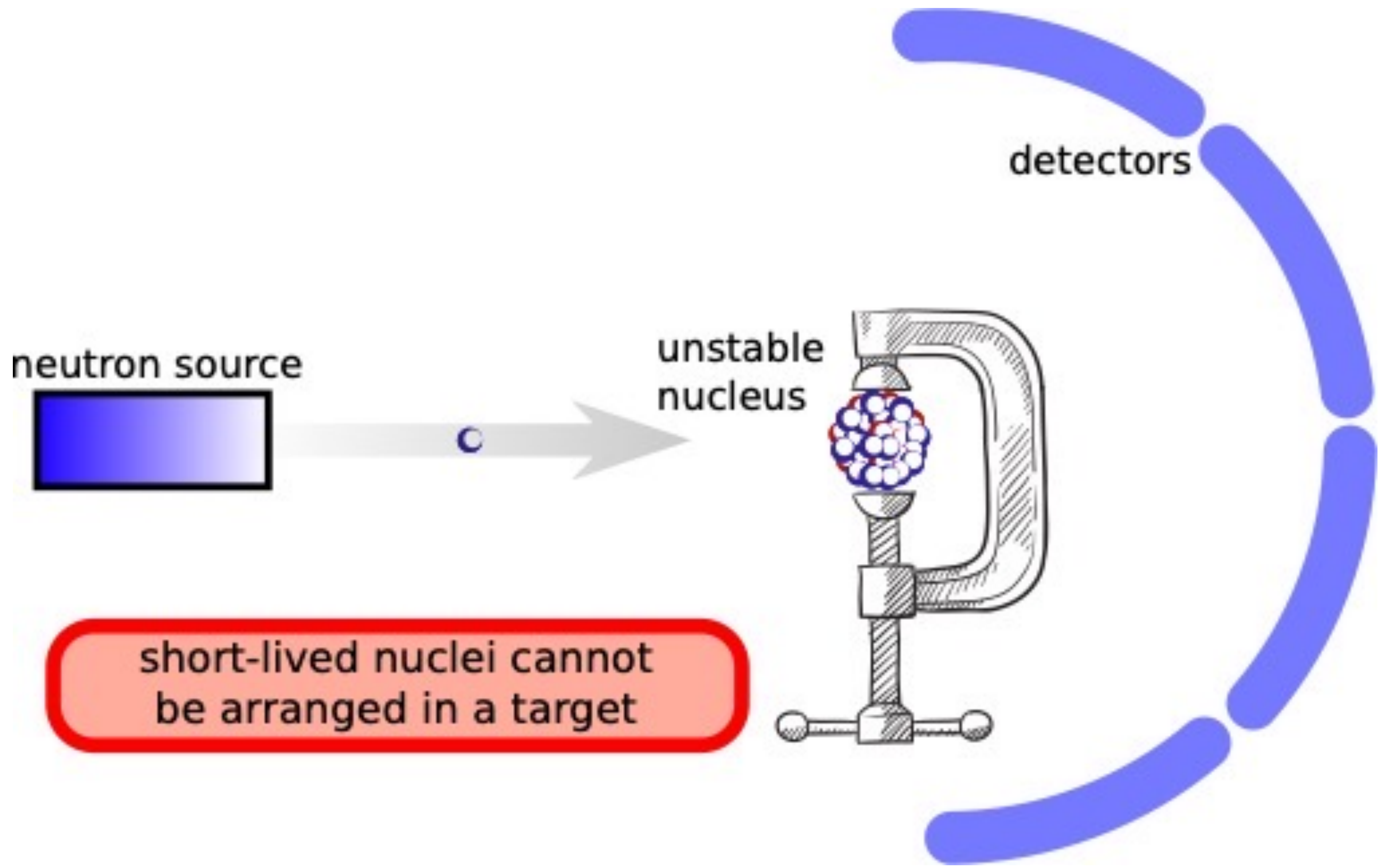

# Measuring cross sections and rates: problems (neutron-induced)

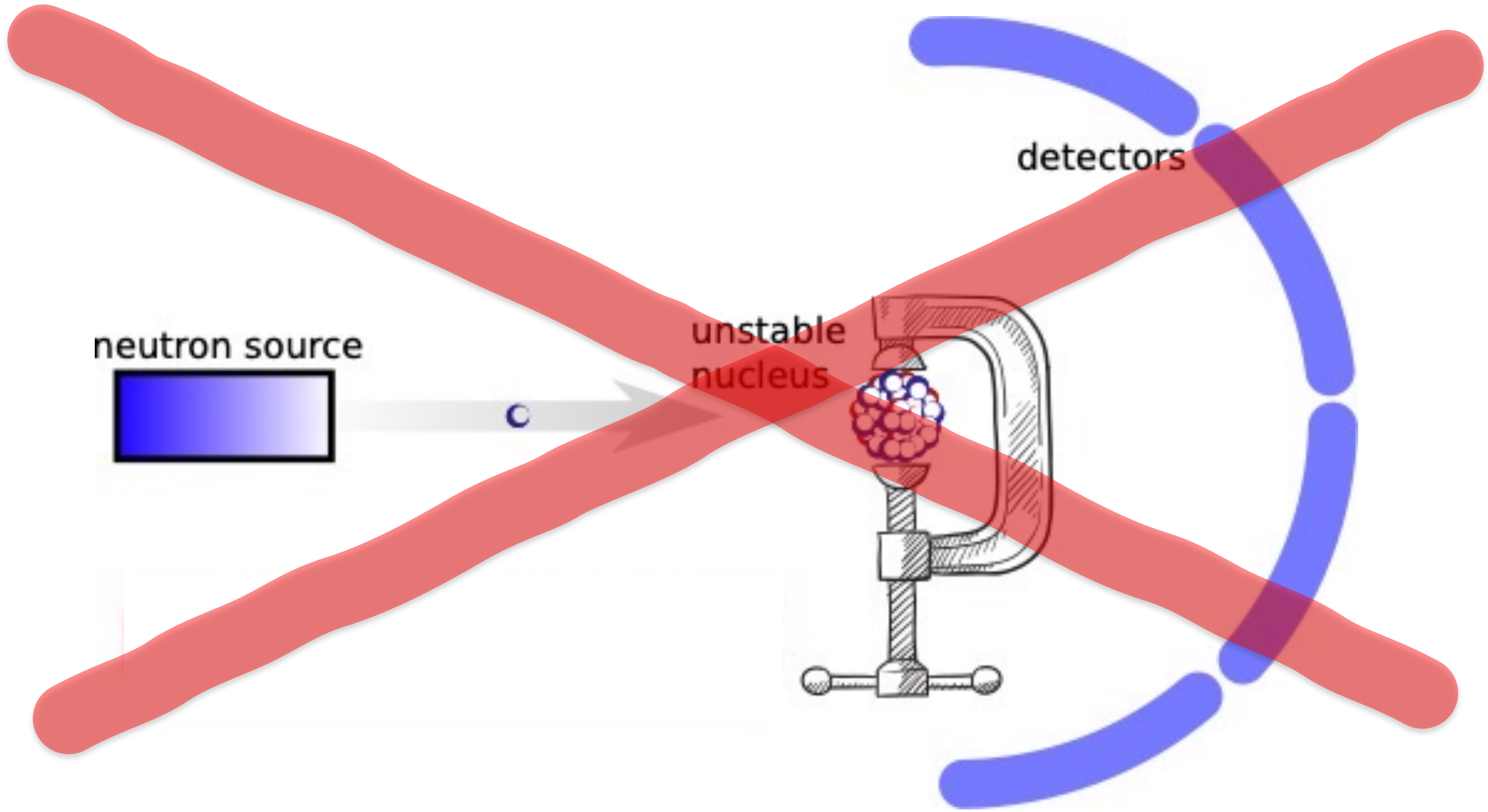

# Measuring cross sections and rates: problems (neutron-induced)

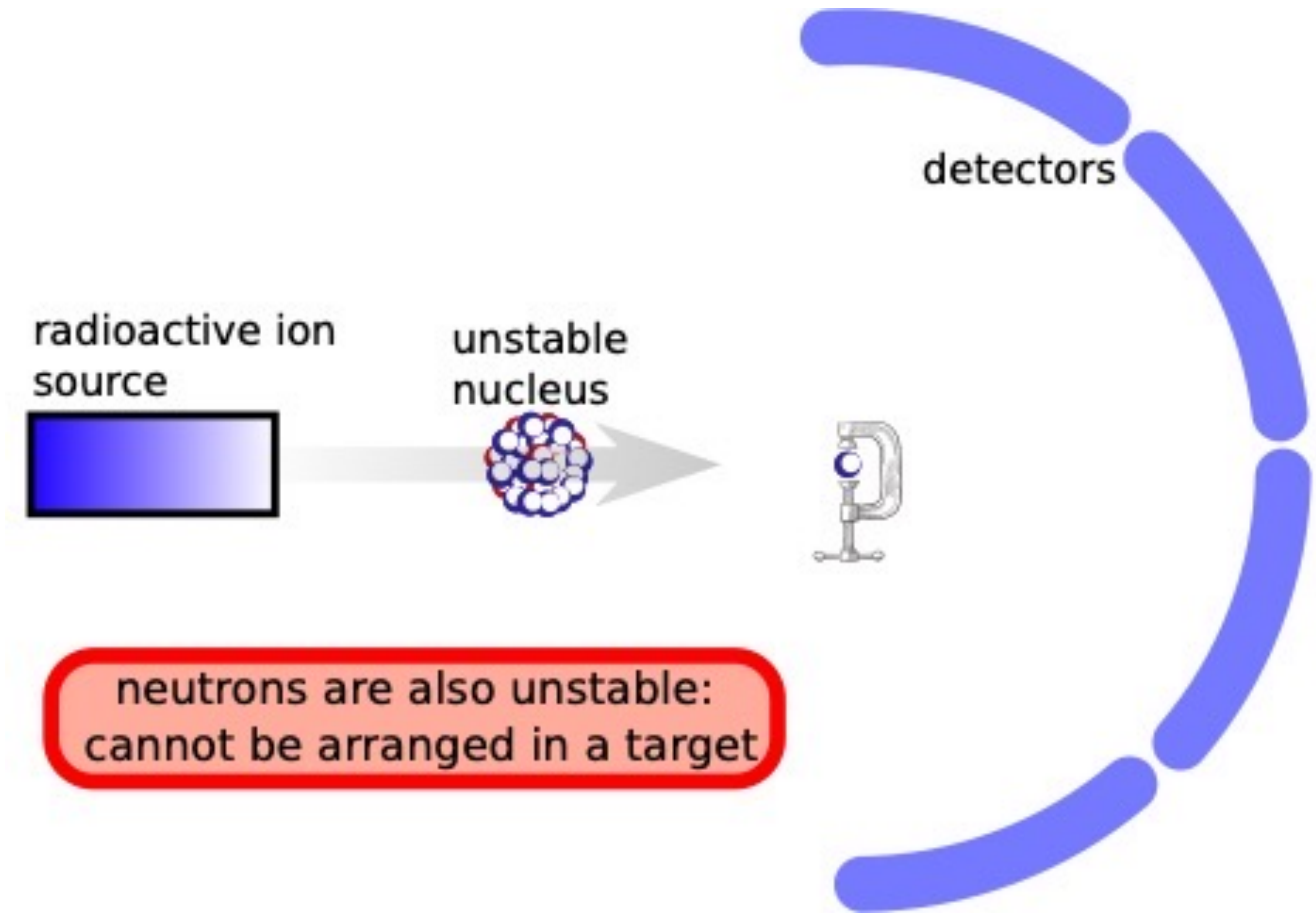

# Measuring cross sections and rates: problems (neutron-induced)

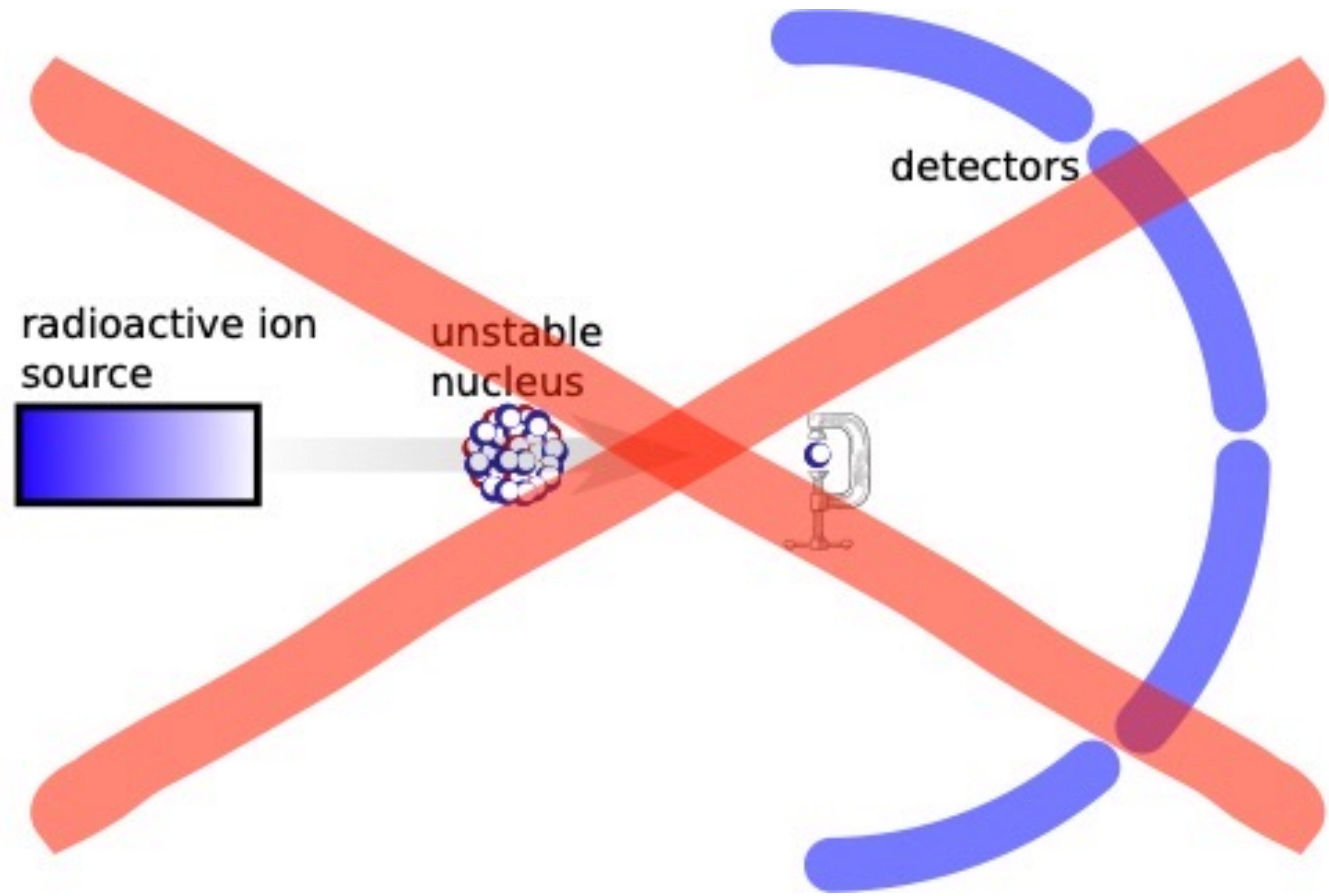

# 2

# Green's Function Transfer (GFT)

# The Green's Function Transfer (GFT) formalism

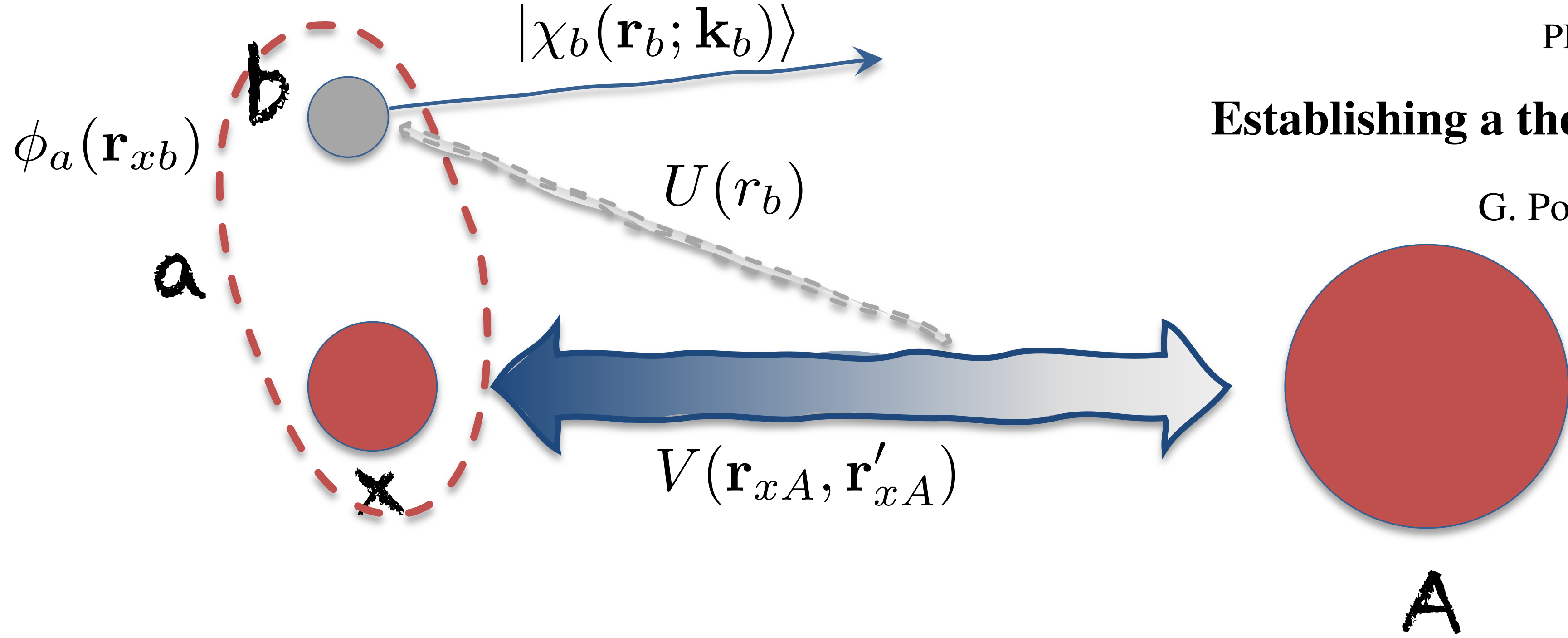


PHYSICAL REVIEW C **92**, 034611 (2015)

**Establishing a theory for deuteron-induced surrogate reactions**

G. Potel,[1,2] F. M. Nunes,[1,3] and I. J. Thompson[2]

$$\psi_0 = \langle e^{i\mathbf{k}_b\mathbf{r}_b}|G(E)\,\mathcal{V}(E)|e^{i\mathbf{k}\mathbf{r}_{xA}}\phi_a\rangle$$

Green's function (reaction)

Optical Potential (structure)

# The Green's Function Transfer (GFT) formalism

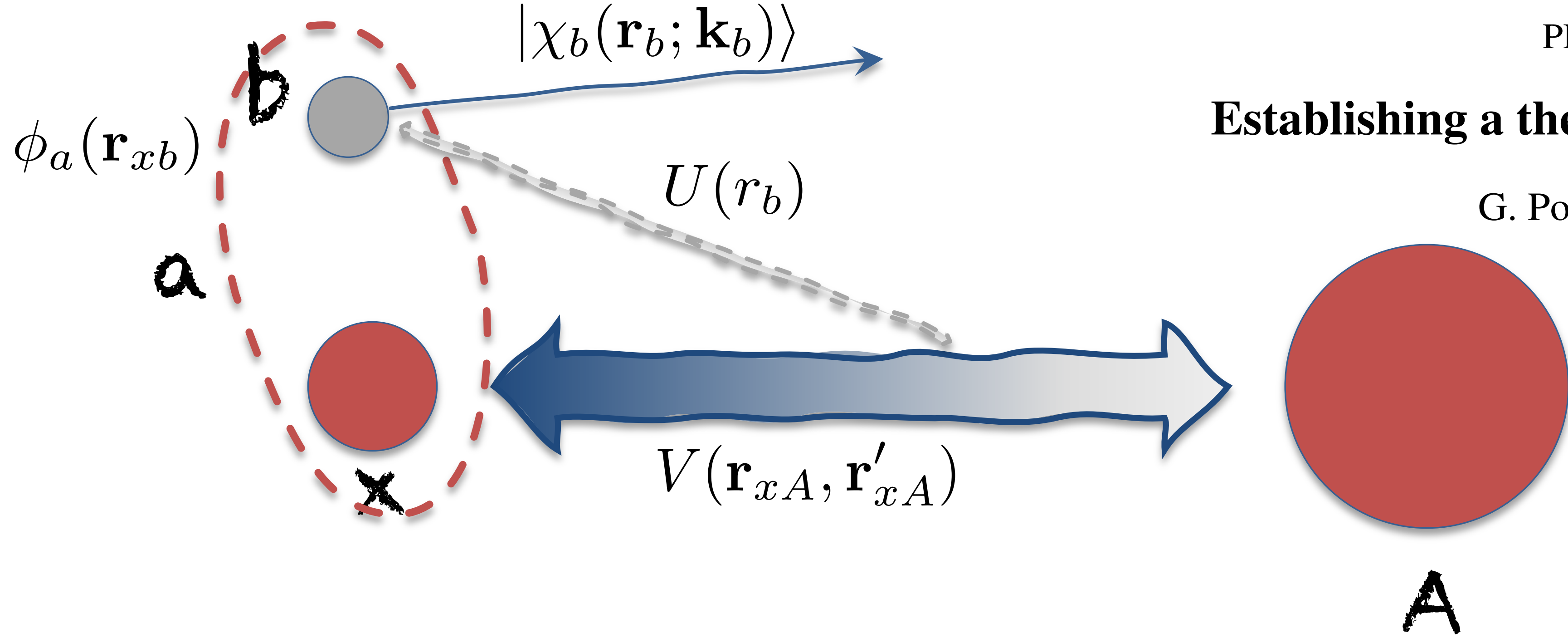


PHYSICAL REVIEW C **92**, 034611 (2015)

**Establishing a theory for deuteron-induced surrogate reactions**

G. Potel,[1,2] F. M. Nunes,[1,3] and I. J. Thompson[2]

$$\psi_0 = \langle e^{i\mathbf{k}_b\mathbf{r}_b}|G(E)\,\mathcal{V}(E)|e^{i\mathbf{k}\mathbf{r}_{xA}}\phi_a\rangle$$

cross section for detecting the spectator b particle

$$\sigma_R(E) = \frac{2\mu}{\hbar k_x}\langle\psi_0|\mathrm{Im}\mathcal{V}(E-E_b)|\psi_0\rangle$$

# The Green's Function Transfer (GFT) formalism

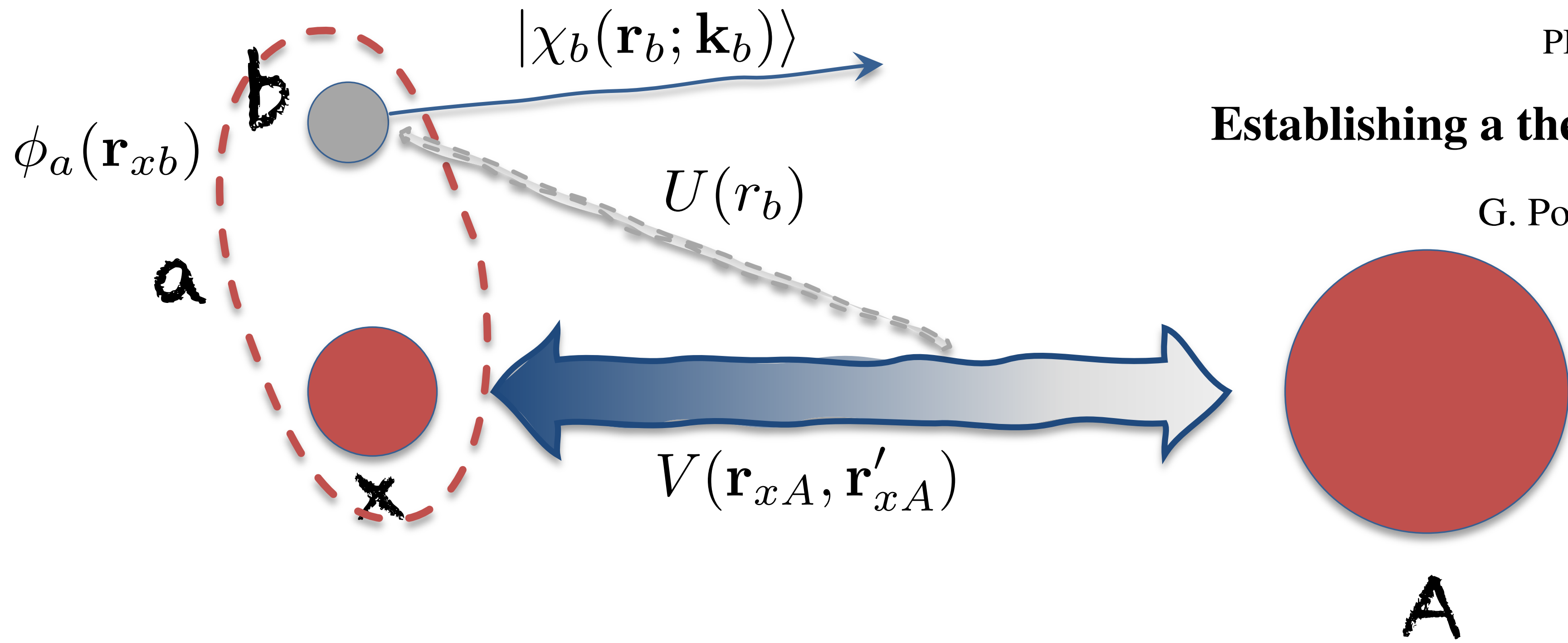


PHYSICAL REVIEW C **92**, 034611 (2015)

**Establishing a theory for deuteron-induced surrogate reactions**

G. Potel,[1,2] F. M. Nunes,[1,3] and I. J. Thompson[2]

$$\psi_0 = \langle e^{i\mathbf{k}_b\mathbf{r}_b}|G(E)\,\mathcal{V}(E)|e^{i\mathbf{k}\mathbf{r}_{xA}}\phi_a\rangle$$

A proposed scheme to enforce structure-reactions consistency

$$G(E) = (E - T - \mathcal{V}(E))^{-1}$$

# 2a

## Applying the GFT to (d,p) reactions

# GFT with the Dispersive Optical Model (DOM); Ca(d,p)

Eur. Phys. J. A (2017) **53**: 178

THE EUROPEAN PHYSICAL JOURNAL A

**Toward a complete theory for predicting inclusive deuteron breakup away from stability**

G. Potel[1,a], G. Perdikakis[1,2,3,b], B.V. Carlson[4,c], M.C. Atkinson[5], W.H. Dickhoff[5], J.E. Escher[6], M.S. Hussein[4,7,8], J. Lei[9,d], W. Li[1], A.O. Macchiavelli[10], A.M. Moro[9], F.M. Nunes[1,11], S.D. Pain[12], and J. Rotureau[1]

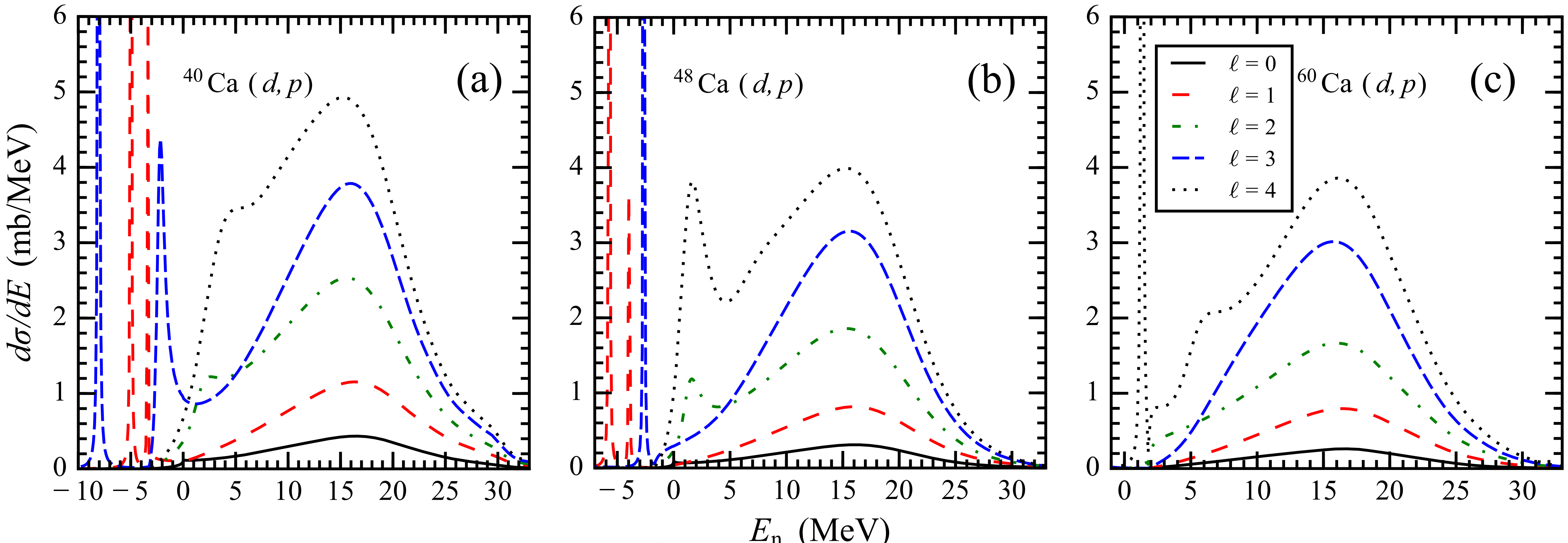


- Dispersive: reproduction of positive and negative energy cross section
- Controlled extrapolation to exotic nuclei

# GFT applied to the Surrogate Method: $^{95}$Mo(d,pγ) with Koning-Delaroche OP

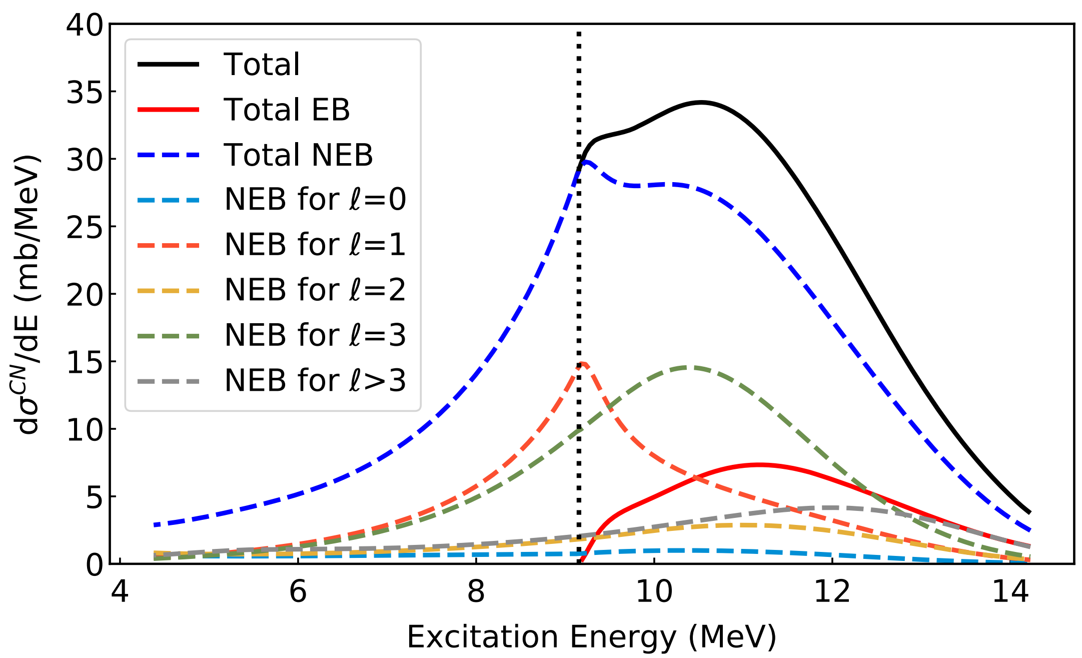


- Absorption of the neutron as a function of excitation energy and spin computed with GFT formalism
- We used the phenomenological Koning-Delaroche OP

# GFT applied to the Surrogate Method: $^{95}$Mo(d,pγ) with Koning-Delaroche OP

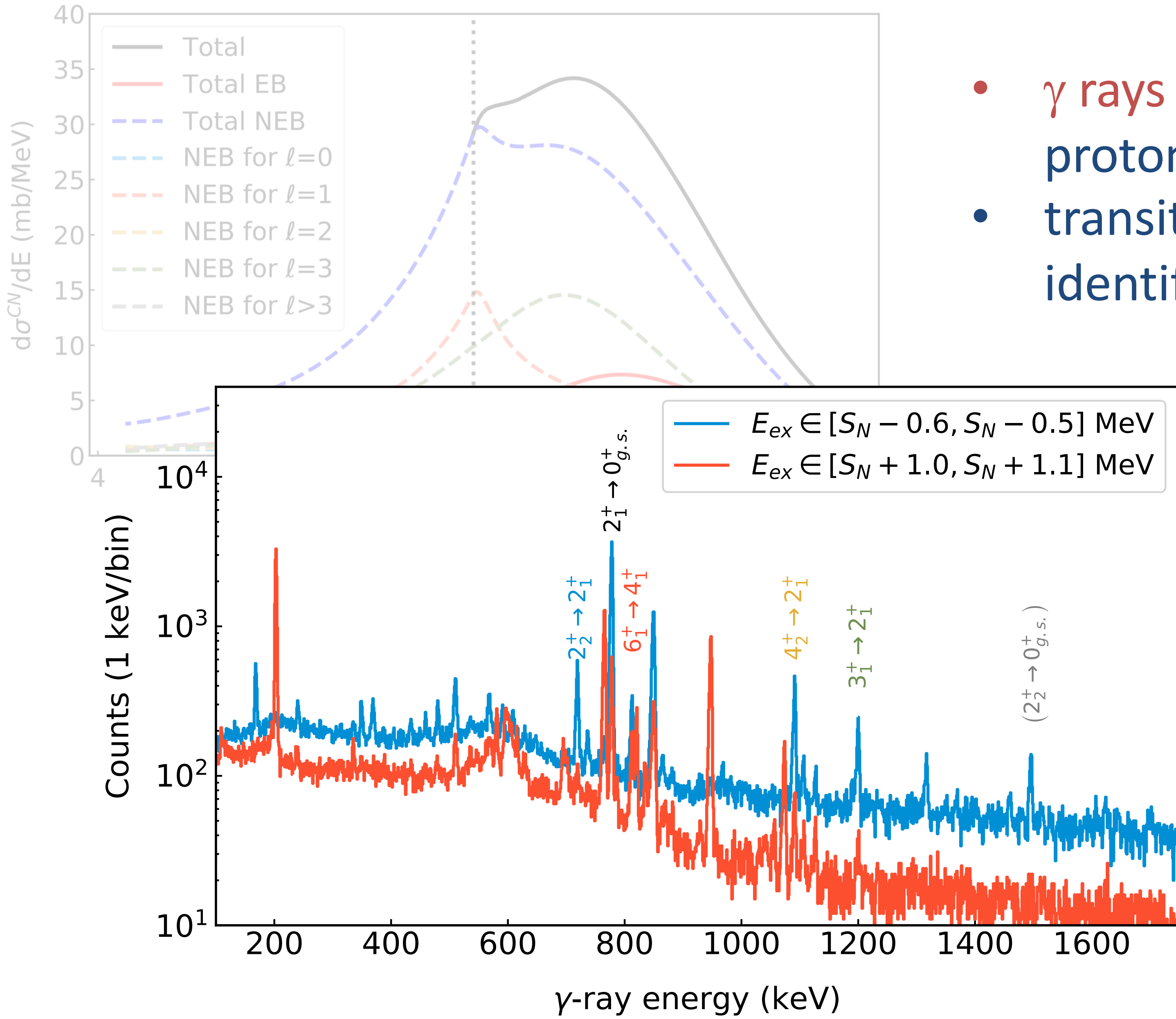


- γ rays observed in coincidence with protons
- transitions from both $^{95}$Mo and $^{96}$Mo are identified

# GFT applied to the Surrogate Method: $^{95}$Mo(d,p$\gamma$) with Koning-Delaroche OP

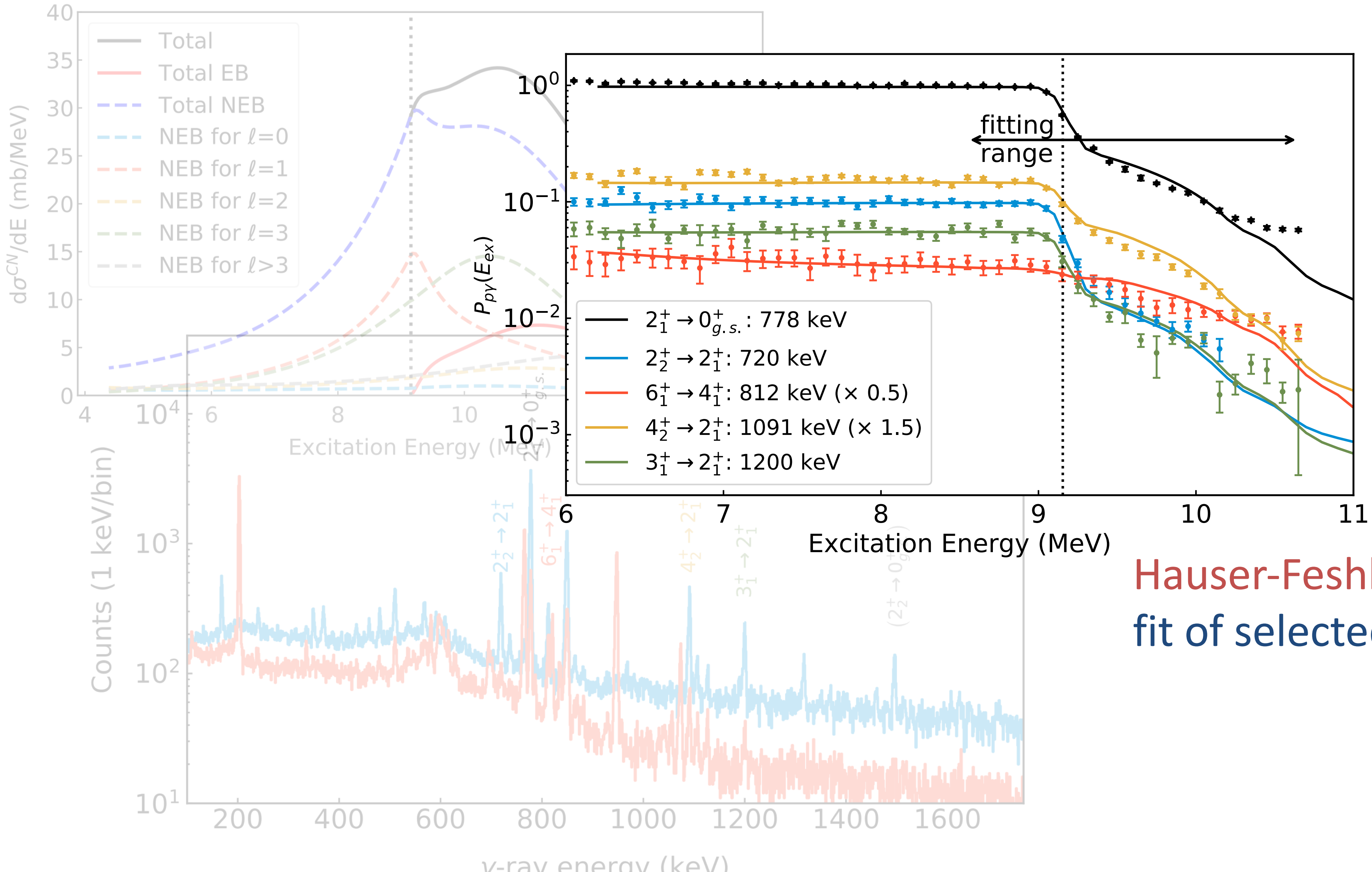


Hauser-Feshbach parameters determined by fit of selected $\gamma$ lines (J. Escher)

# GFT applied to the Surrogate Method: $^{95}$Mo(d,pγ) with Koning-Delaroche OP

PHYSICAL REVIEW LETTERS **122,** 052502 (2019)

**Towards Neutron Capture on Exotic Nuclei: Demonstrating (*d,pγ*) as a Surrogate Reaction for (*n,γ*)**

A. Ratkiewicz,[1,2,*] J. A. Cizewski,[2] J. E. Escher,[1] G. Potel,[3,4] J. T. Burke,[1] R. J. Casperson,[1] M. McCleskey,[5] R. A. E. Austin,[6] S. Burcher,[2] R. O. Hughes,[1,7] B. Manning,[2] S. D. Pain,[8] W. A. Peters,[9] S. Rice,[2] T. J. Ross,[7] N. D. Scielzo,[1] C. Shand,[2,10] and K. Smith[11]

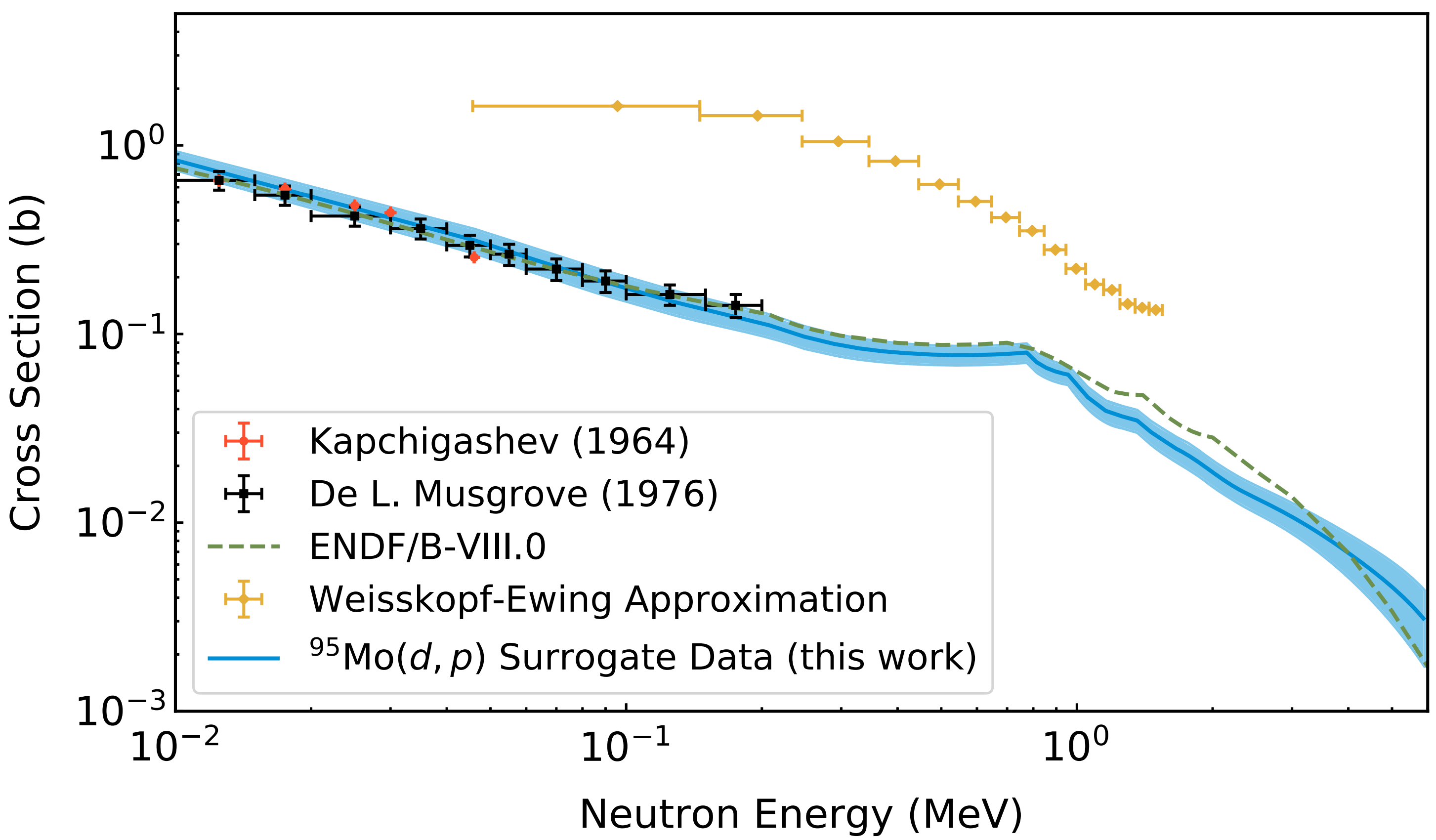


- The obtained Hauser-Feshbach parameters are used to calculate (n,γ)
- We found an excellent agreement with the direct measurement.

# GFT applied to the Surrogate Method: $^{95}$Mo(d,pγ) with Koning-Delaroche OP

PHYSICAL REVIEW LETTERS **122,** 052502 (2019)

**Towards Neutron Capture on Exotic Nuclei: Demonstrating $(d,p\gamma)$ as a Surrogate Reaction for $(n,\gamma)$**

A. Ratkiewicz,[1,2,*] J. A. Cizewski,[2] J. E. Escher,[1] G. Potel,[3,4] J. T. Burke,[1] R. J. Casperson,[1] M. McCleskey,[5] R. A. E. Austin,[6] S. Burcher,[2] R. O. Hughes,[1,7] B. Manning,[2] S. D. Pain,[8] W. A. Peters,[9] S. Rice,[2] T. J. Ross,[7] N. D. Scielzo,[1] C. Shand,[2,10] and K. Smith[11]

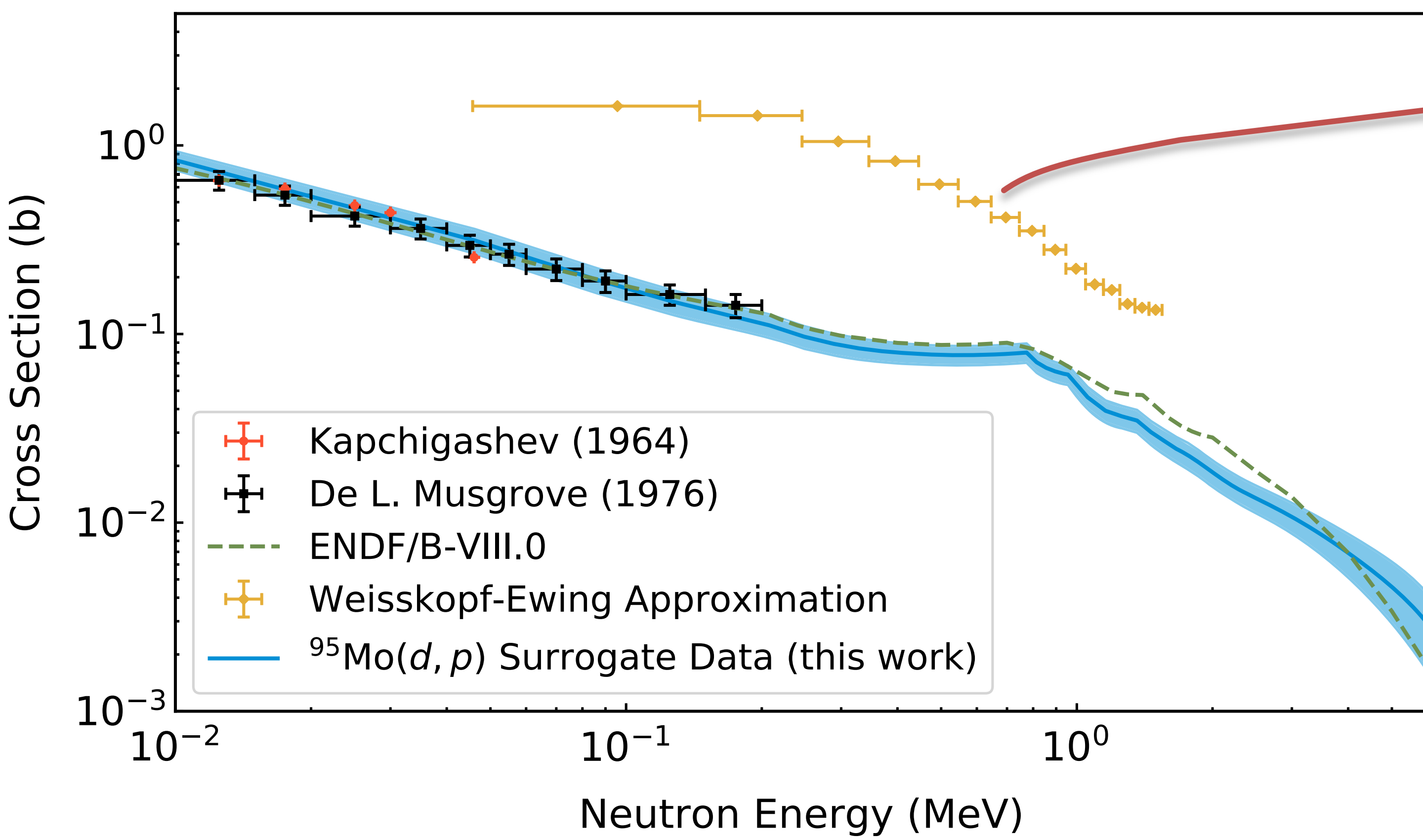


a failure to account for the initial spin distribution (Weisskopf-Ewing approximation) leads to poor results!

- The obtained Hauser-Feshbach parameters are used to calculate (n,γ)
- We found an excellent agreement with the direct measurement.

# GFT with Nuclear Field Theory (NFT): $^{9}Li(d,p)\,^{10}Li$

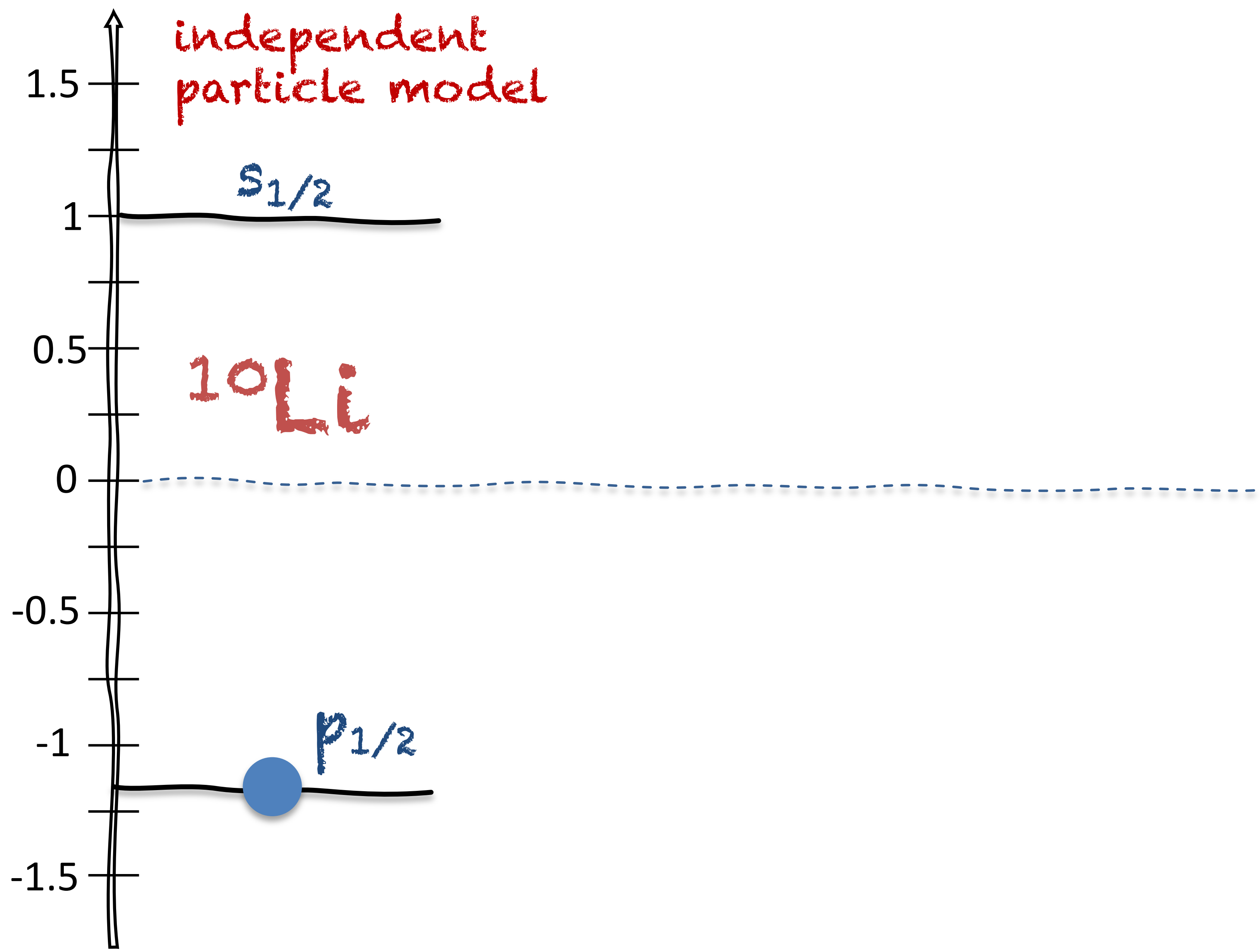

# GFT with Nuclear Field Theory (NFT): $^{9}Li(d,p)\,^{10}Li$

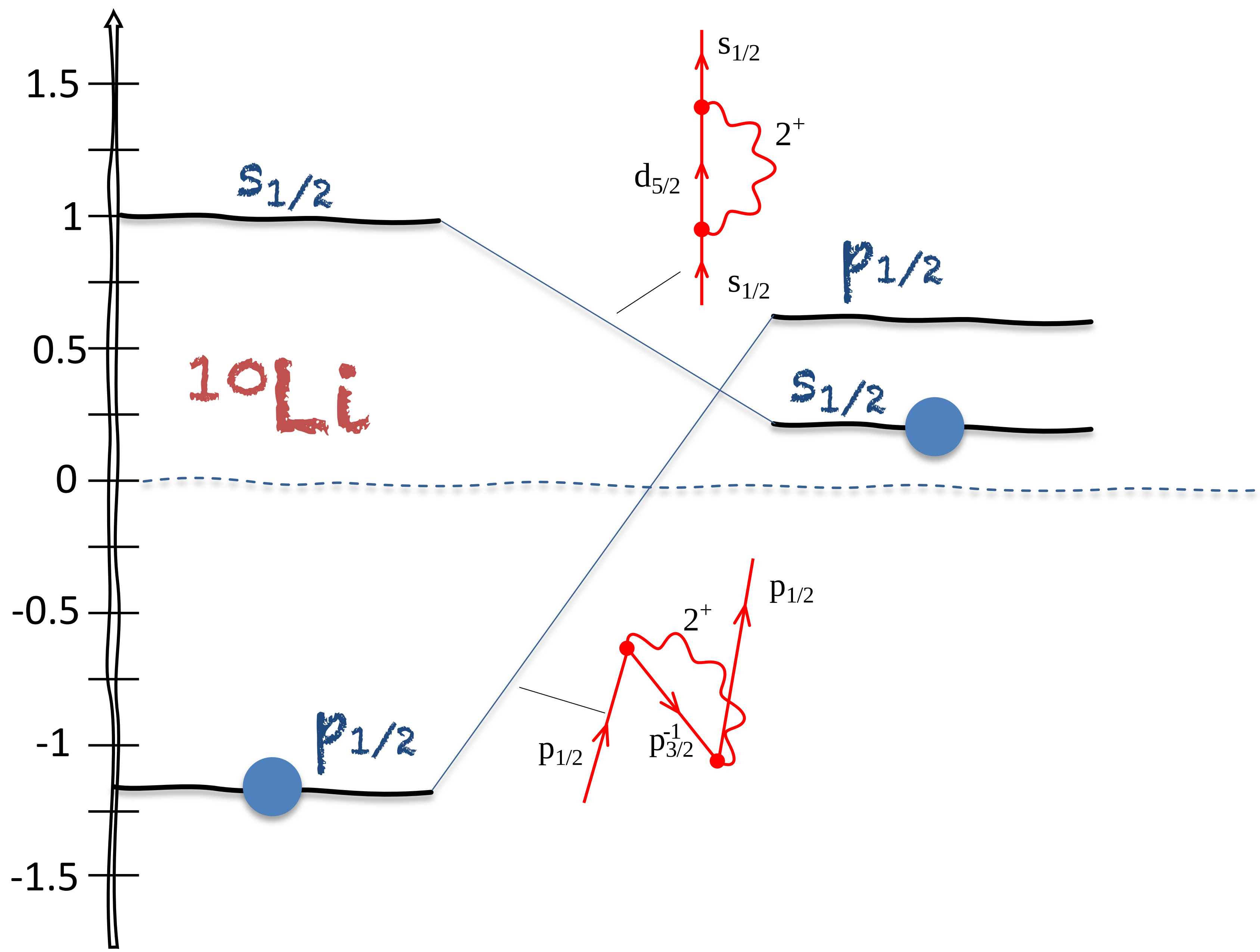

# GFT with Nuclear Field Theory (NFT): $^{9}Li(d,p)\,^{10}Li$

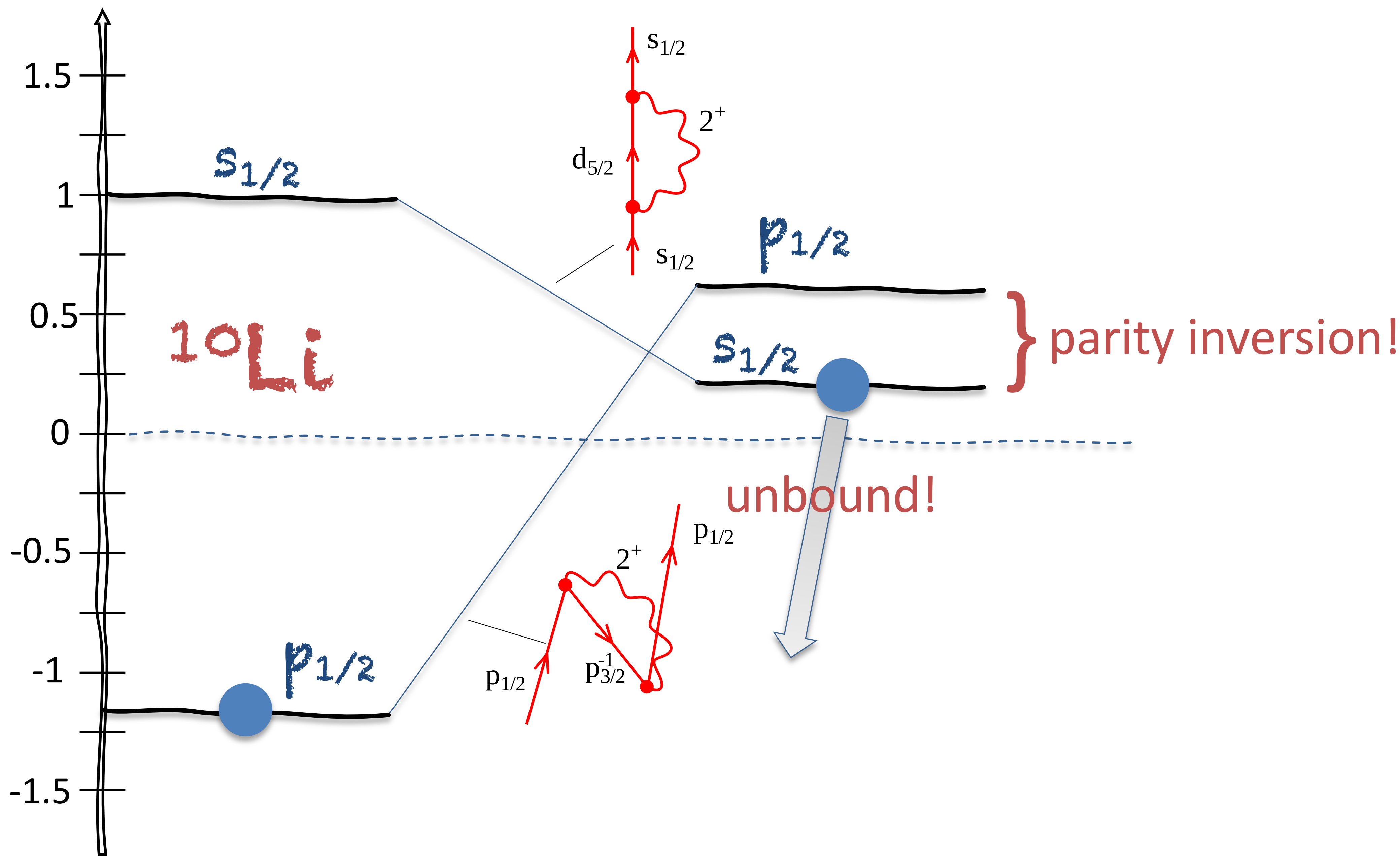

# GFT with Nuclear Field Theory (NFT): $^{9}Li(d,p)\ ^{10}Li$

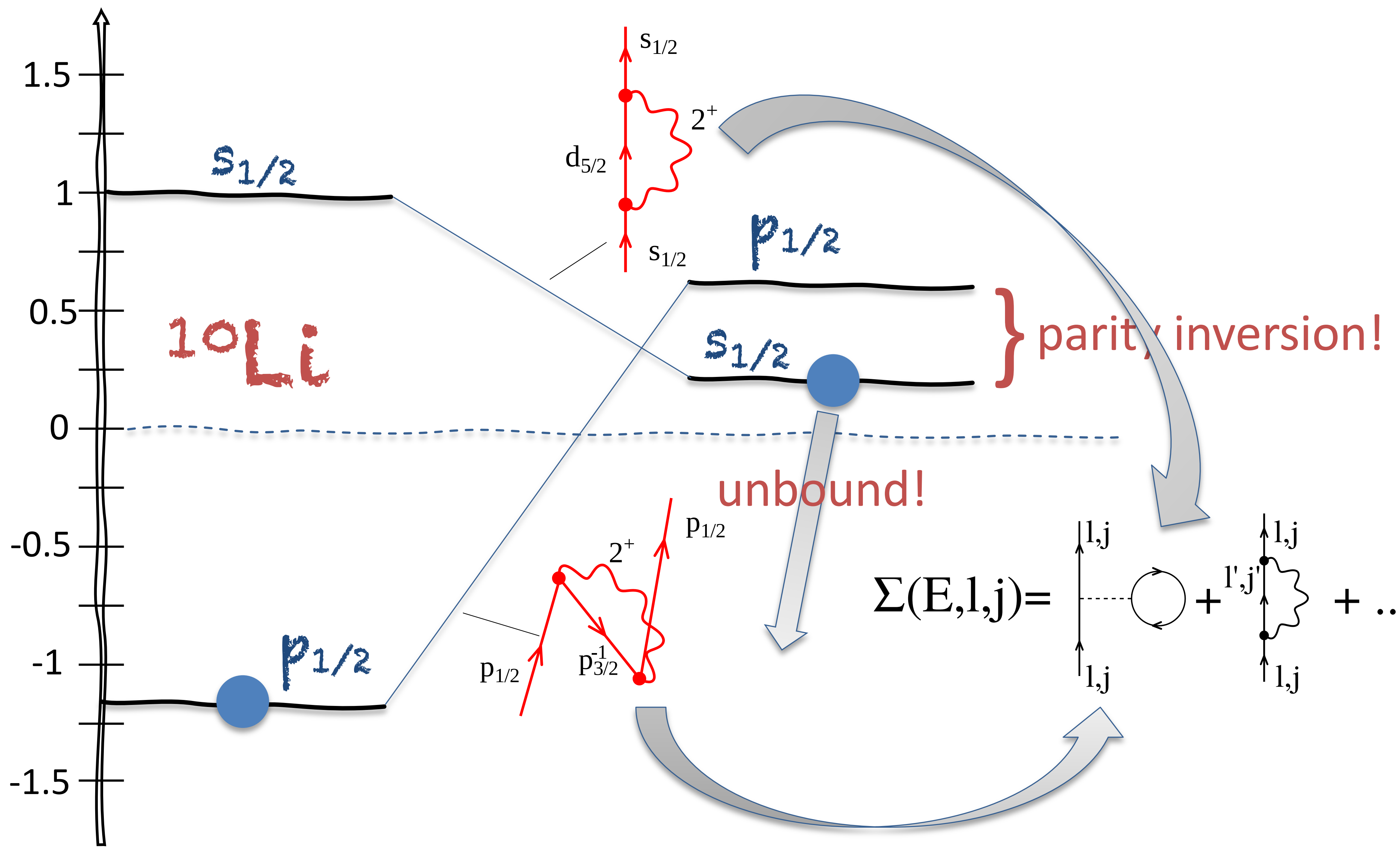

# GFT with Nuclear Field Theory (NFT): $^{9}$Li(d,p) $^{10}$Li

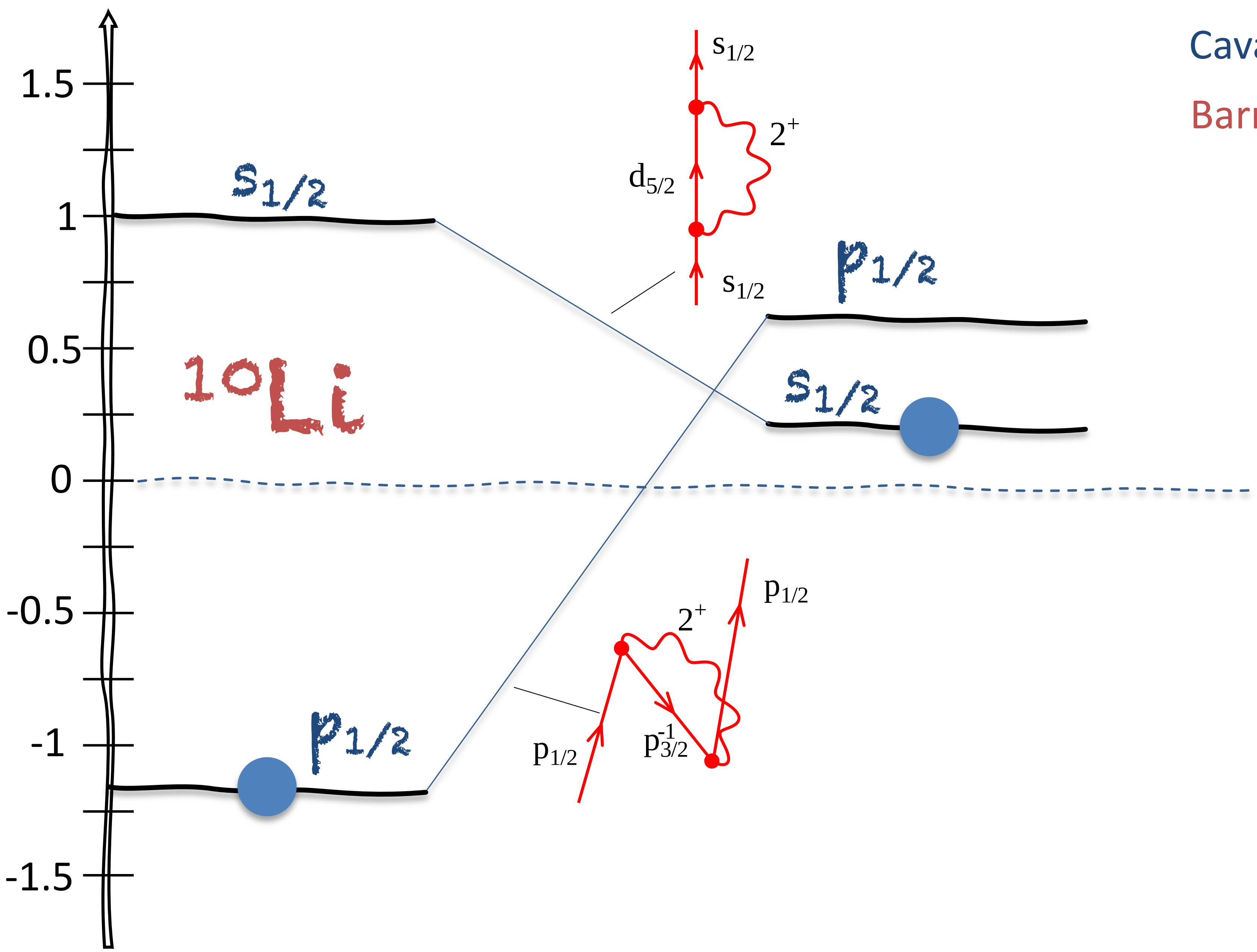


Cavallaro *et al.*, PRL **118**, 012701 (2017)

Barranco, GP, Vigezzi, Broglia PRC **101**, 031305(R) (2020)

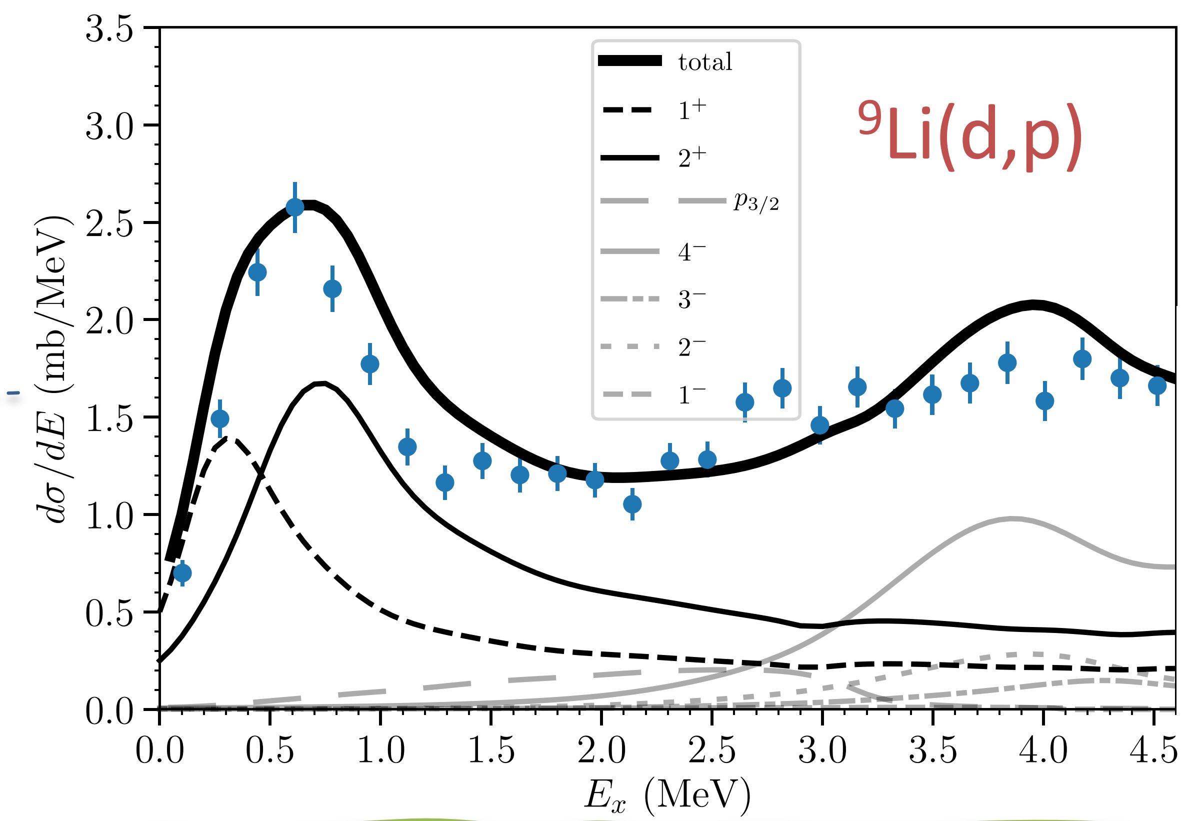


theoretical description validated by experiment

# 3

# Computing the Optical Potential

# The OP accounts for the composite nature of the target nucleus

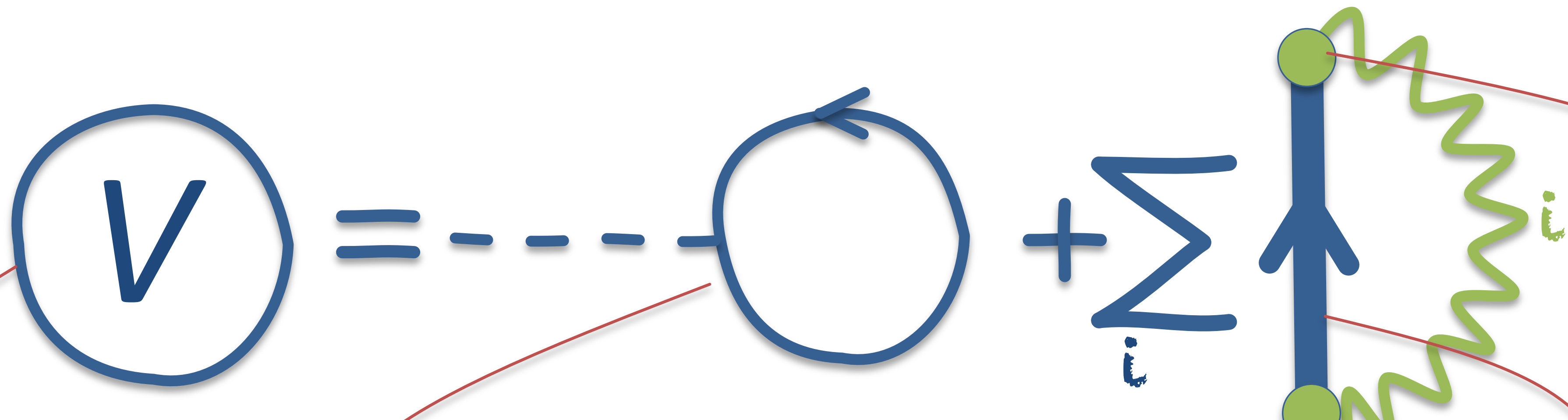


$$V(\mathbf{r},\mathbf{r}';E) = U_0(r) + \sum_i U_{0i}(\mathbf{r})G(E-E_i,\mathbf{r},\mathbf{r}')U_{i0}(\mathbf{r}')$$

- The computed OP is energy dependent, non-local, complex, and dispersive
- The OP verifies the Kramers-Kronig dispersion relations between the real and the imaginary part

# $^{24}$Mg+n with valence shell model

excitation energy $E_i$

angular momentum

parity

| | | | | |
|---|---|---|---|---|
| 0 | 0 | 2 | 1 | 0.584066 |
| 0.701 | 0 | 0 | 1 | −0.716831 |
| 1.169 | 0 | 2 | 1 | 0.488705 |
| 2.033 | 0 | 2 | 1 | −0.288311 |
| 2.529 | 0 | 0 | 1 | 0.318332 |
| 2.701 | 0 | 2 | 1 | 0.542416 |
| 3.859 | 0 | 2 | 1 | 0.0495903 |
| 3.926 | 0 | 1 | −1 | −0.0298132 |
| 4.118 | 0 | 1 | −1 | −0.584623 |
| 4.226 | 0 | 3 | −1 | −0.651056 |
| 4.46 | 0 | 2 | 1 | 0.100777 |
| 4.816 | 0 | 2 | 1 | 0.0975601 |
| 4.945 | 0 | 1 | −1 | 0.516883 |
| 5.065 | 0 | 1 | −1 | −0.0511968 |
| 5.416 | 0 | 0 | 1 | −0.283037 |
| 5.638 | 0 | 3 | −1 | −0.219064 |
| 5.785 | 0 | 2 | 1 | −0.0103979 |
| 5.792 | 0 | 2 | 1 | 0.132477 |
| 5.935 | 0 | 3 | −1 | 0.069005 |
| 5.936 | 0 | 2 | 1 | 0.094658 |
| 6.033 | 0 | 1 | −1 | 0.0353684 |
| 6.12 | 0 | 1 | −1 | −0.159821 |
| 6.243 | 0 | 2 | 1 | −0.174362 |
| 6.35 | 0 | 3 | −1 | 0.122727 |
| 6.385 | 0 | 0 | 1 | 0.182001 |
| 6.417 | 0 | 2 | 1 | 0.115995 |
| 6.609 | 0 | 2 | 1 | 0.100457 |
| 6.739 | 0 | 3 | −1 | 0.157325 |
| 6.771 | 0 | 1 | −1 | 0.419452 |
| 6.801 | 0 | 3 | −1 | 0.160889 |

spectroscopic factor $S_i$

## step 2: Static potential and couplings

$$V(\mathbf{r},\mathbf{r}';E) = U_0(r) + \sum_i U_{0i}(\mathbf{r}) G(E - E_i, \mathbf{r}, \mathbf{r}') U_{i0}(\mathbf{r}')$$

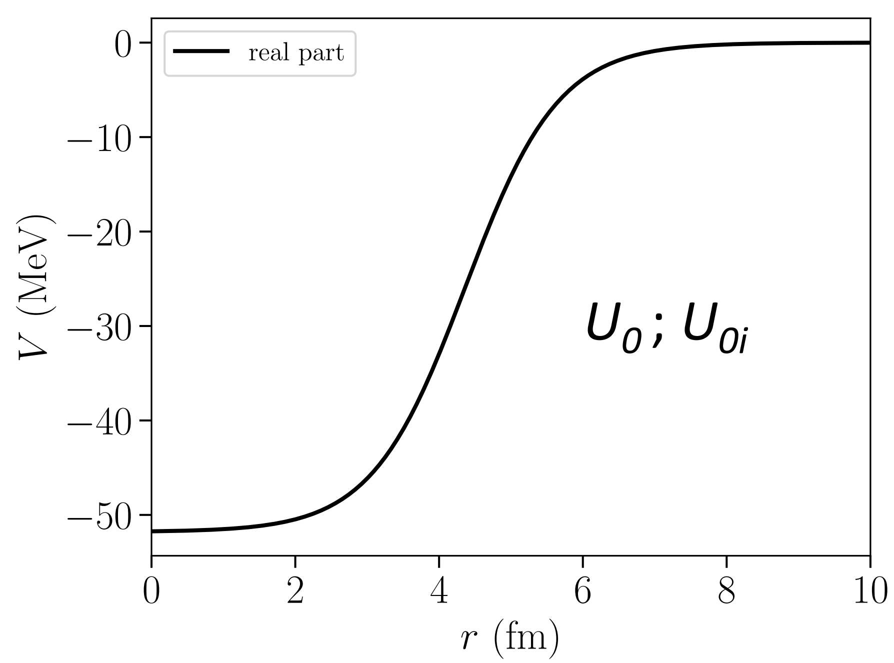


- static potential $U_0$: real, local Woods-Saxon adjusted to reproduce binding energy of $^{25}$Mg
- couplings $U_{0i}$: same Woods-Saxon, but adjusted to each $E_i$ and multiplied by spectroscopic factor $S_i$

can be done better!

# $^{24}$Mg+n with valence shell model

## step 3: Iterative procedure

excitation energy $E_i$

angular momentum

parity

spectroscopic factor $S_i$

| | | | | |
|---|---|---|---|---|
| 0 | 0 | 2 | 1 | 0.584066 |
| 0.701 | 0 | 0 | 1 | −0.716831 |
| 1.169 | 0 | 2 | 1 | 0.488705 |
| 2.033 | 0 | 2 | 1 | −0.288311 |
| 2.529 | 0 | 0 | 1 | 0.318332 |
| 2.701 | 0 | 2 | 1 | 0.542416 |
| 3.859 | 0 | 2 | 1 | 0.0495903 |
| 3.926 | 0 | 1 | −1 | −0.0298132 |
| 4.118 | 0 | 1 | −1 | −0.584623 |
| 4.226 | 0 | 3 | −1 | −0.651056 |
| 4.46 | 0 | 2 | 1 | 0.100777 |
| 4.816 | 0 | 2 | 1 | 0.0975601 |
| 4.945 | 0 | 1 | −1 | 0.516883 |
| 5.065 | 0 | 1 | −1 | −0.0511968 |
| 5.416 | 0 | 0 | 1 | −0.283037 |
| 5.638 | 0 | 3 | −1 | −0.219064 |
| 5.785 | 0 | 2 | 1 | −0.0103979 |
| 5.792 | 0 | 2 | 1 | 0.132477 |
| 5.935 | 0 | 3 | −1 | 0.069005 |
| 5.936 | 0 | 2 | 1 | 0.094658 |
| 6.033 | 0 | 1 | −1 | 0.0353684 |
| 6.12 | 0 | 1 | −1 | −0.159821 |
| 6.243 | 0 | 2 | 1 | −0.174362 |
| 6.35 | 0 | 3 | −1 | 0.122727 |
| 6.385 | 0 | 0 | 1 | 0.182001 |
| 6.417 | 0 | 2 | 1 | 0.115995 |
| 6.609 | 0 | 2 | 1 | 0.100457 |
| 6.739 | 0 | 3 | −1 | 0.157325 |
| 6.771 | 0 | 1 | −1 | 0.419452 |
| 6.801 | 0 | 3 | −1 | 0.160889 |

$$V(\mathbf{r},\mathbf{r}';E) = U_0(r) + \sum_i U_{0i}(\mathbf{r}) G(E-E_i,\mathbf{r},\mathbf{r}') U_{i0}(\mathbf{r}')$$

$$G(\mathbf{r},\mathbf{r}',E) = (E - T - V(\mathbf{r},\mathbf{r}';E))^{-1}$$

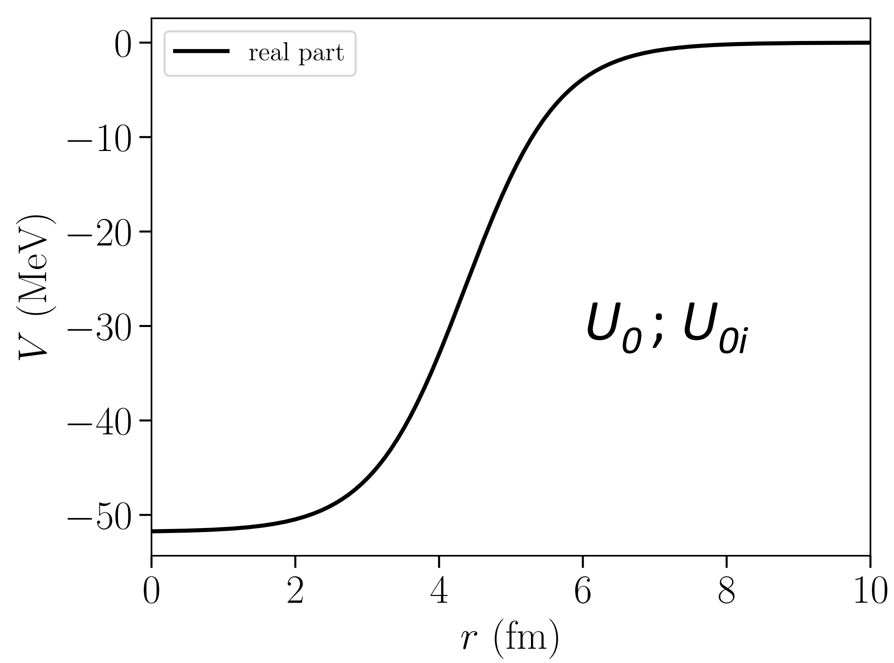


- Iterate until convergence is achieved
- Consistency between potential and Green's function is achieved, as expressed by Dyson's equation:

$$G(\mathbf{r},\mathbf{r}';E) = G_0(\mathbf{r},\mathbf{r}';E) + G_0(\mathbf{r},\mathbf{r}';E)V(\mathbf{r},\mathbf{r}';E)G(\mathbf{r},\mathbf{r}';E)$$

$$G_0(\mathbf{r},\mathbf{r}';E) = (E - T - U_0(r))^{-1}$$

**As a bonus, we obtain the Green's function**

# The dynamical polarization potential is complex, energy-dependent, dispersive, and non-local

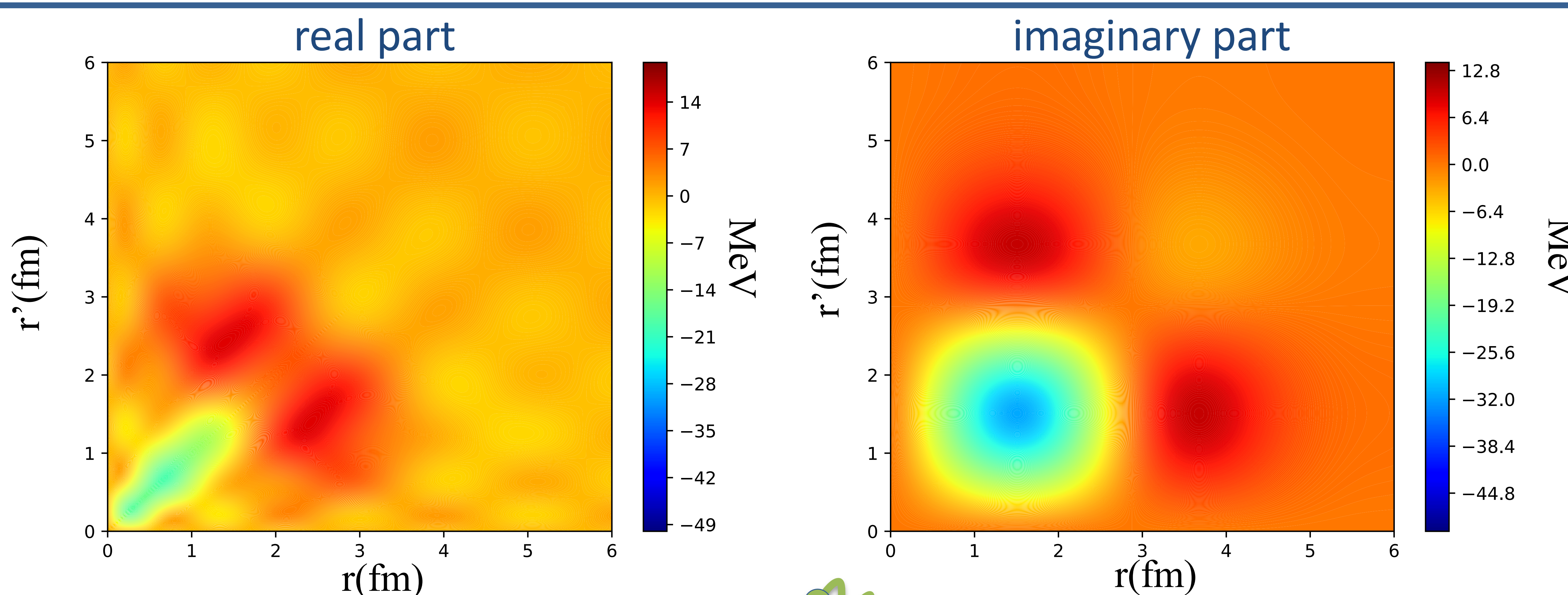


$V_{pol}(r,r';E)=\sum_i$ 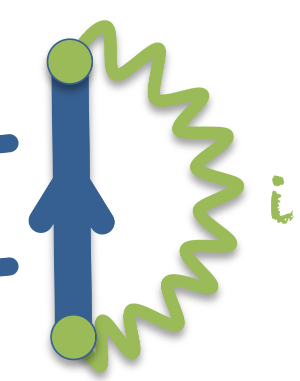

; for $E$=1MeV

# Our $^{24}$Mg calculation compares well with experiment

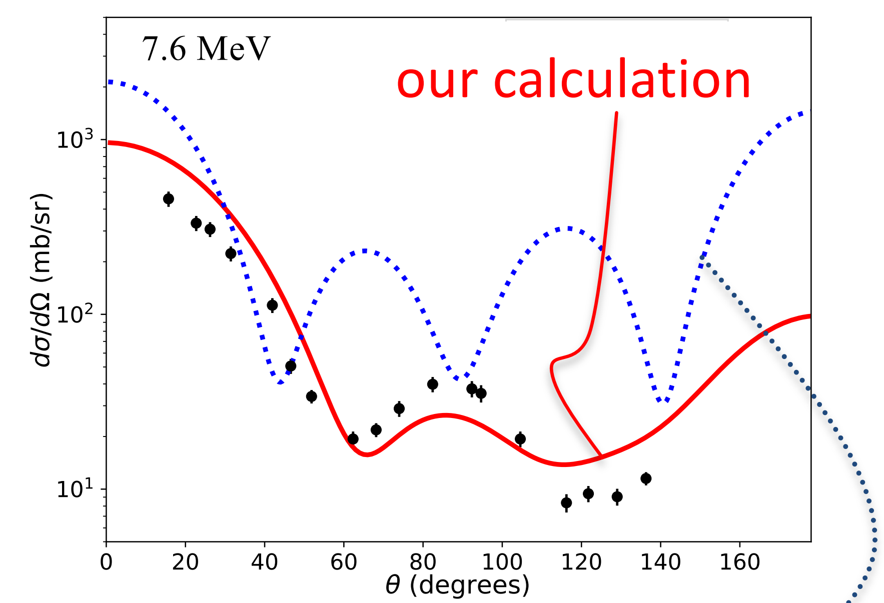


not surprisingly, the static potential alone gives a very wrong result!

# Our $^{24}$Mg calculation compares well with experiment

we check for convergence by looking at the volume integrals as a function of the iteration

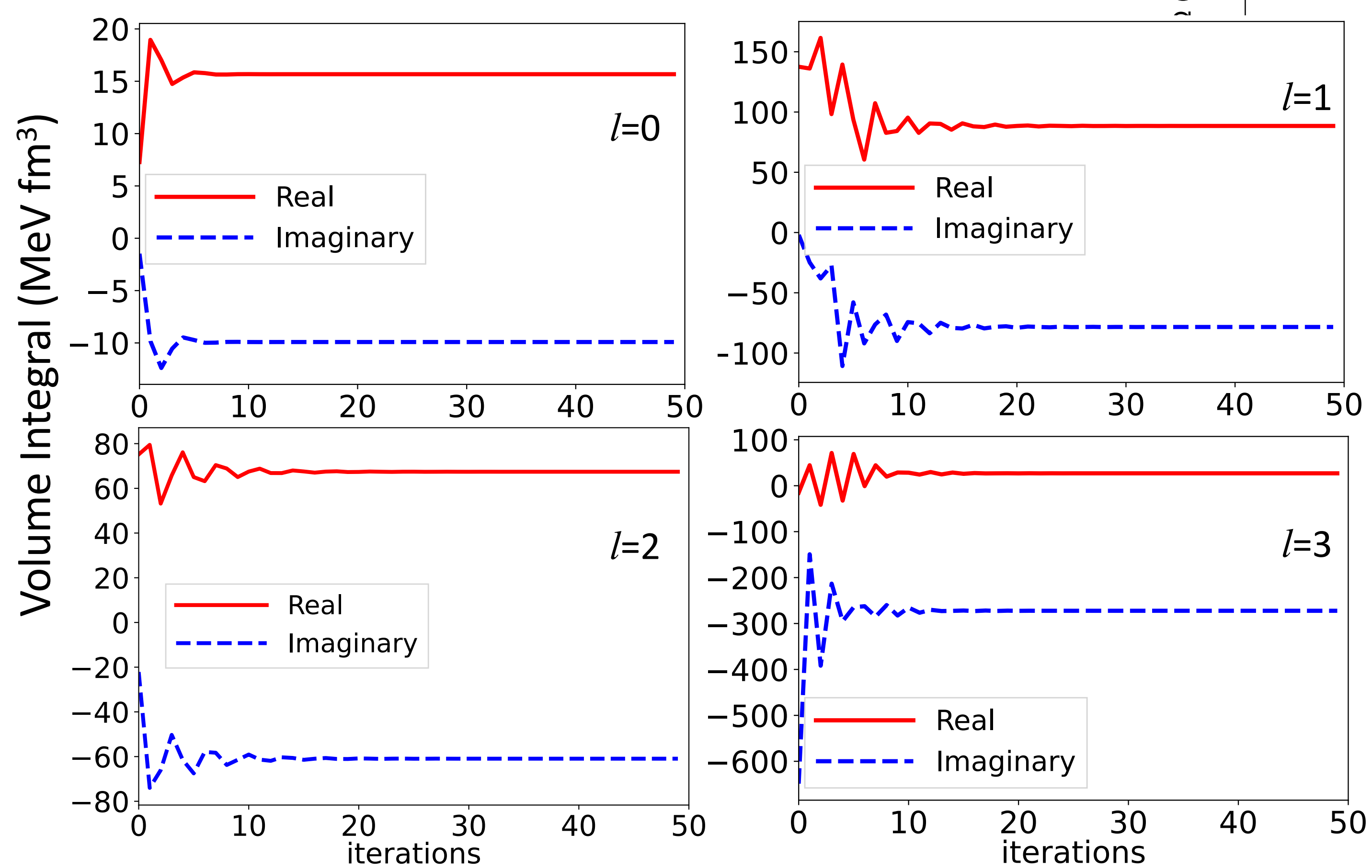


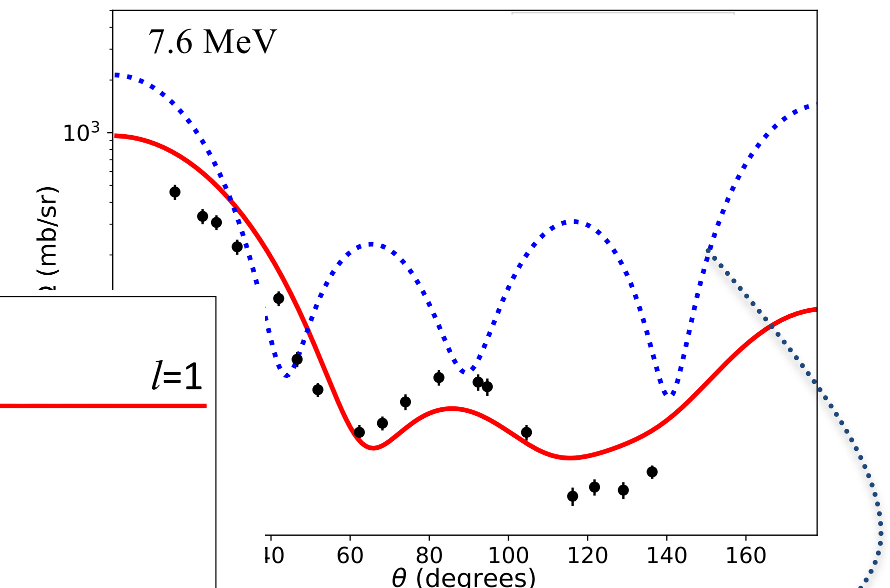


not surprisingly, the static potential alone gives a very wrong result!

# Our $^{24}$Mg calculation compares well with experiment

Koning-Delaroche

our calculation

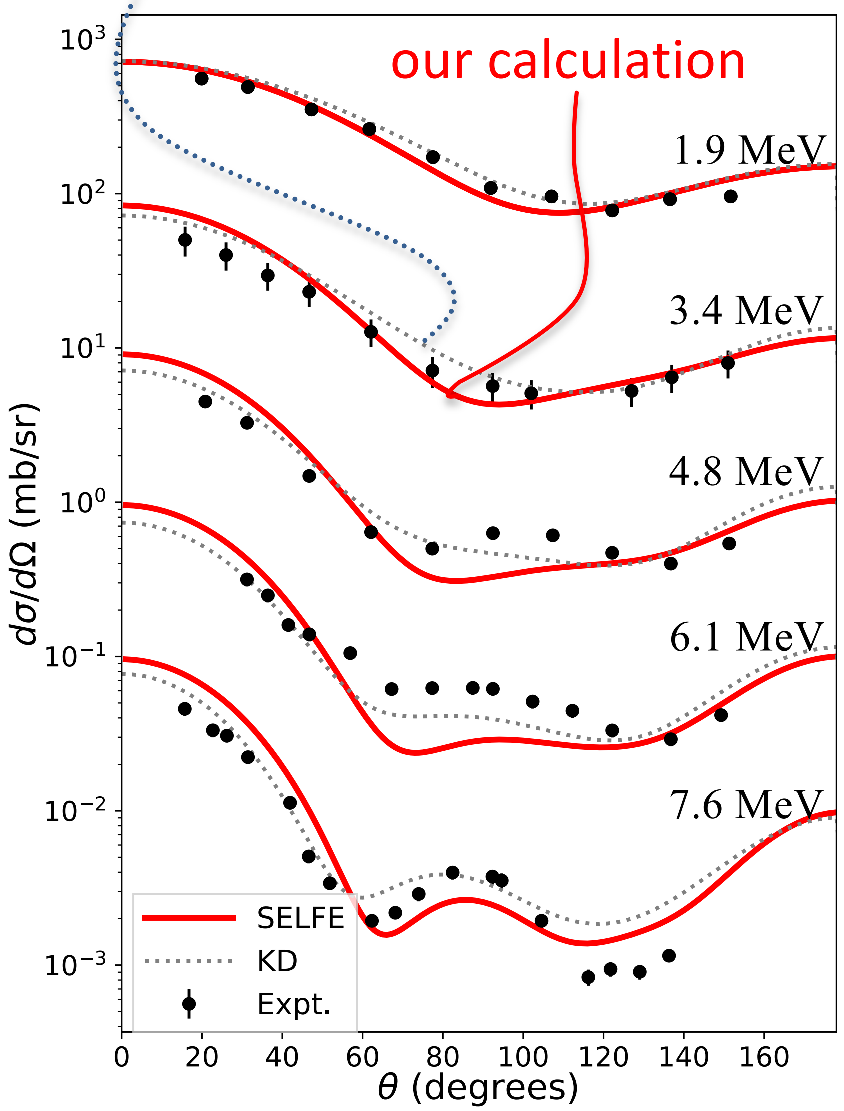


we check for convergence by looking at the volume integrals as a function of the iteration

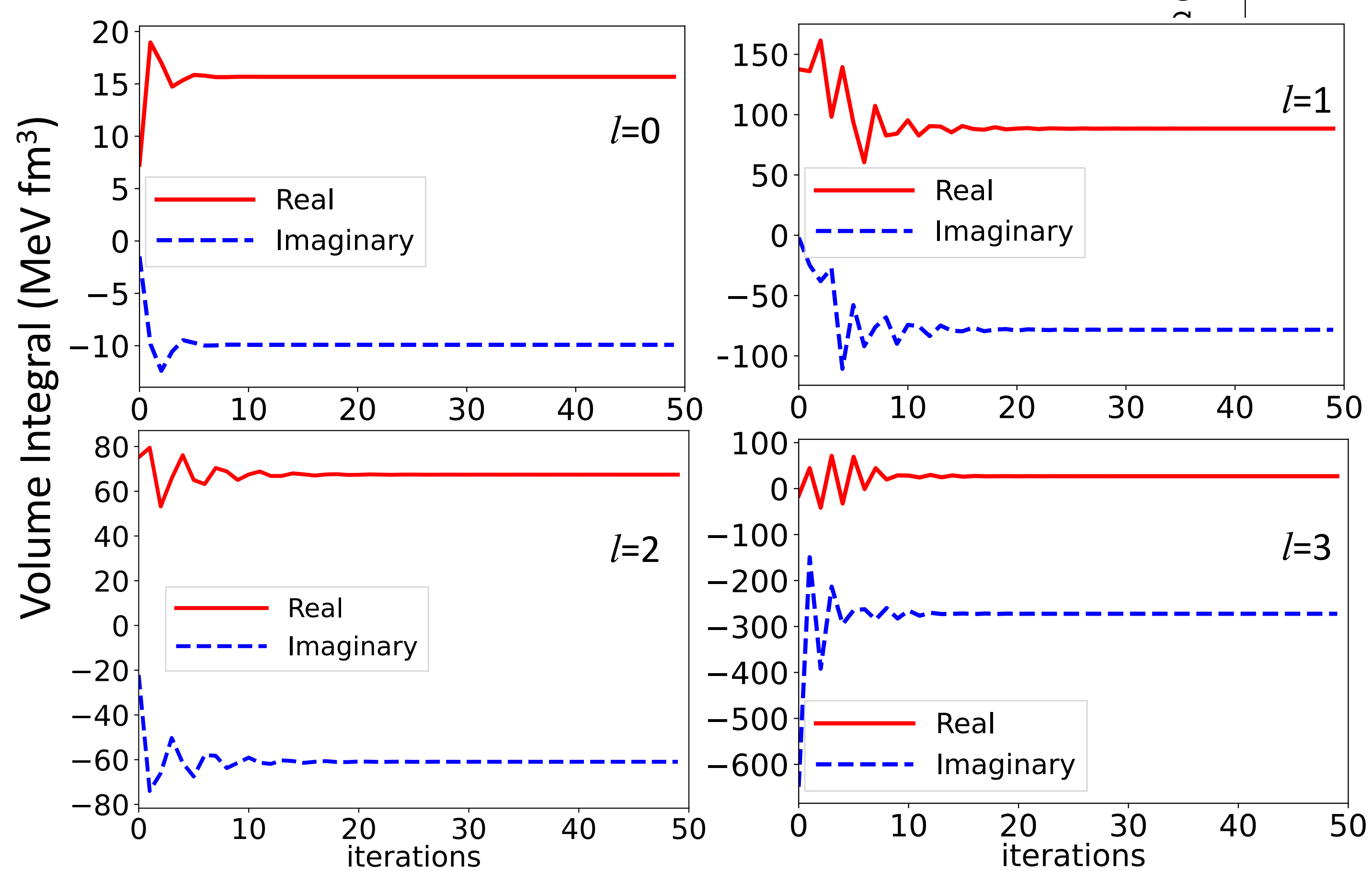


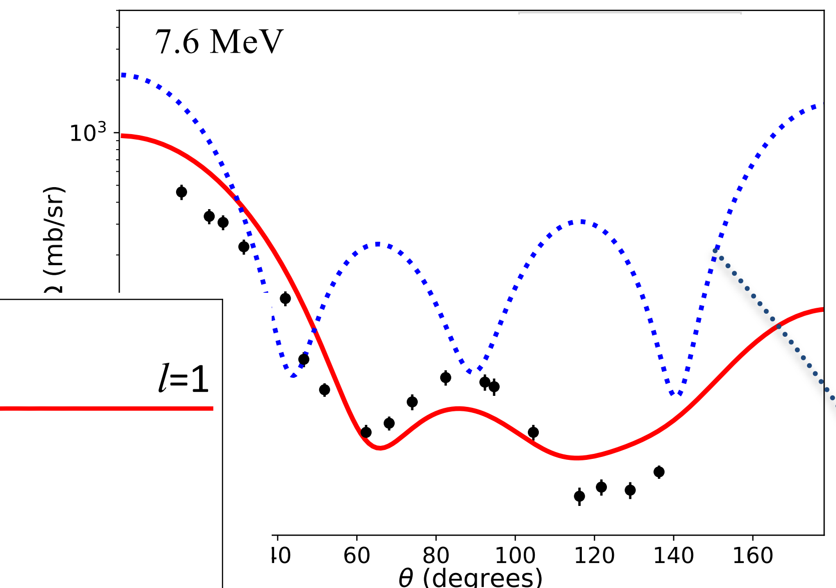


not surprisingly, the static potential alone gives a very wrong result!

**Sargsyan**, GP, Kravvaris, Escher; ArXiv (2024)

# The OP, the level density, and the γ strength function are connected through the same underlying physics

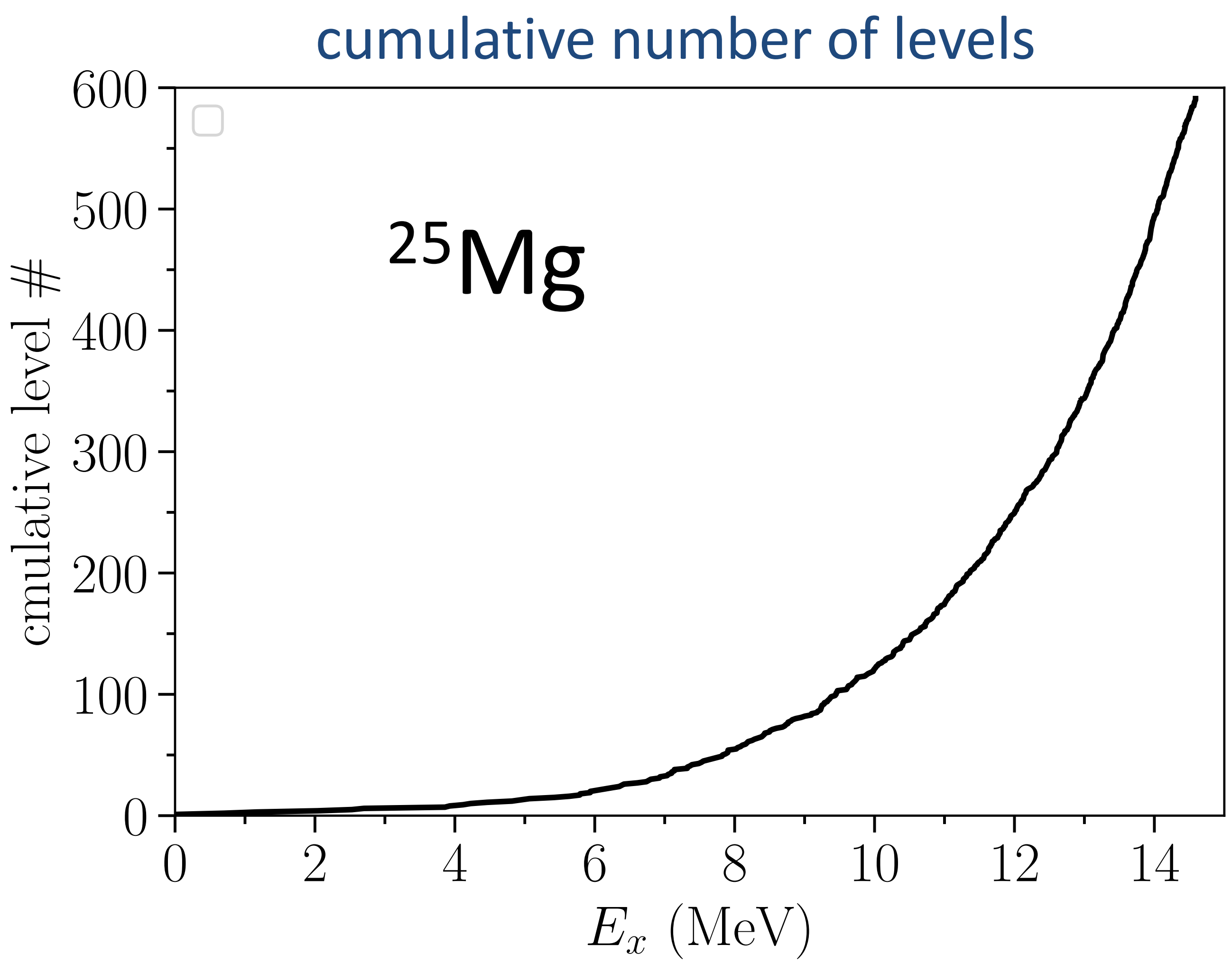


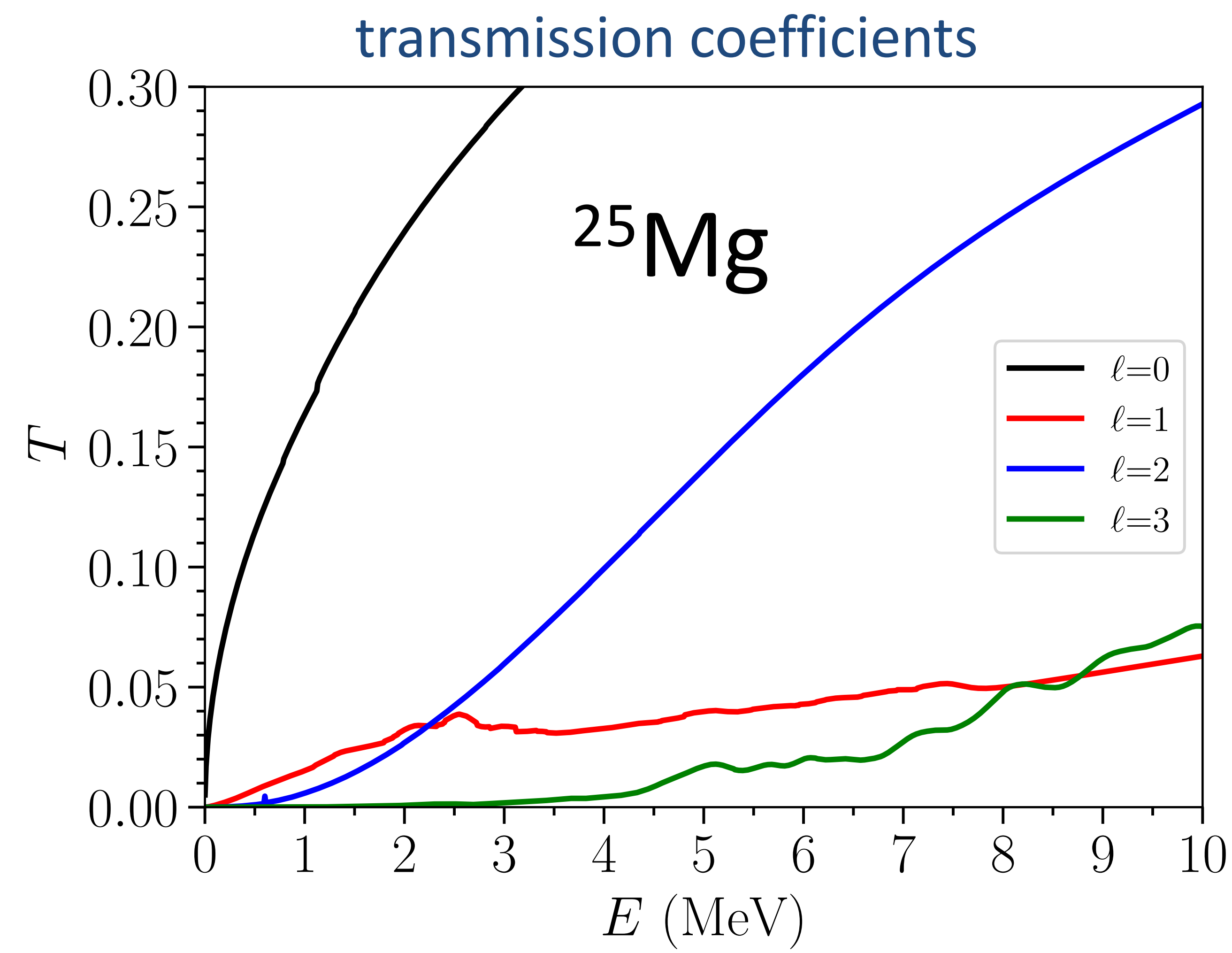


We can explicitly connect with statistical model (Hauser-Feshbach approach) through energy-averaging

# Conclusions and some perspectives

- Phenomenology has to be complemented with theory for reliable extrapolation across different regimes.
- The calculation of the OP provides a flexible and versatile path, including 3-body reactions (with GFT).

what's next?

- Improve microscopic inputs.
- Disentangle direct, pre-equilibrium, and compound reactions.
- Explore the limits of validity of the statistical model.
- Symmetry-breaking systems (deformation, pairing).
- R-Matrix parametrization of indirect reactions.

Collaborators:

- J. Escher, K. Kravvaris,
- E. Vigezzi (INFN, Milano)
- F. Barranco (University of Seville)
- G. Sargsyan, F. Nunes (MSU)
- C. Hebborn (CNRS, Paris)

**$^{95}$Mo:** A. Ratkiewicz, J. Escher, J. Burke, R. Casperson, R. Hughes, N. Scielzo (LLNL), J. Cizewski, S. Burcher, B. Manning, S. Rice, C. Shand (Rutgers), M. McCleskey (TAMU), R. Austin (St Mary's), S. Pain (ORNL), W. Peters (U of Tennessee), T. Ross (U of Richmond) and K. Smith (LANL).

# Thank you!

UNIVERSIDAD D SEVILLA
1505

# BACKUP SLIDES

# It works for $^{11}$Be, too!

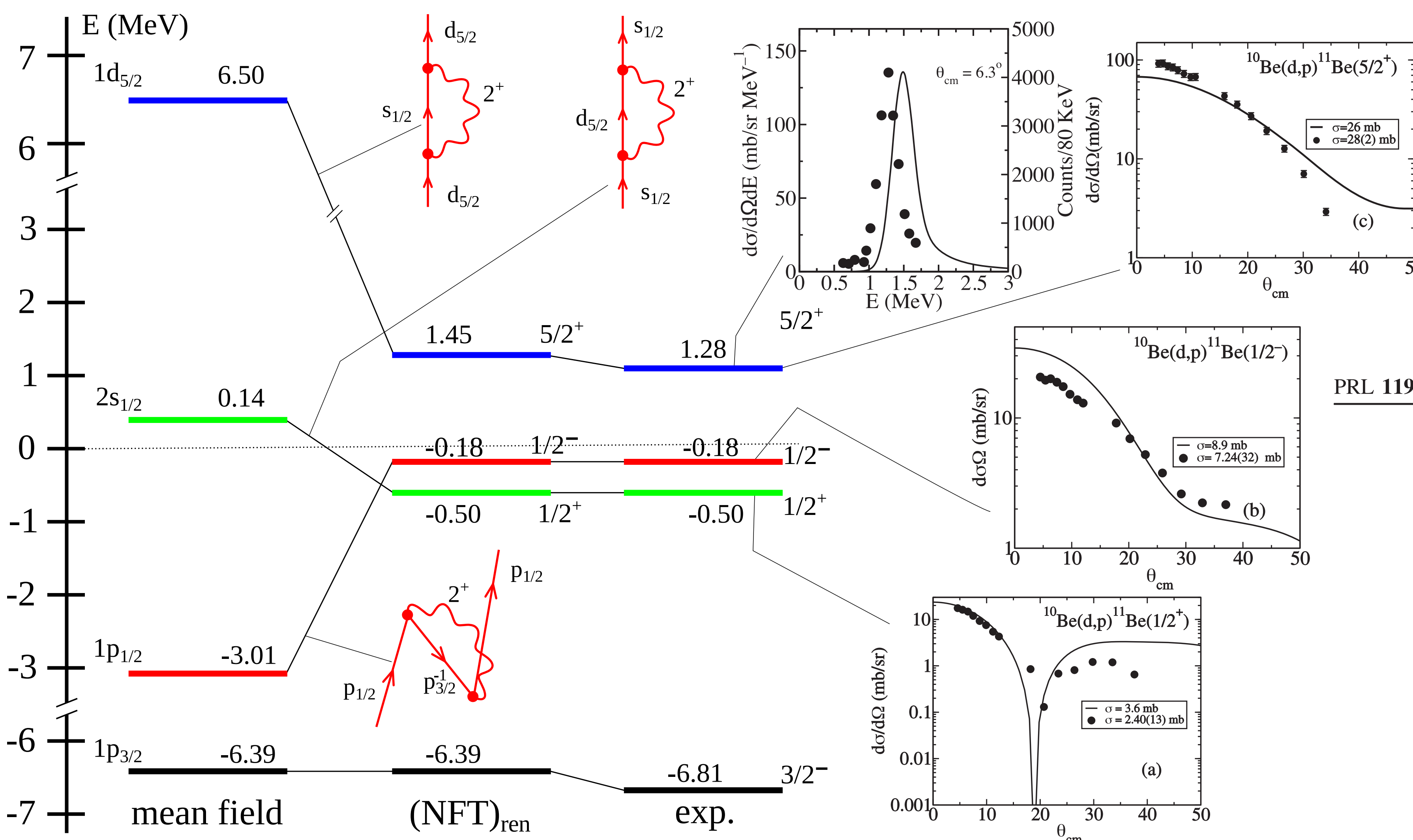


Barranco, GP, Broglia, Vigezzi PRL **119**, 082501 (2017)

PRL **119,** 082501 (2017) PHYSICAL REVIEW LETTERS week ending 25 AUGUST 2017

**Structure and Reactions of $^{11}$Be: Many-Body Basis for Single-Neutron Halo**

F. Barranco,[1] G. Potel,[2] R. A. Broglia,[3,4] and E. Vigezzi[5]

[1]*Departamento de Fisica Aplicada III, Escuela Superior de Ingenieros, Universidad de Sevilla, Camino de los Descubrimientos, 41092 Sevilla, Spain*
[2]*National Superconducting Cyclotron Laboratory, Michigan State University, East Lansing, Michigan 48824, USA*
[3]*The Niels Bohr Institute, University of Copenhagen, DK-2100 Copenhagen, Denmark*
[4]*Dipartimento di Fisica, Università degli Studi Milano, Via Celoria 16, I-20133 Milano, Italy*
[5]*INFN Sezione di Milano, Via Celoria 16, I-20133 Milano, Italy*

# Part 5

## Teaser: connections with R-Matrix and Hauser-Feshbach

# The GFT formalism suggests an *R*-matrix parametrization for the indirect cross section

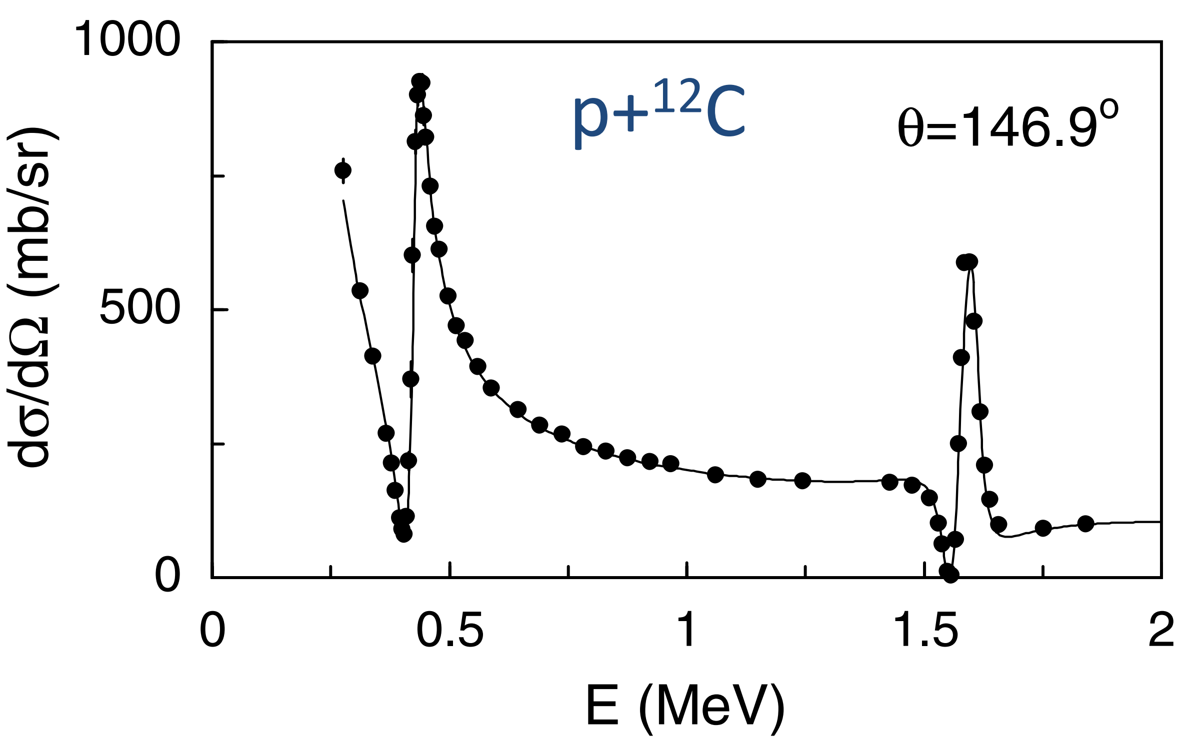

# The GFT formalism suggests an *R*-matrix parametrization for the indirect cross section

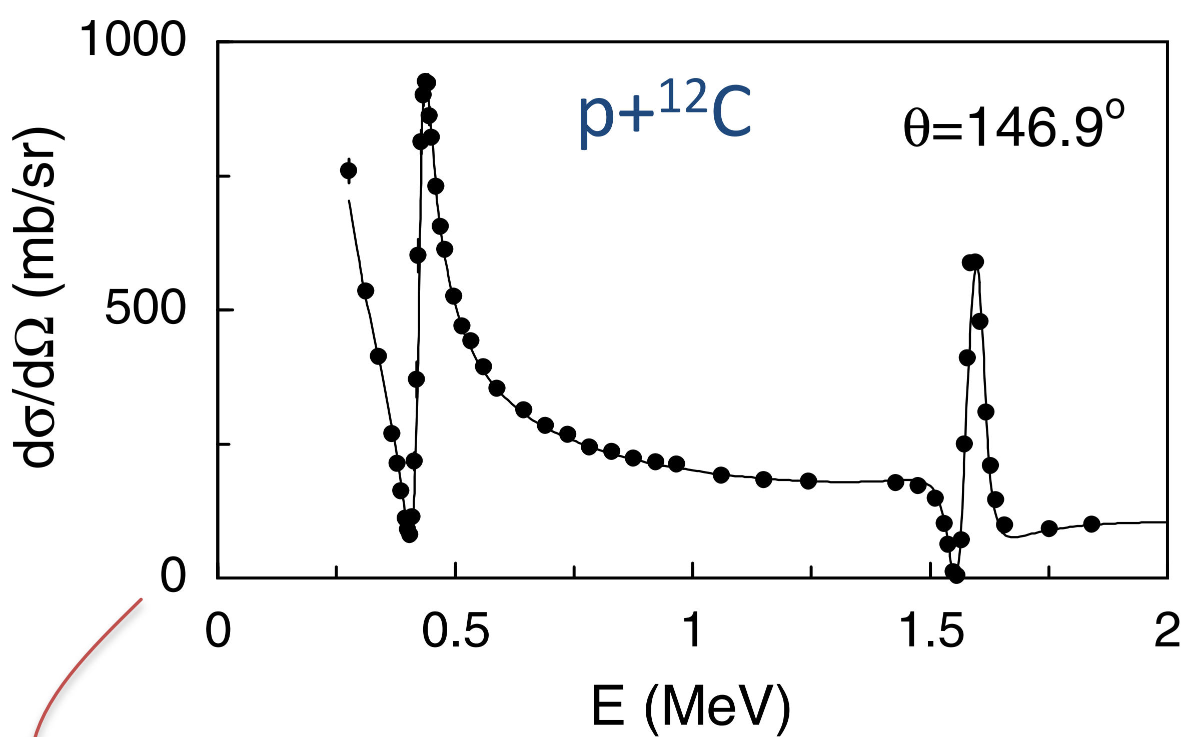


$$T_{i0}(E) = \sqrt{P_i(E)P_0(E)} \sum_{pq} \frac{\gamma_{ip}\gamma_{0q}}{(E_p - E)\delta_{pq} - \sum_c \gamma_{ic}\gamma_{jc}(S_c(E) + iP_c(E))}$$

T-matrix partial widths and energy parameters fitted from data

# The GFT formalism suggests an *R*-matrix parametrization for the indirect cross section

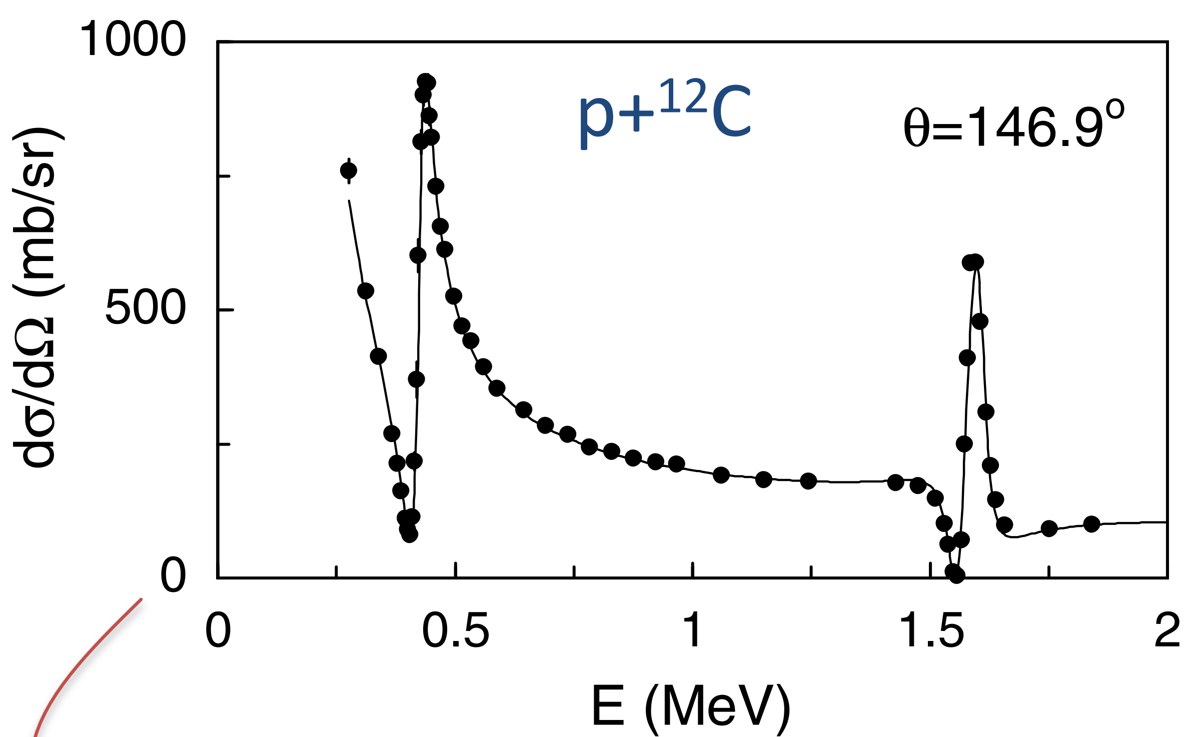


$$\frac{d\sigma(E)}{d\sigma} \propto |T_{i0}(E)|^2$$

$$T_{i0}(E) = \sqrt{P_i(E)P_0(E)} \sum_{pq} \frac{\gamma_{ip}\gamma_{0q}}{(E_p - E)\delta_{pq} - \sum_c \gamma_{ic}\gamma_{jc}(S_c(E) + iP_c(E))}$$

T-matrix partial widths and energy parameters fitted from data

# The GFT formalism suggests an *R*-matrix parametrization for the indirect cross section

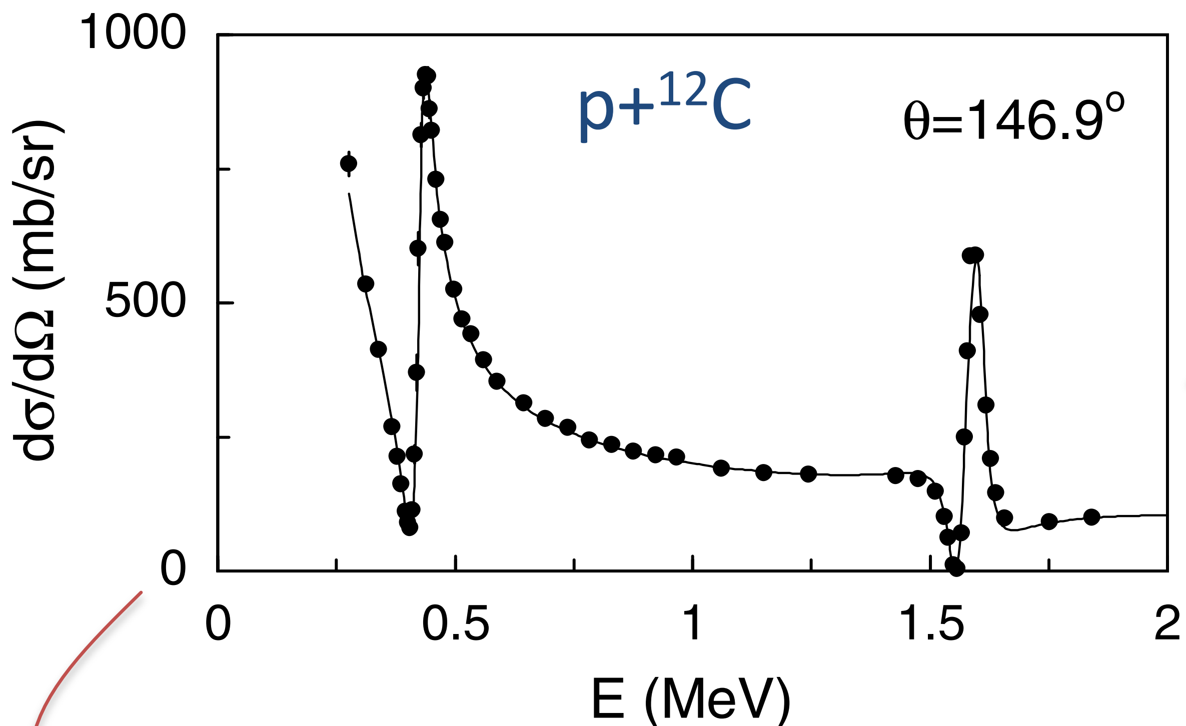


Rep. Prog. Phys. **73** (2010) 036301 (44pp)

**The *R*-matrix theory**

P Descouvemont[1] and D Baye[1,2]

$$\frac{d\sigma(E)}{d\sigma} \propto |T_{i0}(E)|^2$$

$$T_{i0}(E) = \sqrt{P_i(E)P_0(E)} \sum_{pq} \frac{\gamma_{ip}\gamma_{0q}}{(E_p - E)\delta_{pq} - \sum_c \gamma_{ic}\gamma_{jc}(S_c(E) + iP_c(E))}$$

T-matrix partial widths and energy parameters fitted from data

# The GFT formalism suggests an *R*-matrix parametrization for the indirect cross section

connection between direct and indirect R-matrix parameters

example:

- direct: $\alpha$ scattering ($T_{i0}(E)$)
- indirect: ($^6$Li,d). ($T^I_{i0}(E)$)

# The GFT formalism suggests an *R*-matrix parametrization for the indirect cross section

connection between direct and indirect R-matrix parameters

example:

- direct: α scattering ($T_{i0}(E)$)
- indirect: ($^6$Li,d). ($T^I_{i0}(E)$)

indirect T-matrix

$$T^I_{i0}(E) = \int T_{i0}(E_k)\, g(\mathbf{k}; E)\, d\mathbf{k}.$$

direct T-matrix

# The GFT formalism suggests an *R*-matrix parametrization for the indirect cross section

connection between direct and indirect R-matrix parameters

example:

- direct: α scattering ($T_{i0}(E)$)
- indirect: ($^6$Li,d). ($T^I_{i0}(E)$)

indirect T-matrix

$$E_k = \frac{\hbar^2 k^2}{2\mu}$$

$$T^I_{i0}(E) = \int T_{i0}(E_k)\, g(\mathbf{k}; E)\, d\mathbf{k}.$$

direct T-matrix

# The GFT formalism suggests an *R*-matrix parametrization for the indirect cross section

connection between direct and indirect R-matrix parameters

example:

- direct: α scattering ($T_{i0}(E)$)
- indirect: ($^6$Li,d). ($T^I_{i0}(E)$)

indirect T-matrix

$$T^I_{i0}(E) = \int T_{i0}(E_k)\, g(\mathbf{k}; E)\, d\mathbf{k}.$$

direct T-matrix

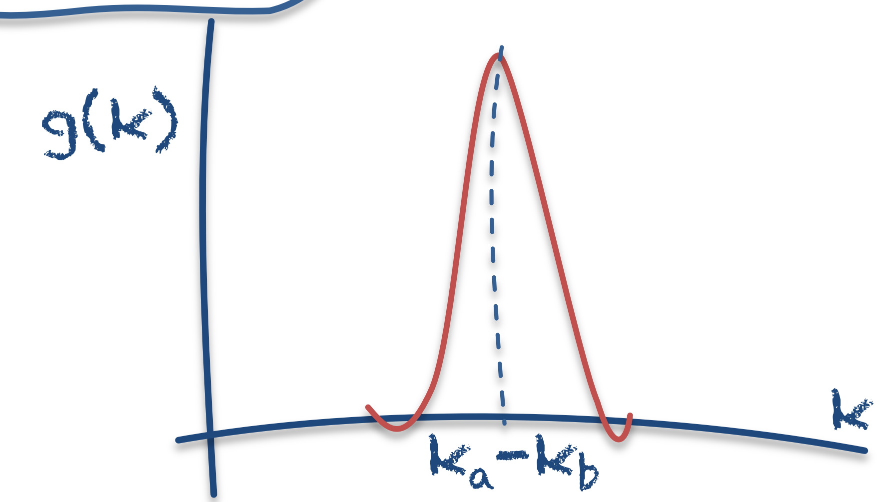


broadening factor

$$g(\mathbf{k}; E) = \int \psi^{HM}(\mathbf{r}_{xA}; E)\, F^*(\mathbf{r}_{xA}, \mathbf{k})\, d\mathbf{r}_{xA}$$

# The GFT formalism suggests an *R*-matrix parametrization for the indirect cross section

connection between direct and indirect R-matrix parameters

example:

- direct: α scattering
- indirect: ($^6$Li,d)

indirect T-matrix

$$T^I_{i0} = \int \sqrt{P_i(E_k)P_0(E_k)} \sum_{pq} \frac{\gamma_{ip}\gamma_{0q}}{(E_p - E_k)\delta_{pq} - \sum_c \gamma_{ic}\gamma_{jc}(S_c(E_k) + iP_c(E_k))} g(\mathbf{k})\, d\mathbf{k}.$$

$$E_k = \frac{\hbar^2 k^2}{2\mu}$$

broadening factor

$$g(\mathbf{k}) = \int \psi^{HM}(\mathbf{r}_{xA})\, F^*(\mathbf{r}_{xA}, \mathbf{k})\, d\mathbf{r}_{xA}$$

# The GFT formalism suggests an *R*-matrix parametrization for the indirect cross section

connection between direct and indirect R-matrix parameters

example:

- direct: α scattering
- indirect: ($^6$Li,d)

indirect T-matrix

$$T^I_{i0} = \int \sqrt{P_i(E_k) P_0(E_k)} \sum_{pq} \frac{\gamma_{ip}\gamma_{0q}}{(E_p - E_k)\delta_{pq} - \sum_c \gamma_{ic}\gamma_{jc}(S_c(E_k) + iP_c(E_k))} \, g(\mathbf{k}) \, d\mathbf{k}.$$

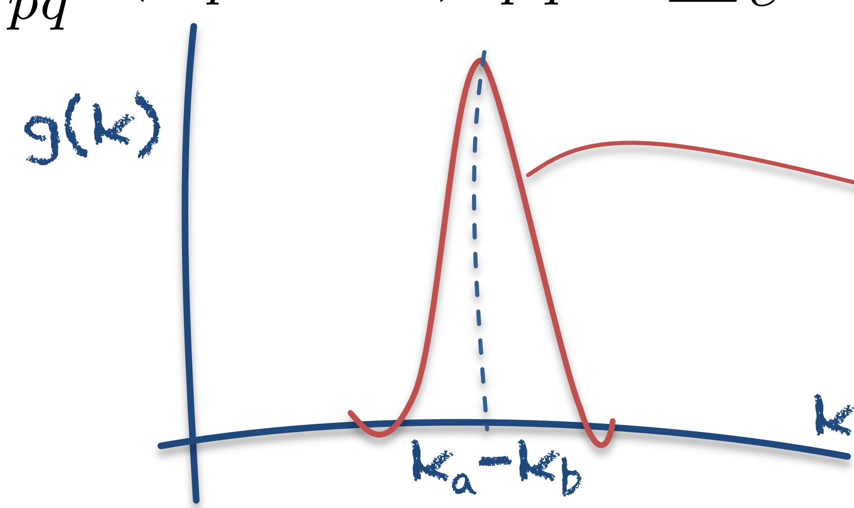


$$g(\mathbf{k}) = \int \psi^{HM}(\mathbf{r}_{xA}) \, F^*(\mathbf{r}_{xA}, \mathbf{k}) \, d\mathbf{r}_{xA}$$

## The GFT formalism suggests an *R*-matrix parametrization for the indirect cross section

- If the broadening distribution is narrow, the T-matrix can be evaluated at the peak
- This is essentially the approximation made by Barker in *Aust. J. Phys*. **20** (341) 1967 for isolated resonances

$$T_{i0}^{I} = \int \sqrt{P_i(E_k)P_0(E_k)} \sum_{pq} \frac{\gamma_{ip}\gamma_{0q}}{(E_p - E_k)\delta_{pq} - \sum_c \gamma_{ic}\gamma_{jc}(S_c(E_k) + iP_c(E_k))} g(\mathbf{k})\, d\mathbf{k}.$$

$$\Downarrow$$

$$T_{i0}^{I} \approx \sqrt{P_i(E_k^{max})P_0(E_k^{max})} \sum_{pq} \frac{\gamma_{ip}\gamma_{0q}}{(E_p - E_k^{max})\delta_{pq} - \sum_c \gamma_{ic}\gamma_{jc}(S_c(E_k^{max}) + iP_c(E_k^{max}))} \int g(\mathbf{k})\, d\mathbf{k}.$$

# $^{40}$Ca OP calculated in a weak coupling, collective model approximation

$$V(\mathbf{r},\mathbf{r}';E) = U_0(r) + \sum_i U_{0i}(\mathbf{r}) G(E - E_i, \mathbf{r}, \mathbf{r}') U_{i0}(\mathbf{r}')$$

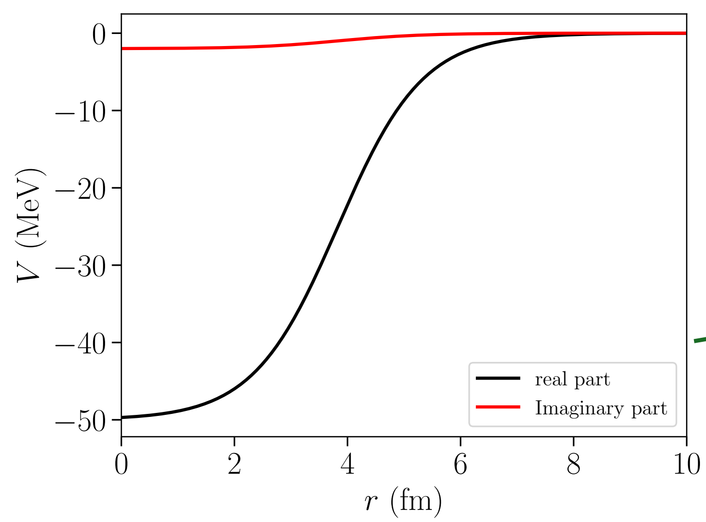


- the static potential is a simple Woods-Saxon
- a small imaginary part *W* is included to account for the lack of absorption of the model
- this is a consequence of the over-simplification of the spectrum
- The small imaginary part spoils dispersivity

From Rao, Reeves, and Satchler, NPA **207** (1973) 182

# $^{40}$Ca OP calculated in a weak coupling, collective model approximation

$$V(\mathbf{r},\mathbf{r}';E) = U_0(r) + \sum_i U_{0i}(\mathbf{r})G(E-E_i,\mathbf{r},\mathbf{r}')U_{i0}(\mathbf{r}')$$

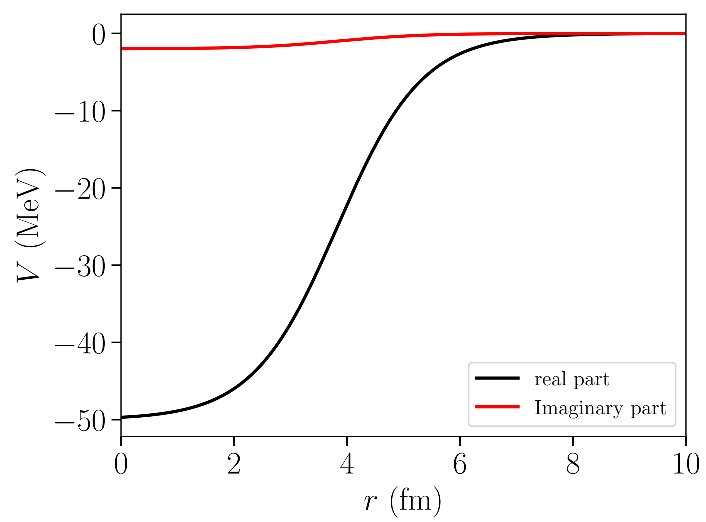


- the spectrum of $^{40}$Ca is approximated by 6 collective vibrational states
- the deformation parameters $\beta_\lambda$ are constrained by the experimental inelastic scattering cross section

$$\left|\Phi(^{41}\mathrm{Ca})\right\rangle_i \approx \left|\Phi(^{40}\mathrm{Ca})\right\rangle_i \otimes \left|\chi(n)\right\rangle_i$$

| $\lambda_n^\pi$ | $1^-$ | $2^+$ | $2^+$ | $3^-$ | $4^+$ | $5^-$ |
|---|---|---|---|---|---|---|
| $E_n$ (MeV) | 18.0 | 3.9 | 8.0 | 3.73 | 8.0 | 4.48 |
| $\beta_\lambda(n)$ | 0.087 | 0.143 | 0.309 | 0.354 | 0.254 | 0.192 |
| $\sigma_A$ (mb) | 17 | 43 | 176 | 164 | 78 | 37 |

From Rao, Reeves, and Satchler, NPA **207** (1973) 182

# $^{40}$Ca OP calculated in a weak coupling, collective model approximation

$$V(\mathbf{r},\mathbf{r}';E) = U_0(r) + \sum_i U_{0i}(\mathbf{r})G(E-E_i,\mathbf{r},\mathbf{r}')U_{i0}(\mathbf{r}')$$

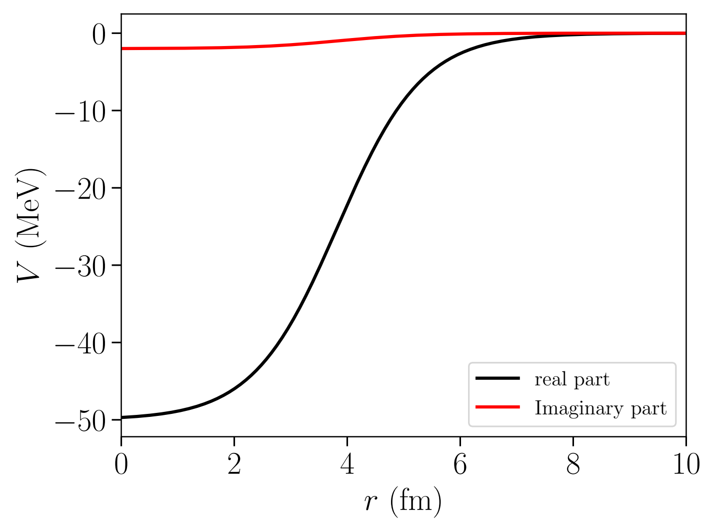


- the couplings are surface peaked
- by construction, the experimental contribution of each vibrational state to the absorption cross section is reproduced

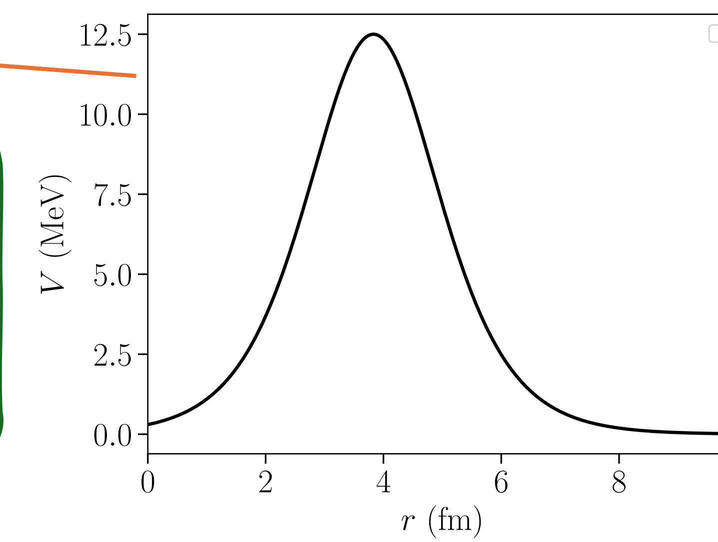


$$U_{0i}(\mathbf{r}) \sim \beta_i \frac{dU(r)}{dr} Y^{\lambda_i}(\hat{r})$$

| $\lambda_n^\pi$ | $1^-$ | $2^+$ | $2^+$ | $3^-$ | $4^+$ | $5^-$ |
|---|---|---|---|---|---|---|
| $E_n$ (MeV) | 18.0 | 3.9 | 8.0 | 3.73 | 8.0 | 4.48 |
| $\beta_\lambda(n)$ | 0.087 | 0.143 | 0.309 | 0.354 | 0.254 | 0.192 |
| $\sigma_A$ (mb) | 17 | 43 | 176 | 164 | 78 | 37 |

From Rao, Reeves, and Satchler, NPA **207** (1973) 182

# We benchmark our results against Rao *et al.*, and look at the effect of iterations

p+$^{40}$Ca elastic scattering at 30.3 MeV

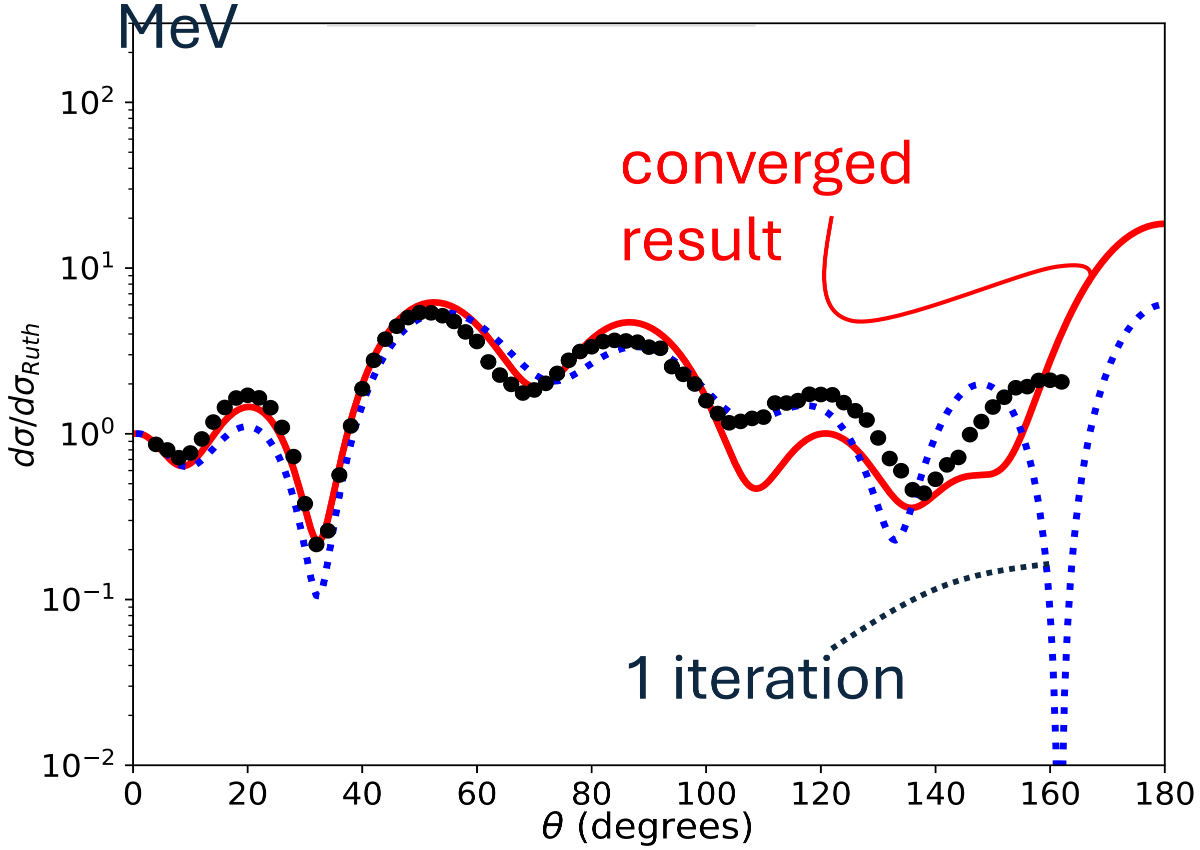


n+$^{40}$Ca elastic scattering at 30.3 MeV

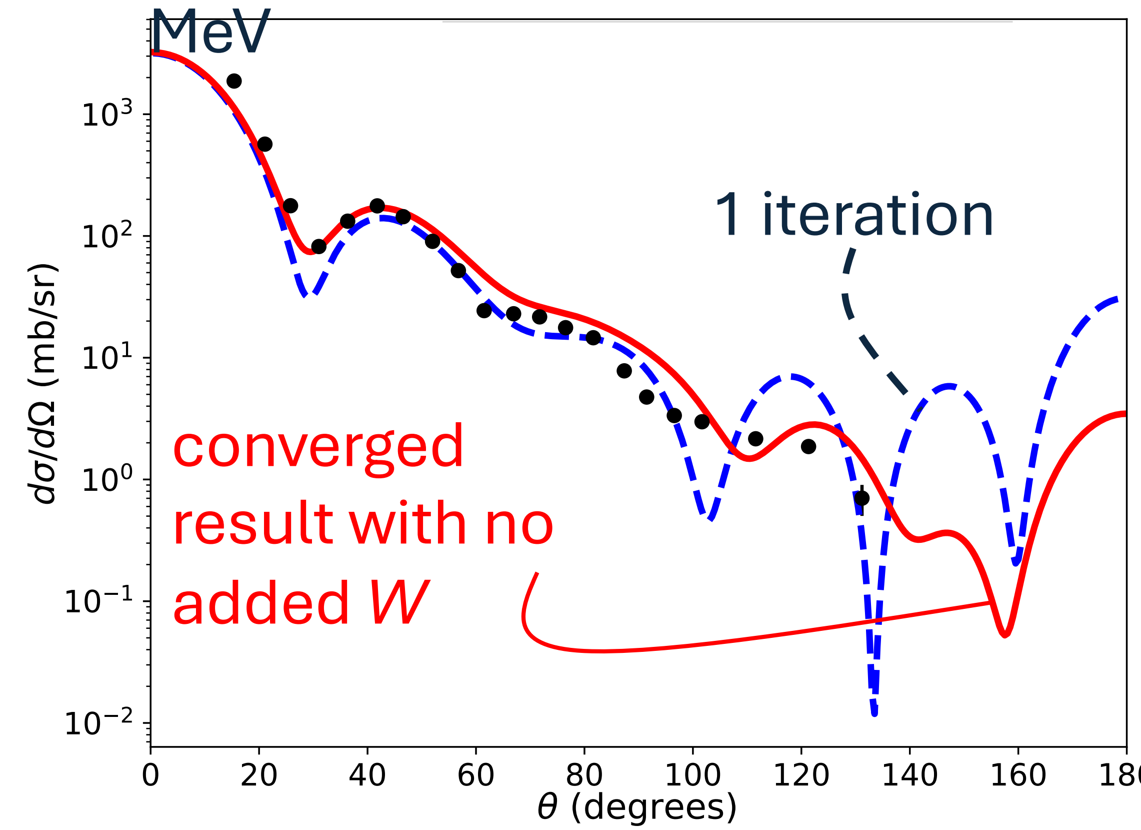


- 1 iteration calculation agrees with Rao et al. (not shown)
- Converged result different at large angles

- Good result for neutrons just by removing Coulomb
- Added non-dispersive imaginary part W not needed for the converged result

# *ab initio* methods applied to reactions (NCSMC)

PHYSICAL REVIEW LETTERS **129,** 042503 (2022)

***Ab Initio*** **Prediction of the $^4$He$(d,\gamma)^6$Li Big Bang Radiative Capture**

C. Hebborn,[1,2,*] G. Hupin,[3] K. Kravvaris,[2] S. Quaglioni,[2] P. Navrátil,[4] and P. Gysbers[4,5]
[1]*Facility for Rare Isotope Beams, East Lansing, Michigan 48824, USA*
[2]*Lawrence Livermore National Laboratory, P.O. Box 808, L-414, Livermore, California 94551, USA*
[3]*Université Paris-Saclay, CNRS/IN2P3, IJCLab, 91405 Orsay, France*
[4]*TRIUMF, 4004 Wesbrook Mall, Vancouver British Columbia V6T 2A3, Canada*
[5]*Department of Physics and Astronomy, University of British Columbia, Vancouver, British Columbia V6T 1Z1, Canada*

$$|\Psi^{J^\pi T}\rangle = \sum_\lambda c_\lambda^{J^\pi T}|A\lambda J^\pi T\rangle + \sum_\nu \int_0^{+\infty} dr\, r^2 \frac{\gamma_\nu^{J^\pi T}(r)}{r}\hat{\mathcal{A}}_\nu|\Phi_{\nu r}^{J^\pi T}\rangle$$

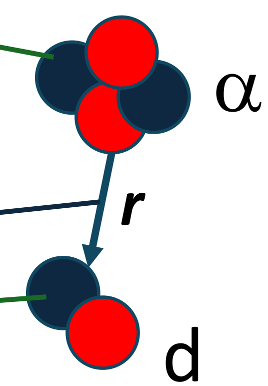


continuum scattering wf

clusters in NCSM

NCSMC wf used in T-matrix

$$\sigma(E) = \frac{64\pi^4}{4\pi\epsilon_0\hbar v}\sum_{\kappa\lambda}\frac{k_\gamma^{2\lambda+1}}{[(2\lambda+1)!!]^2}\frac{\lambda+1}{\lambda} \times \sum_{J_i l_i s_i}\frac{\hat{J}_f^2}{\hat{s}_P^2\hat{s}_T^2\hat{l}_i^2}|\langle\Psi^{J_f^{\pi_f}T_f}||\mathcal{M}^{\kappa\lambda}||\Psi_{l_i s_i}^{J_i^{\pi_i}T_i}\rangle|^2$$

electromagnetic operator

T-matrix

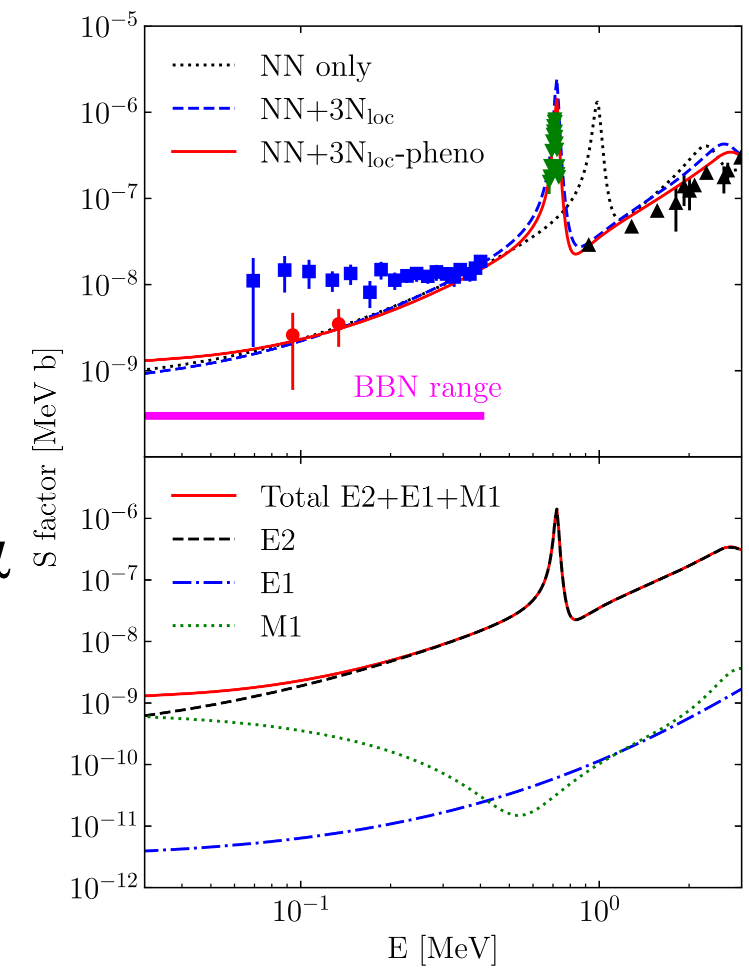


- solution of 6-body Hamiltonian with chiral NN interaction
- No Core Shell Model with Continuum (NCSMC) combines NCSM with scattering wf
- only possible for very light nuclei

# Nuclear reactions of astrophysical interest (light elements)

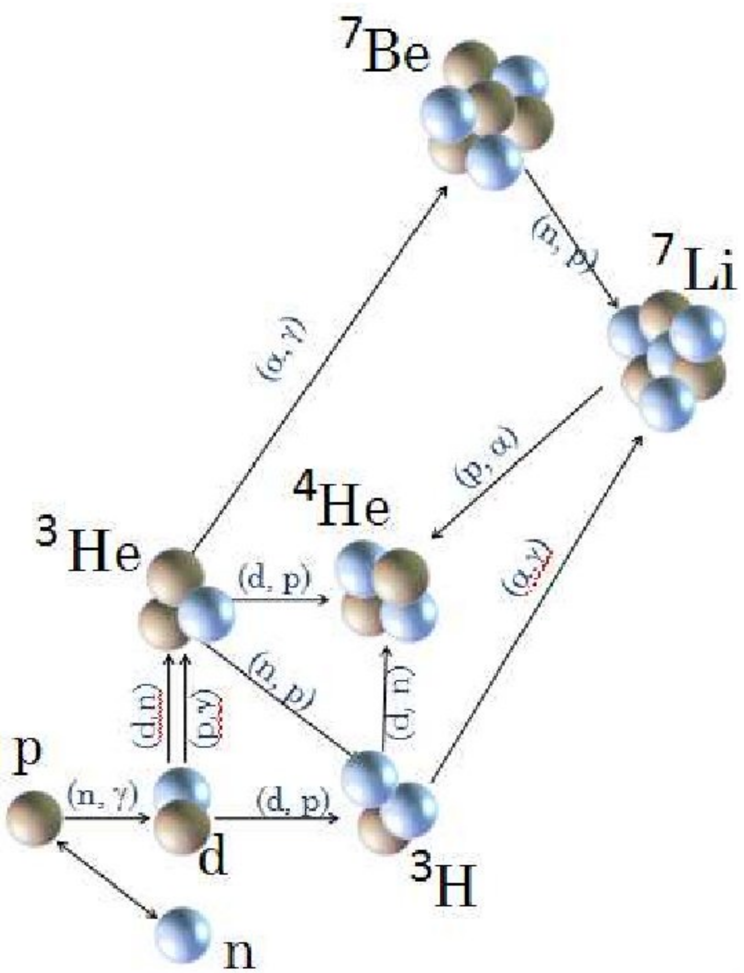


Big Bang nucleosynthesis

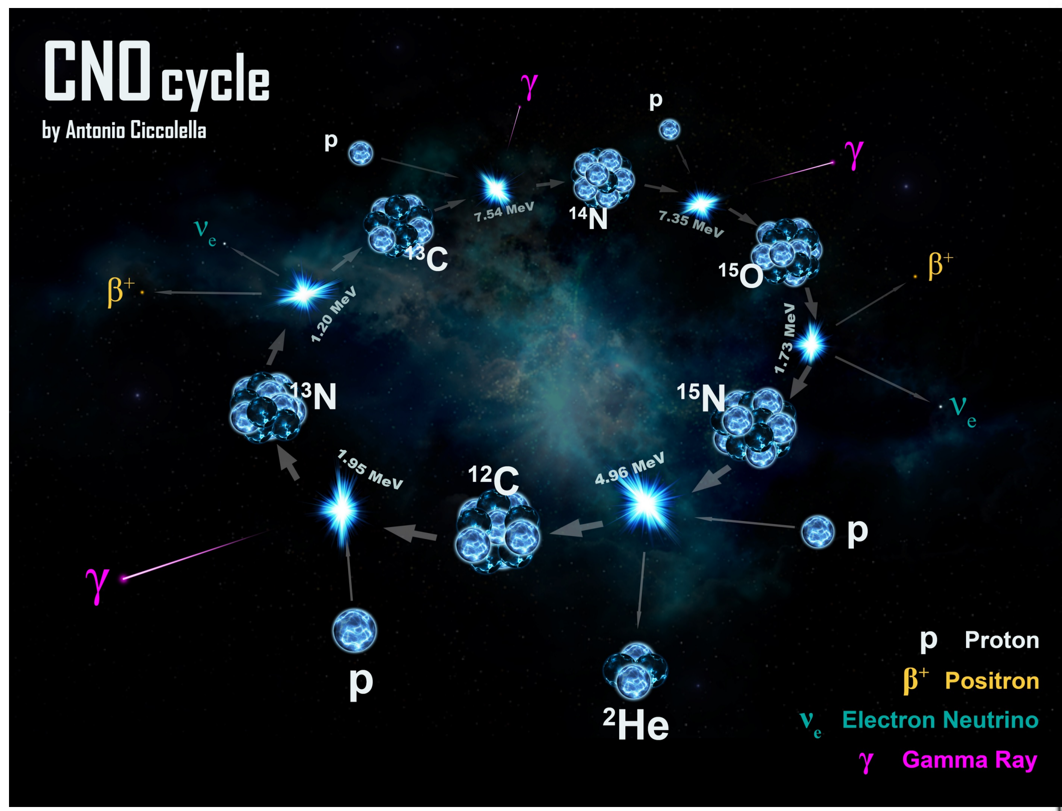


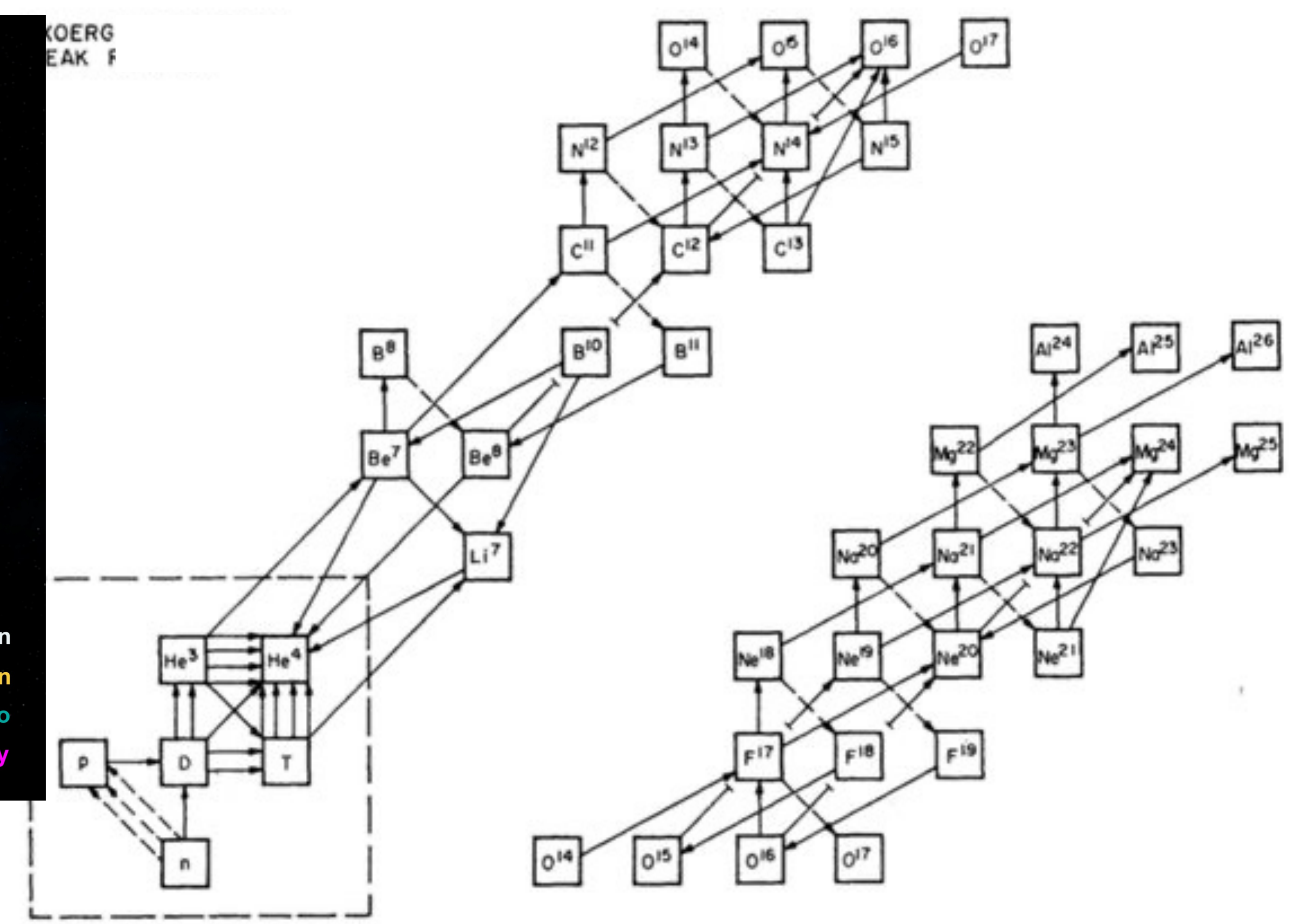

reaction networks

# Nuclear reactions of astrophysical interest (heavy elements)

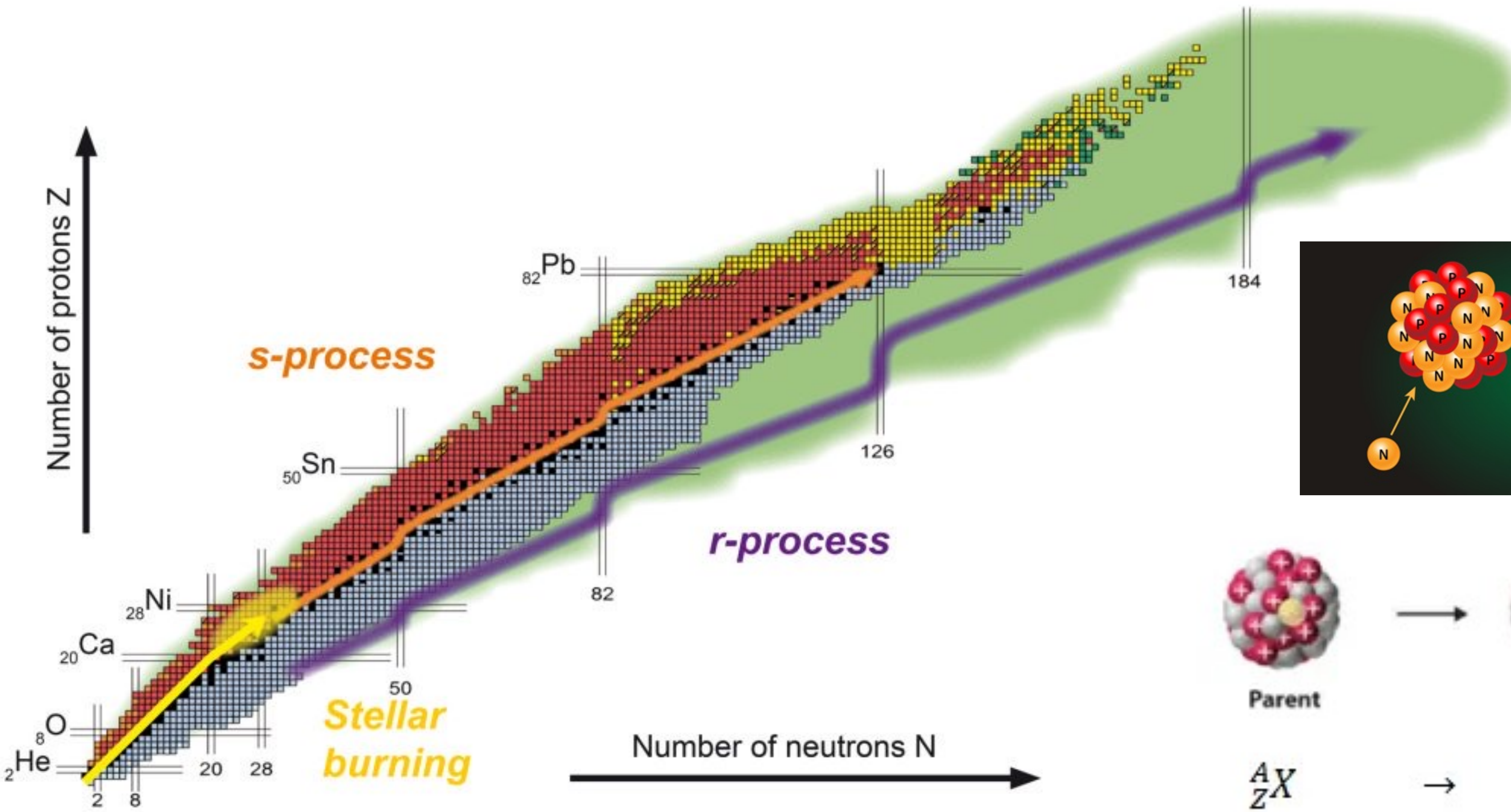


neutron capture

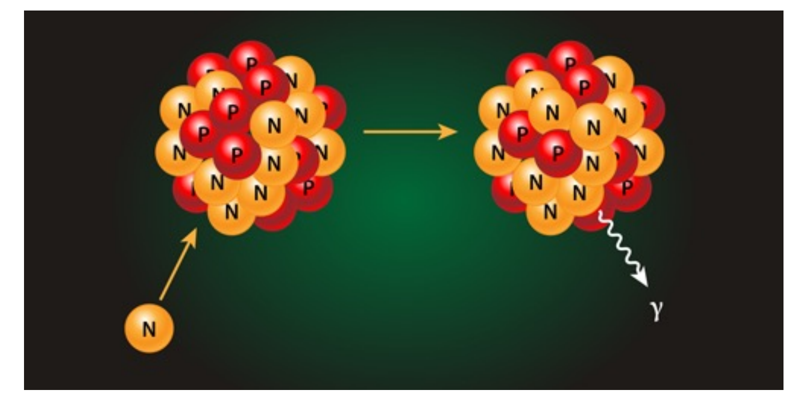


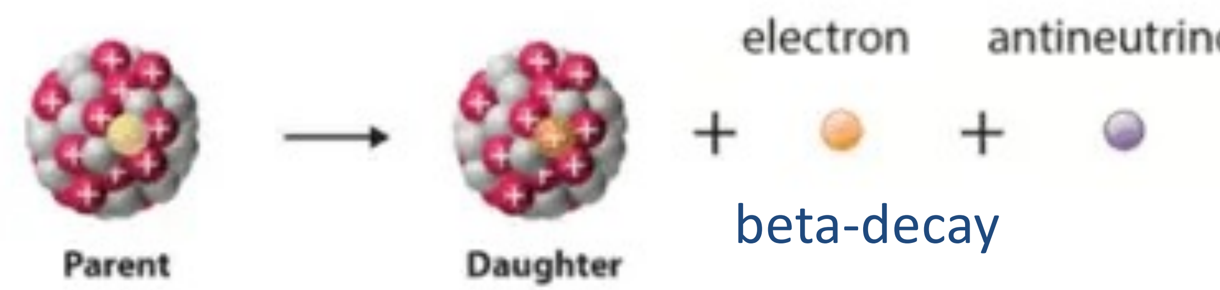


beta-decay

$$ {}^{A}_{Z}X \rightarrow {}_{Z+1}^{A}Y + \beta^{-} + \bar{\nu_e} $$

# Both elastic and absorption cross sections can be calculated from the OP

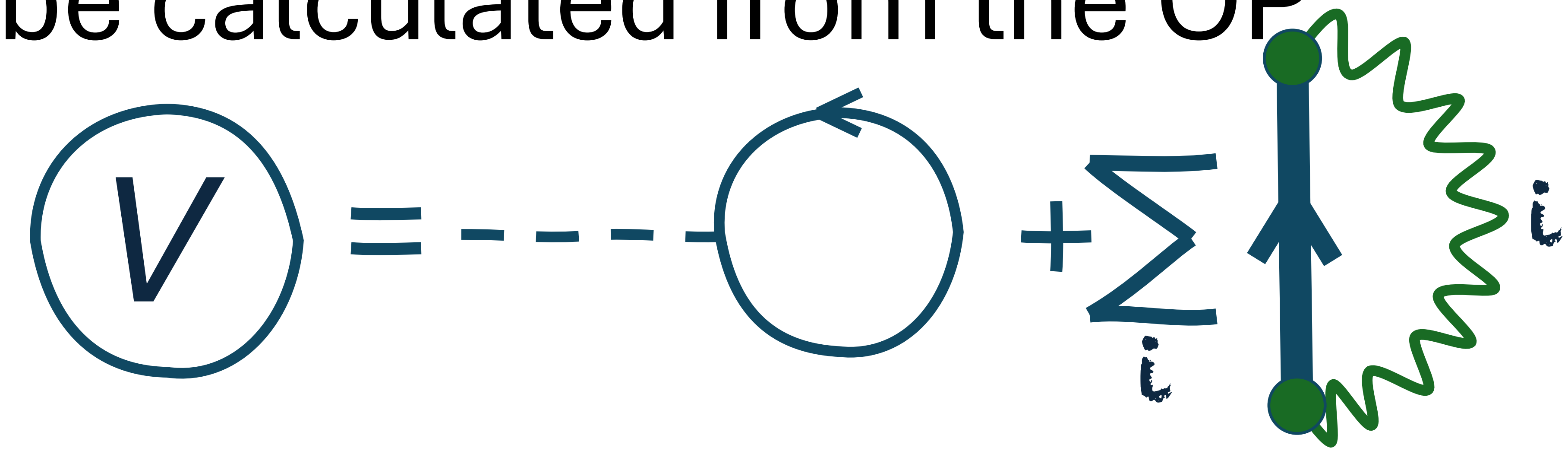


$$\left(E - T - V(\mathbf{r}, \mathbf{r}'; E)\right)\phi = 0$$

elastic scattering from phase shifts

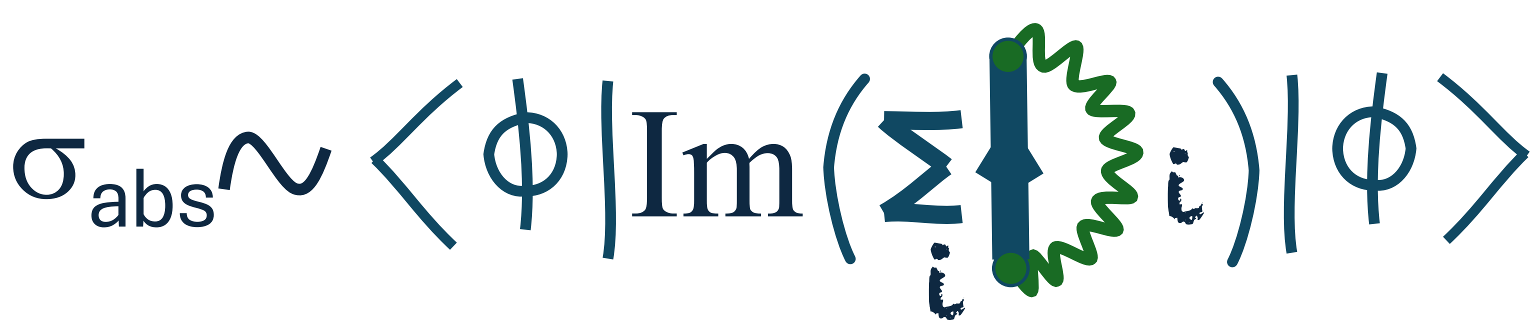


absorption from imaginary part of polarization potential

# 2-body scattering in a nutshell

elastic scattering between 2 nuclei x and A

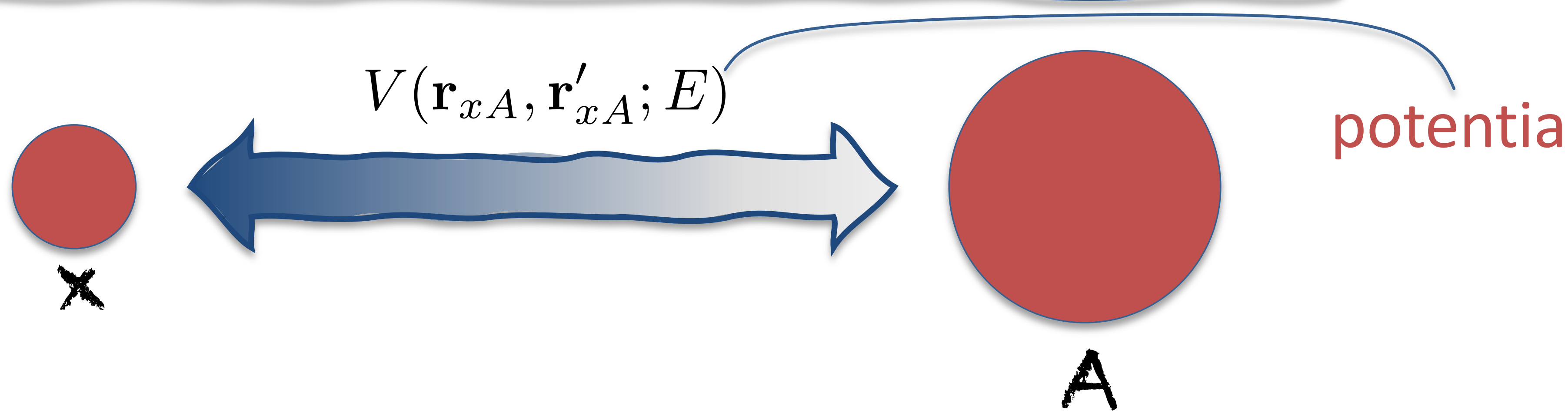

# 2-body scattering in a nutshell

elastic scattering between 2 nuclei x and A

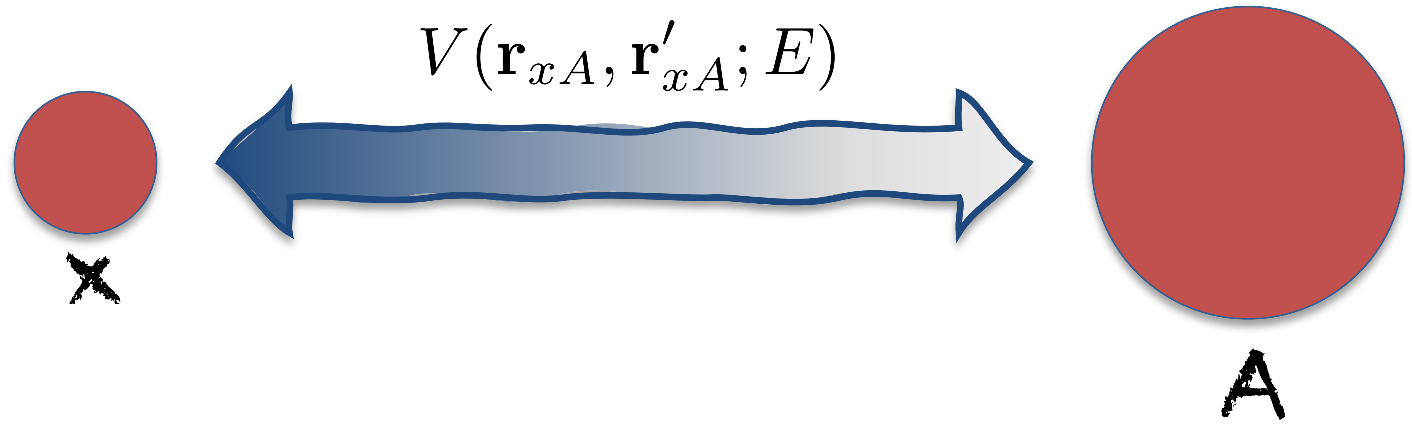


$$\psi_0(r_{xA}, E) = e^{i\mathbf{k}\mathbf{r}_{xA}} + G(E)\,V(E)\,e^{i\mathbf{k}\mathbf{r}_{xA}}$$

Lippmann-Schwinger equation

# 2-body scattering in a nutshell

elastic scattering between 2 nuclei x and A

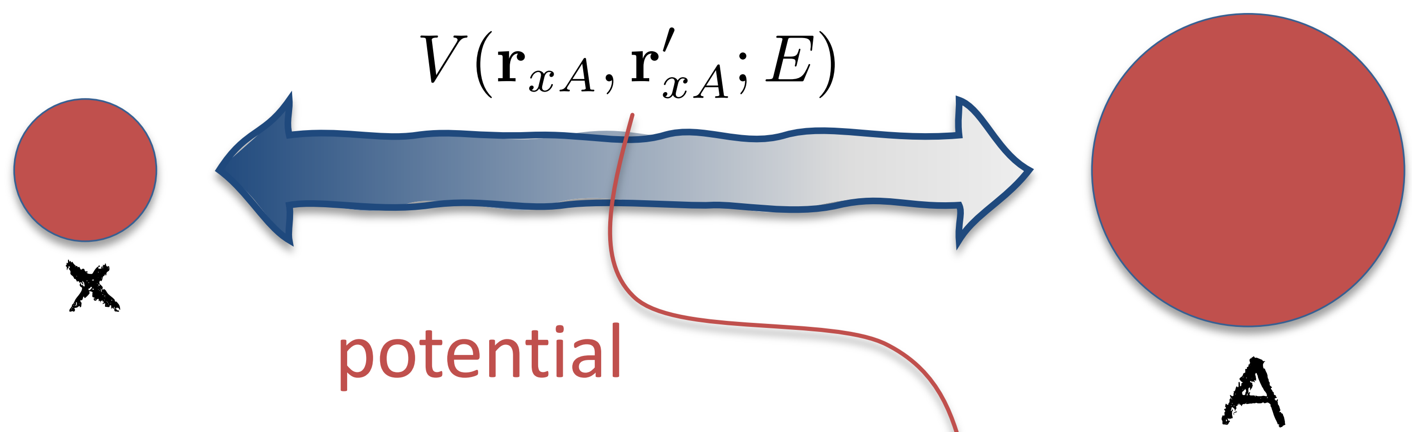


$$\psi_0(r_{xA}, E) = e^{i\mathbf{k}\mathbf{r}_{xA}} + G(E)\, V(E)\, e^{i\mathbf{k}\mathbf{r}_{xA}}$$

# 2-body scattering in a nutshell

elastic scattering between 2 nuclei x and A

$$V(\mathbf{r}_{xA}, \mathbf{r}'_{xA}; E)$$

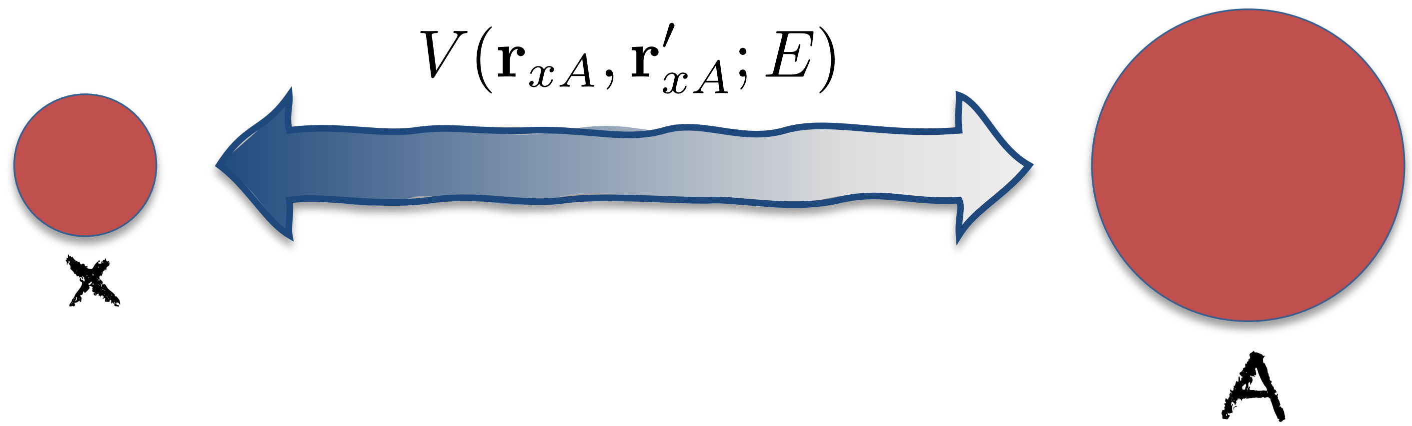


$$\psi_0(r_{xA}, E) = e^{i\mathbf{k}\mathbf{r}_{xA}} + G(E)\, V(E)\, e^{i\mathbf{k}\mathbf{r}_{xA}}$$

Green's function

$$G(E) = (E - T_x - V(E))^{-1}$$

# 2-body scattering in a nutshell

elastic scattering between 2 nuclei x and A

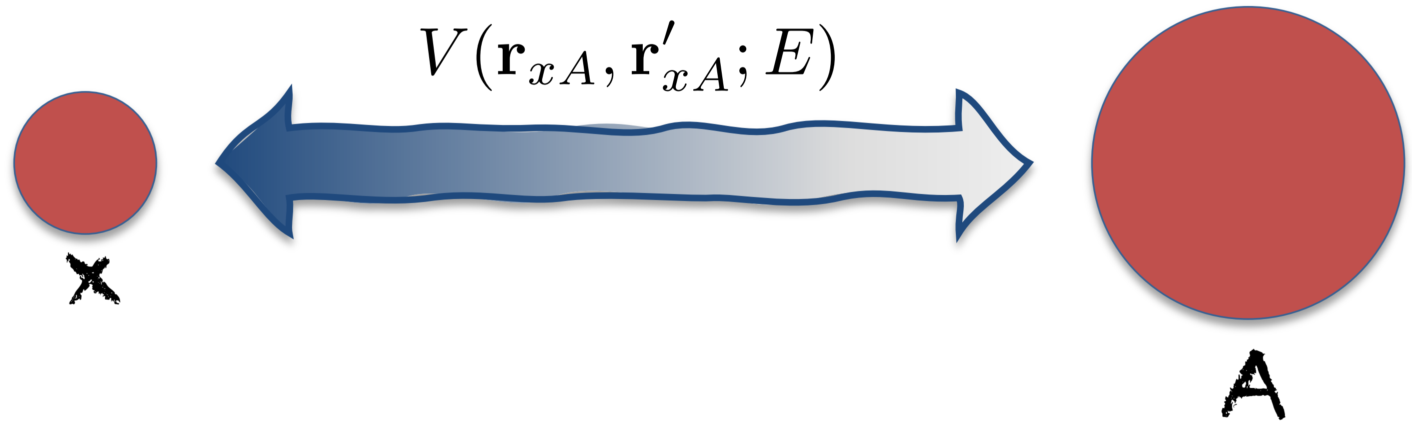


$$\psi_0(r_{xA}, E) = e^{i\mathbf{k}\mathbf{r}_{xA}} + G(E)\, V(E)\, e^{i\mathbf{k}\mathbf{r}_{xA}}$$

Green's function

$$G(E) = (E - T_x - V(E))^{-1}$$

reaction cross section

$$\sigma_R = \frac{2\mu}{\hbar k_x} \langle \psi_0 | \mathrm{Im} V | \psi_0 \rangle$$

# Part 2

Expanding the scope
to 3-body scattering: GFT

# The Green's Function Transfer (GFT) formalism

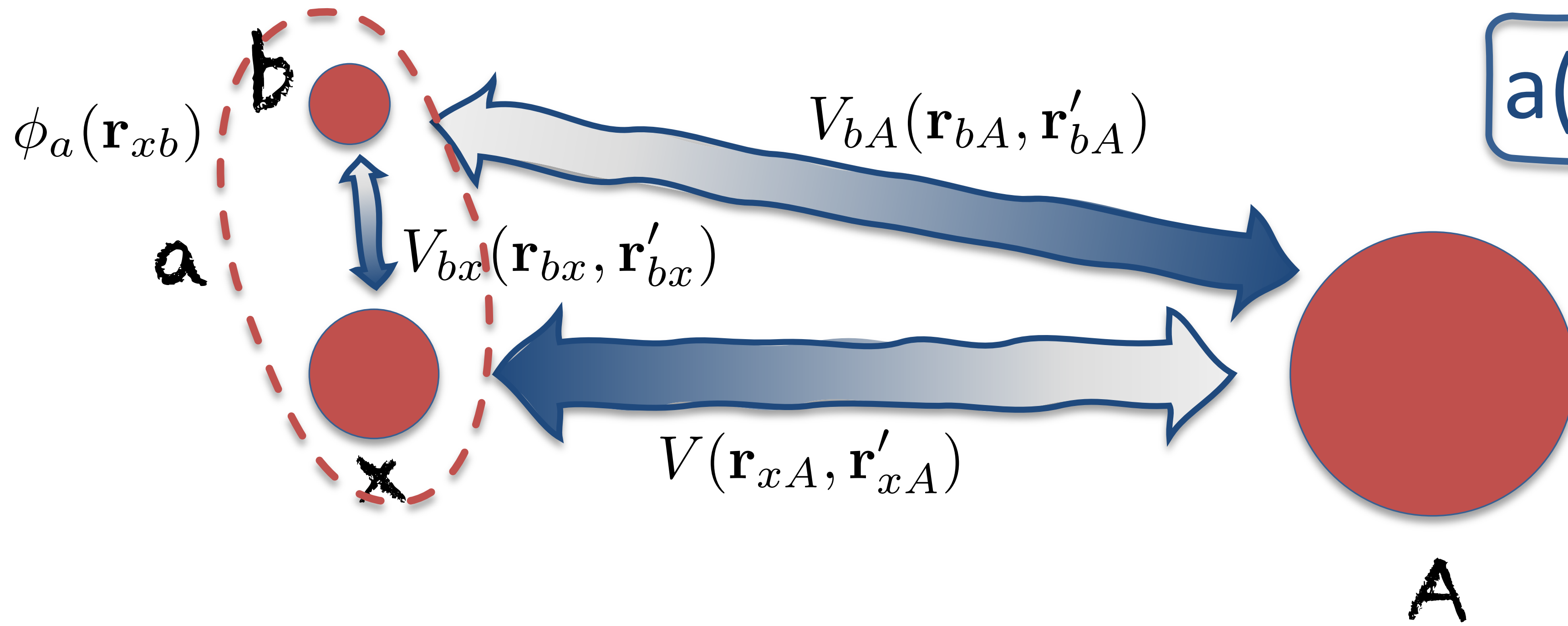


a(=b+x)+A → b+B(=A+x)

# The Green's Function Transfer (GFT) formalism

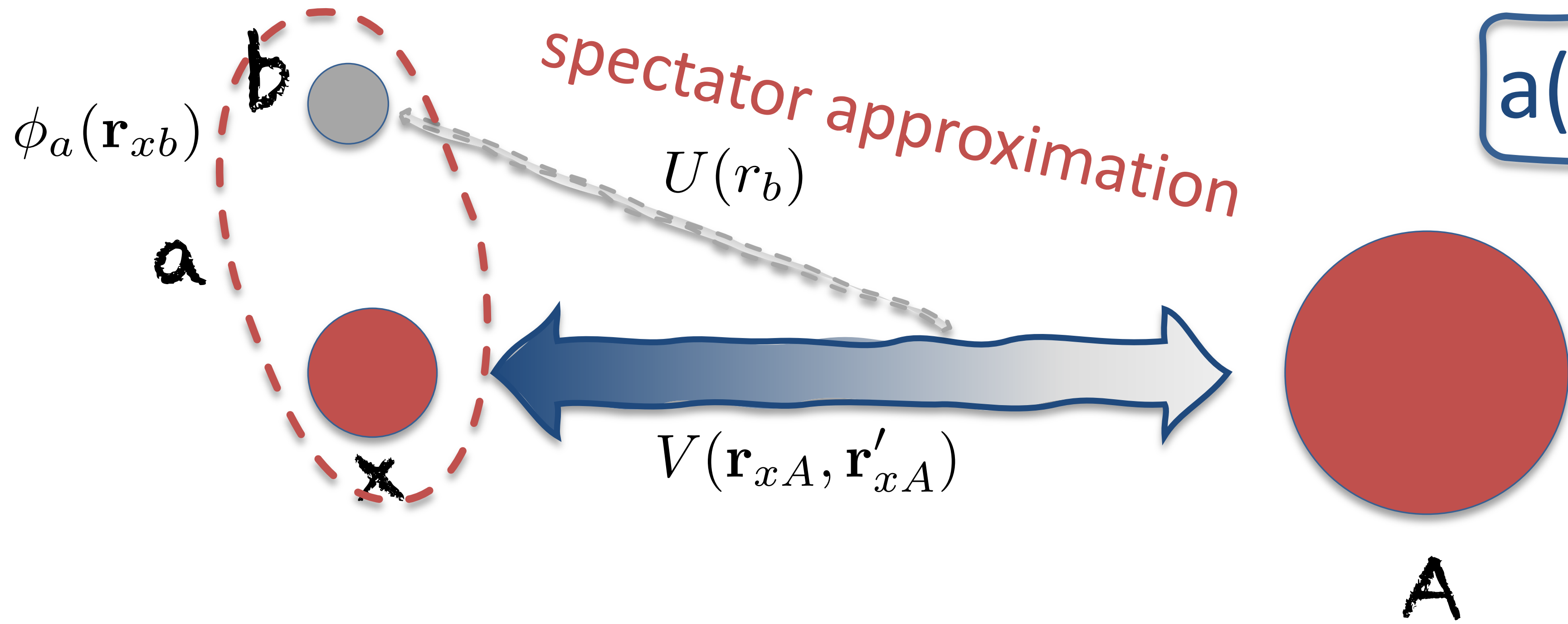


a(=b+x)+A ➡ b+B(=A+x)

# The Green's Function Transfer (GFT) formalism

a(=b+x)+A ⟶ b+B(=A+x)

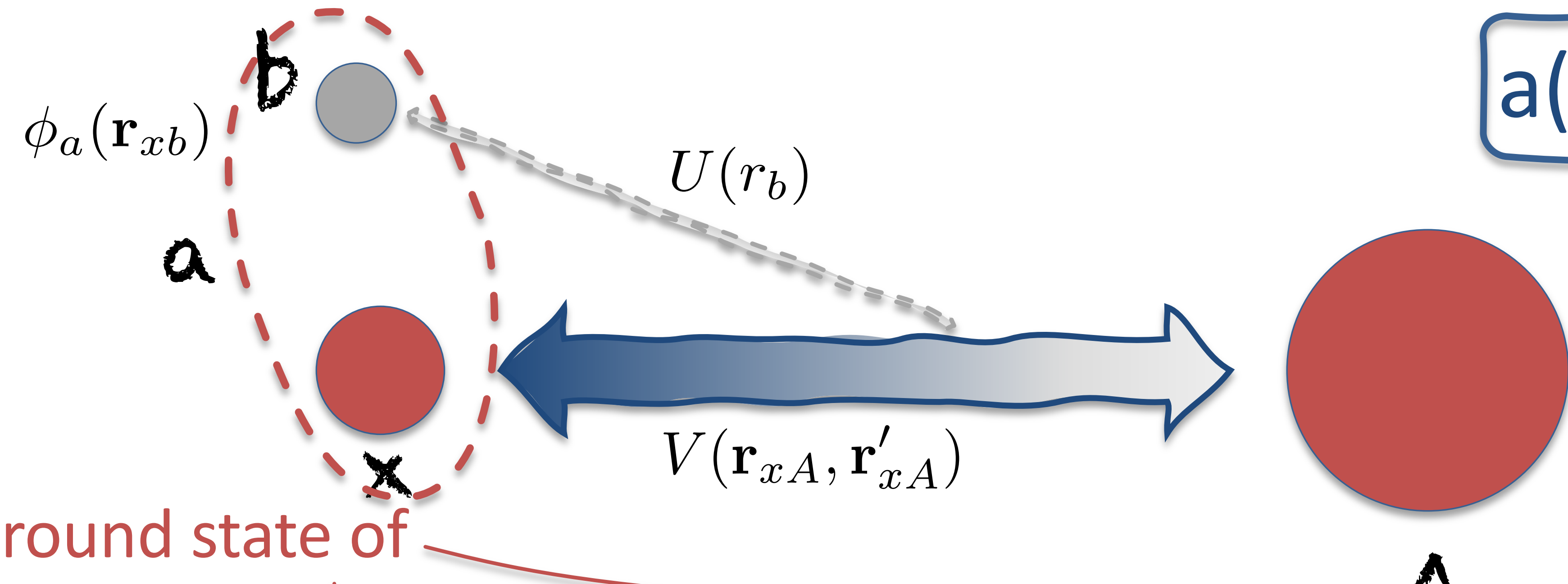


intrinsic ground state of nucleus a

$$\Psi_0(\mathbf{r}_{xA}, \mathbf{r}_b) = e^{i\mathbf{k}\mathbf{r}_a}\phi_a(\mathbf{r}_{xb}) + G(E-E_b)\mathcal{P}(\mathbf{r}_b)\left[V(E-E_b) + U_b(\mathbf{r}_b)\right]e^{i\mathbf{k}\mathbf{r}_a}\phi_a(\mathbf{r}_{xb})$$

# The Green's Function Transfer (GFT) formalism

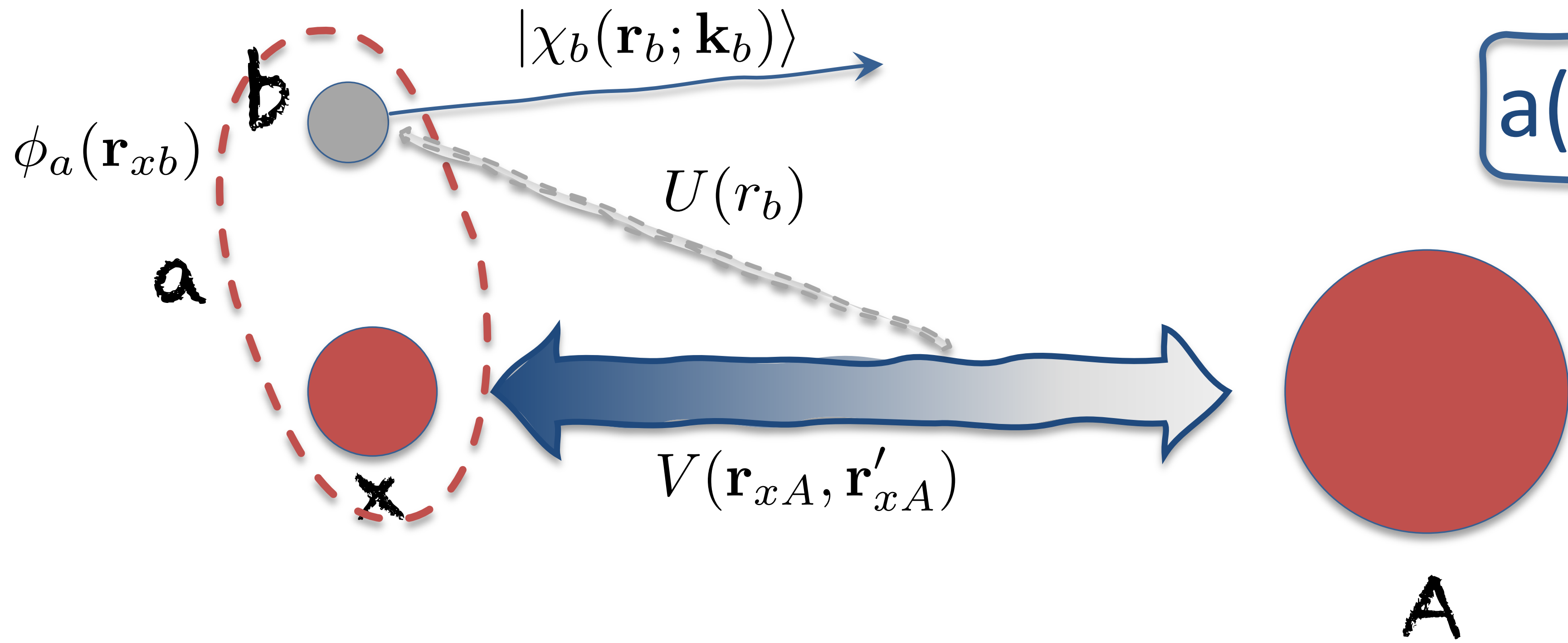


a(=b+x)+A ➡ b+B(=A+x)

$$\Psi_0(\mathbf{r}_{xA},\mathbf{r}_b) = e^{i\mathbf{k}\mathbf{r}_a}\phi_a(\mathbf{r}_{xb}) + G(E-E_b)\mathcal{P}(\mathbf{r}_b)\left[V(E-E_b)+U_b(r_b)\right]e^{i\mathbf{k}\mathbf{r}_a}\phi_a(\mathbf{r}_{xb})$$

projector over b states $\mathcal{P}(\mathbf{r}_b) = \int |\chi_b(\mathbf{r}_b;\mathbf{k}_b)\rangle\langle\chi_b(\mathbf{r}_b;\mathbf{k}_b)|\, d\mathbf{k}_b$

$$E_b = \frac{\hbar^2 k_b^2}{2\mu_b}$$

# The Green's Function Transfer (GFT) formalism

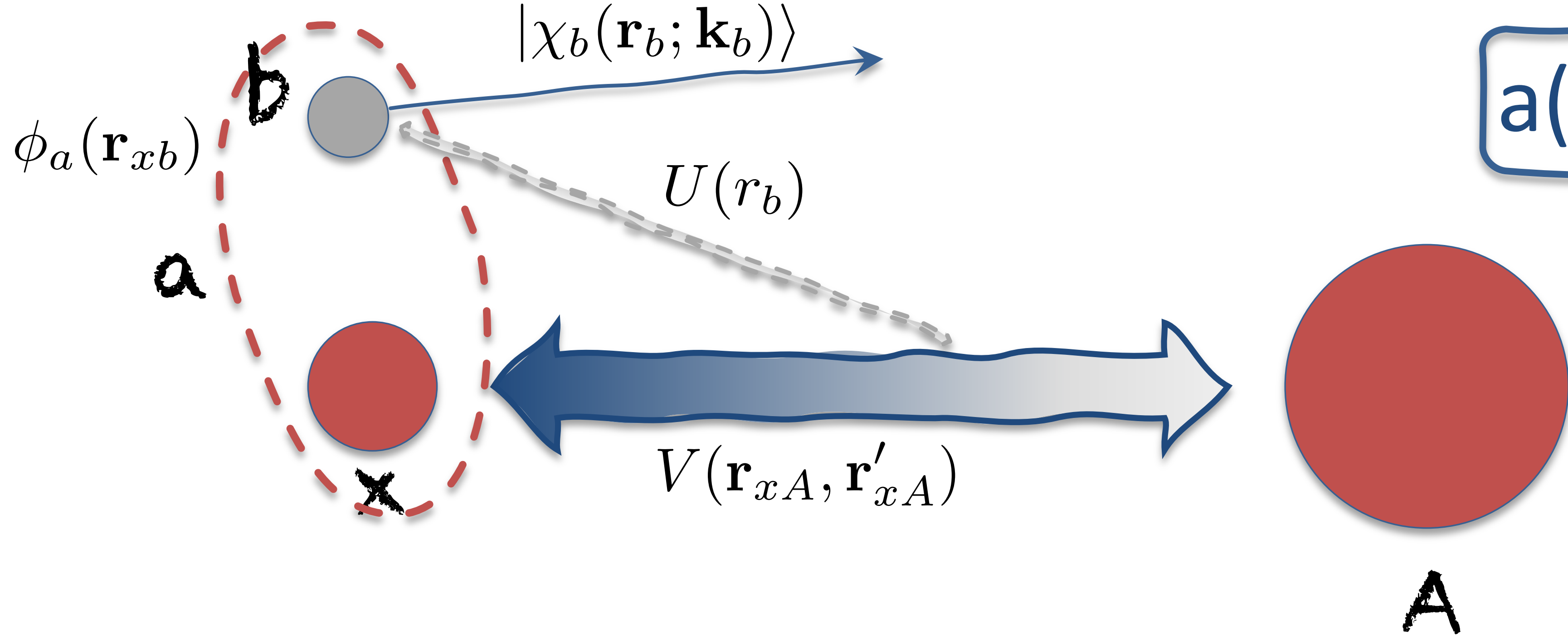


a(=b+x)+A ➡ b+B(=A+x)

$$\Psi_0(\mathbf{r}_{xA},\mathbf{r}_b) = e^{i\mathbf{k}\mathbf{r}_a}\phi_a(\mathbf{r}_{xb}) + G(E-E_b)\mathcal{P}(\mathbf{r}_b)\big[V(E-E_b)+U_b(\mathbf{r}_b)\big]e^{i\mathbf{k}\mathbf{r}_a}\phi_a(\mathbf{r}_{xb})$$

Green's function $G(E) = (E - T_x - V(E))^{-1}$

Same as for x-A scattering!

# The Green's Function Transfer (GFT) formalism

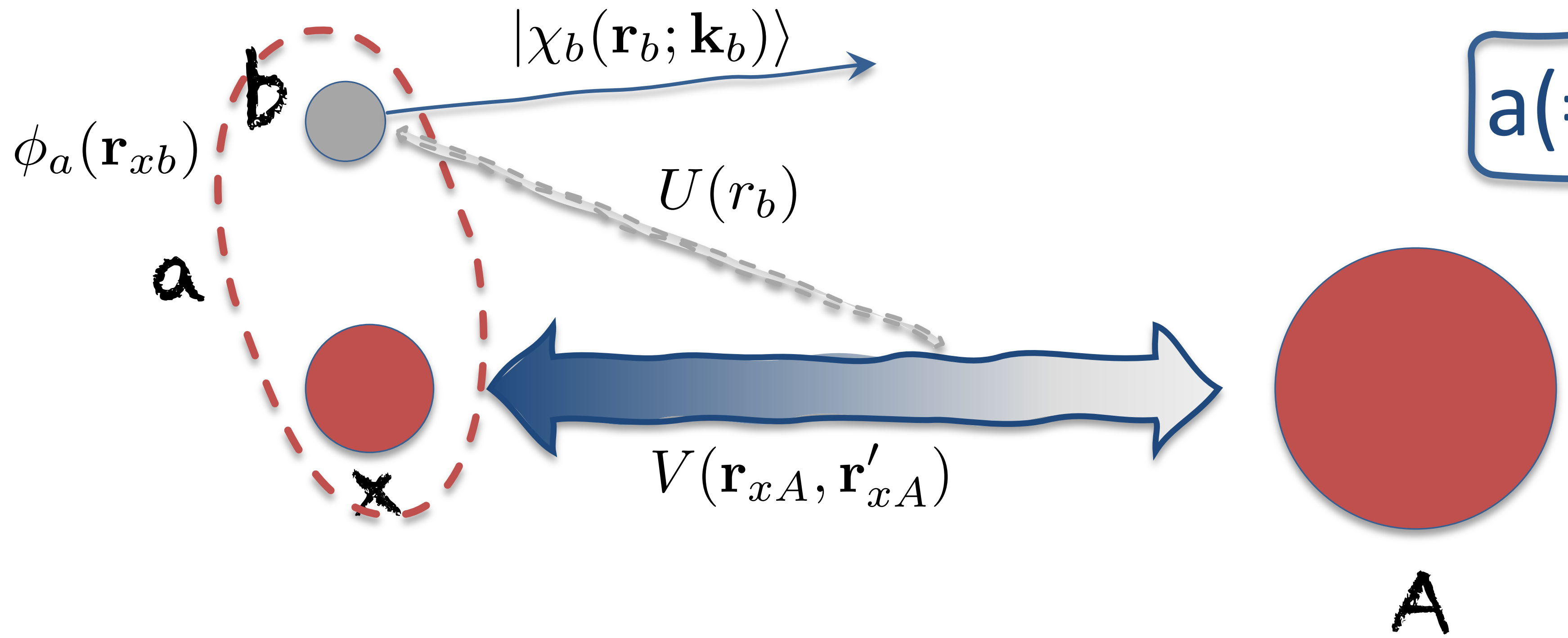


a(=b+x)+A ➡ b+B(=A+x)

$$\Psi_0(\mathbf{r}_{xA},\mathbf{r}_b) = e^{i\mathbf{k}\mathbf{r}_a}\phi_a(\mathbf{r}_{xb}) + G(E-E_b)\mathcal{P}(\mathbf{r}_b)\left[V(E-E_b)+U_b(\mathbf{r}_b)\right]e^{i\mathbf{k}\mathbf{r}_a}\phi_a(\mathbf{r}_{xb})$$

factorized propagator

# The Green's Function Transfer (GFT) formalism

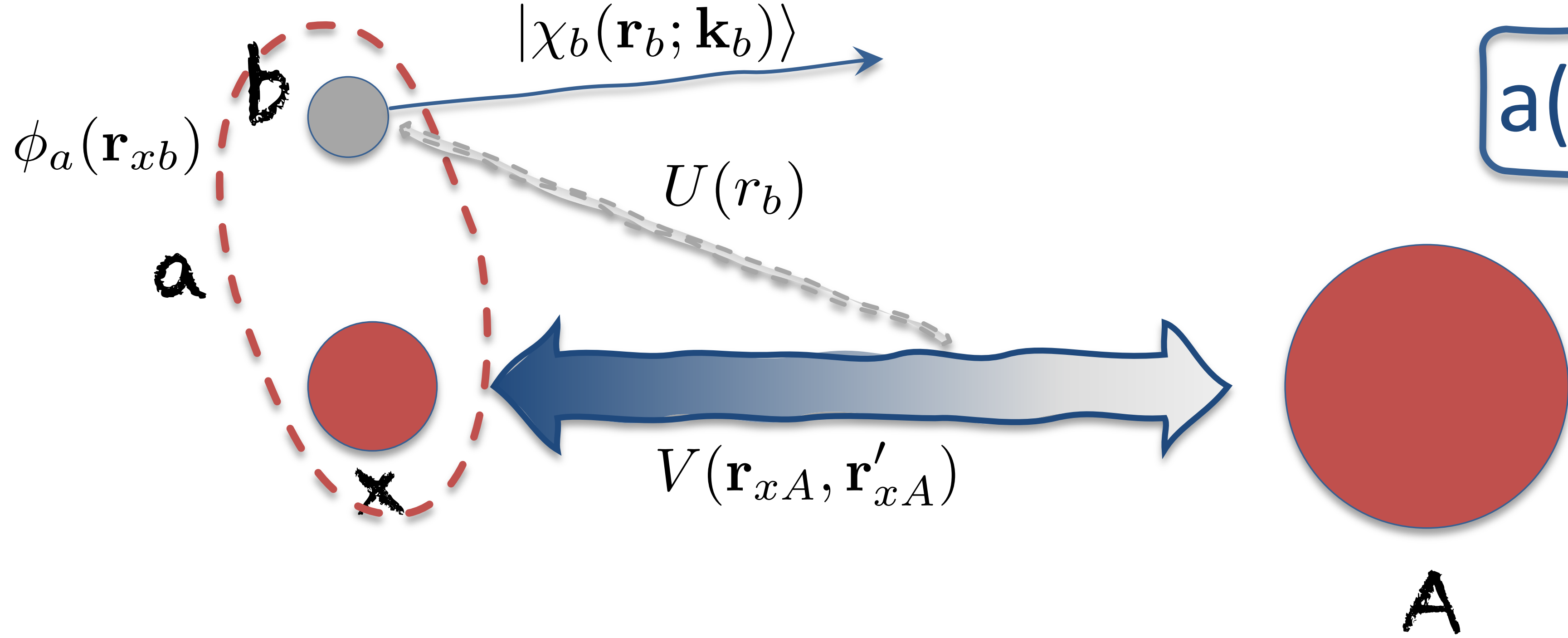


a(=b+x)+A → b+B(=A+x)

$$\langle\chi_b(\mathbf{r}_b;\mathbf{k}_b)|\Psi_0(\mathbf{r}_{xA},\mathbf{r}_b) = \langle\chi_b(\mathbf{r}_b;\mathbf{k}_b)|\left(e^{i\mathbf{k}\mathbf{r}_a}\phi_a(\mathbf{r}_{xb}) + G(E-E_b)\mathcal{P}(\mathbf{r}_b)\left[V(E-E_b)+U_b(\mathbf{r}_b)\right]e^{i\mathbf{k}\mathbf{r}_a}\phi_a(\mathbf{r}_{xb})\right)$$

project over b state to get x-A wavefunction

# The Green's Function Transfer (GFT) formalism

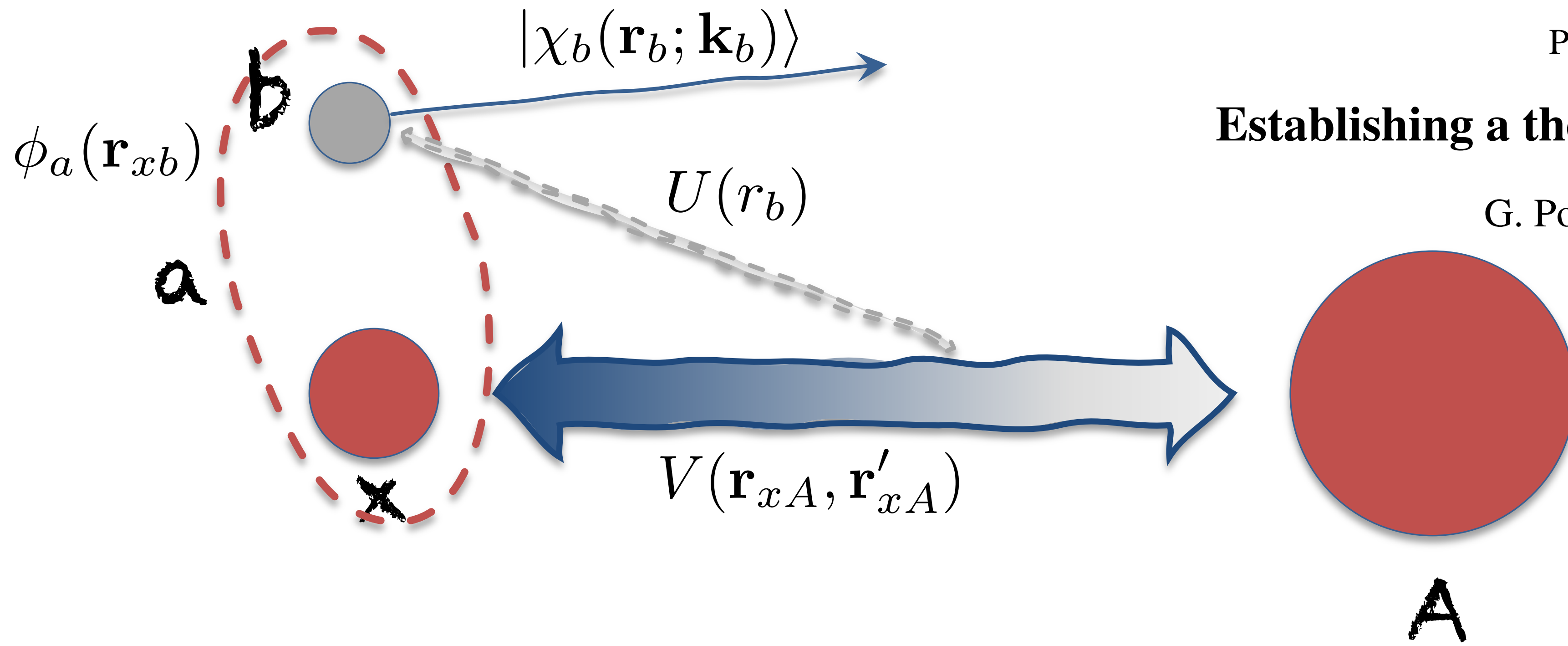


PHYSICAL REVIEW C **92**, 034611 (2015)

**Establishing a theory for deuteron-induced surrogate reactions**

G. Potel,[1,2] F. M. Nunes,[1,3] and I. J. Thompson[2]

$$\psi_0^I(\mathbf{r}_{xA},E) = \psi^{HM}(\mathbf{r}_a) + G(E-E_b)\big[V(E-E_b)\psi^{HM} + \langle\chi_b|U_b(\mathbf{r}_b)\big]e^{i\mathbf{k}\mathbf{r}_a}\phi_a(\mathbf{r}_{xb})$$

$$\psi^{HM}(\mathbf{r}_{xA}) = \int \chi_b^*(\mathbf{r}_{bB},\mathbf{k}_b)\phi_a(\mathbf{r}_{xb})e^{i\mathbf{k}\mathbf{r}_a}\,d\mathbf{r}_{xb}$$

Hussein-McVoy term

$$\sigma_R^I(E,E_b) = \frac{2\mu}{\hbar k_x}\langle\psi_0^I|\mathrm{Im}\mathcal{V}(E-E_b)|\psi_0^I\rangle$$

inclusive x–A cross section

## Let us now introduce explicitly some internal structure $\xi$. Can we treat structure and reactions on the same footing?

$$\psi_0(r_{xA}, \xi, E) = e^{i\mathbf{k}\mathbf{r}_{xA}} \phi_0(\xi) + \mathbf{G}(E)\,\mathbf{V}(E)\, e^{i\mathbf{k}\mathbf{r}_{xA}} \phi_0(\xi)$$

## Let us now introduce explicitly some internal structure $\xi$. Can we treat structure and reactions on the same footing?

$$\psi_0(r_{xA},\xi,E) = e^{i\mathbf{k}\mathbf{r}_{xA}}\phi_0(\xi) + \mathbf{G}(E)\,\mathbf{V}(E)\,e^{i\mathbf{k}\mathbf{r}_{xA}}\phi_0(\xi)$$

project on observed scattered direction

$$\langle e^{i\mathbf{k}_f\mathbf{r}_{xA}}\phi_0(\xi)|\psi_0(r_{xA},\xi,E)\rangle = \langle e^{i\mathbf{k}_f\mathbf{r}_{xA}}\phi_0(\xi)|\mathbf{G}(E)\,\mathbf{V}(E)|e^{i\mathbf{k}\mathbf{r}_{xA}}\phi_0(\xi)\rangle$$

## Let us now introduce explicitly some internal structure $\xi$. Can we treat structure and reactions on the same footing?

$$\psi_0(r_{xA},\xi,E) = e^{i\mathbf{k}\mathbf{r}_{xA}}\phi_0(\xi) + \mathbf{G}(E)\,\mathbf{V}(E)\,e^{i\mathbf{k}\mathbf{r}_{xA}}\phi_0(\xi)$$

$$\langle e^{i\mathbf{k}_f\mathbf{r}_{xA}}\phi_0(\xi)|\psi_0(r_{xA},\xi,E)\rangle = \langle e^{i\mathbf{k}_f\mathbf{r}_{xA}}\phi_0(\xi)|G(E)\,\mathcal{V}(E)|e^{i\mathbf{k}\mathbf{r}_{xA}}\phi_0(\xi)\rangle$$

optical potential

## Let us now introduce explicitly some internal structure $\xi$. Can we treat structure and reactions on the same footing?

$$\psi_0(r_{xA},\xi,E) = e^{i\mathbf{k}\mathbf{r}_{xA}}\phi_0(\xi) + \mathbf{G}(E)\,\mathbf{V}(E)\,e^{i\mathbf{k}\mathbf{r}_{xA}}\phi_0(\xi)$$

$$\langle e^{i\mathbf{k}_f\mathbf{r}_{xA}}\phi_0(\xi)|\psi_0(r_{xA},\xi,E)\rangle = \langle e^{i\mathbf{k}_f\mathbf{r}_{xA}}\phi_0(\xi)|G(E)\,\mathcal{V}(E)|e^{i\mathbf{k}\mathbf{r}_{xA}}\phi_0(\xi)\rangle$$

classification according to asymptotic behavior

$$\lim_{r_{xA}\to\infty} = 0 \to \text{structure}$$

## Let us now introduce explicitly some internal structure $\xi$. Can we treat structure and reactions on the same footing?

$$\psi_0(r_{xA},\xi,E) = e^{i\mathbf{k}\mathbf{r}_{xA}}\phi_0(\xi) + \mathbf{G}(E)\,\mathbf{V}(E)\,e^{i\mathbf{k}\mathbf{r}_{xA}}\phi_0(\xi)$$

$$\langle e^{i\mathbf{k}_f\mathbf{r}_{xA}}\phi_0(\xi)|\psi_0(r_{xA},\xi,E)\rangle = \langle e^{i\mathbf{k}_f\mathbf{r}_{xA}}\phi_0(\xi)|G(E)\,\mathcal{V}(E)|e^{i\mathbf{k}\mathbf{r}_{xA}}\phi_0(\xi)\rangle$$

classification according to asymptotic behavior

$$\lim_{r_{xA}\to\infty} = 0 \to \text{structure}$$

$$\lim_{r_{xA}\to\infty} = \text{oscillatory} \to \text{reaction}$$

## Let us now introduce explicitly some internal structure $\xi$. Can we treat structure and reactions on the same footing?

$$\psi_0(r_{xA},\xi,E) = e^{i\mathbf{k}\mathbf{r}_{xA}}\phi_0(\xi) + \mathbf{G}(E)\,\mathbf{V}(E)\,e^{i\mathbf{k}\mathbf{r}_{xA}}\phi_0(\xi)$$

$$\langle e^{i\mathbf{k}_f\mathbf{r}_{xA}}\phi_0(\xi)|\psi_0(r_{xA},\xi,E)\rangle = \langle e^{i\mathbf{k}_f\mathbf{r}_{xA}}\phi_0(\xi)|G(E)\,\mathcal{V}(E)|e^{i\mathbf{k}\mathbf{r}_{xA}}\phi_0(\xi)\rangle$$

classification according to asymptotic behavior

$$\lim_{r_{xA}\to\infty} = 0 \to \text{structure}$$

$$\lim_{r_{xA}\to\infty} = \text{oscillatory} \to \text{reaction}$$

some possible implementations of structure-reactions consistency

- ab-initio,
- EFT,
- QRPA+G-matrix,
- ...

## Let us now introduce explicitly some internal structure $\xi$. Can we treat structure and reactions on the same footing?

$$\psi_0(r_{xA}, \xi, E) = e^{i\mathbf{k}\mathbf{r}_{xA}}\phi_0(\xi) + \mathbf{G}(E)\,\mathbf{V}(E)\,e^{i\mathbf{k}\mathbf{r}_{xA}}\phi_0(\xi)$$

$$\langle e^{i\mathbf{k}_f\mathbf{r}_{xA}}\phi_0(\xi)|\psi_0(r_{xA}, \xi, E)\rangle = \langle e^{i\mathbf{k}_f\mathbf{r}_{xA}}\phi_0(\xi)|G(E)\,\mathcal{V}(E)|e^{i\mathbf{k}\mathbf{r}_{xA}}\phi_0(\xi)\rangle$$

A proposed scheme to enforce structure-reactions consistency

$$\psi_i(r_{xA}, \xi) \rightarrow \mathcal{V}(E) \rightarrow G(E) = (E - T - \mathcal{V}(E))^{-1}$$

# DWBA vs GFT

$$\sigma_{i0}^{DWBA} \sim |\langle \psi_i | V | \psi_0 \rangle|^2 \qquad \sigma_R^{GFT}(E) \sim \langle G(E)\,(\mathcal{V}(E) + U_b)\,\psi^{HM} | \mathrm{Im}\mathcal{V}(E) | G(E)\,(\mathcal{V}(E) + U_b)\,\psi^{HM} \rangle$$

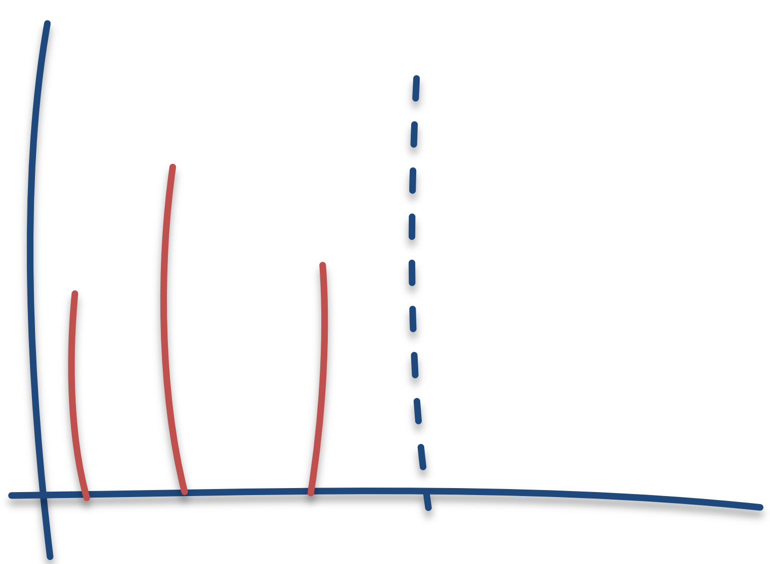

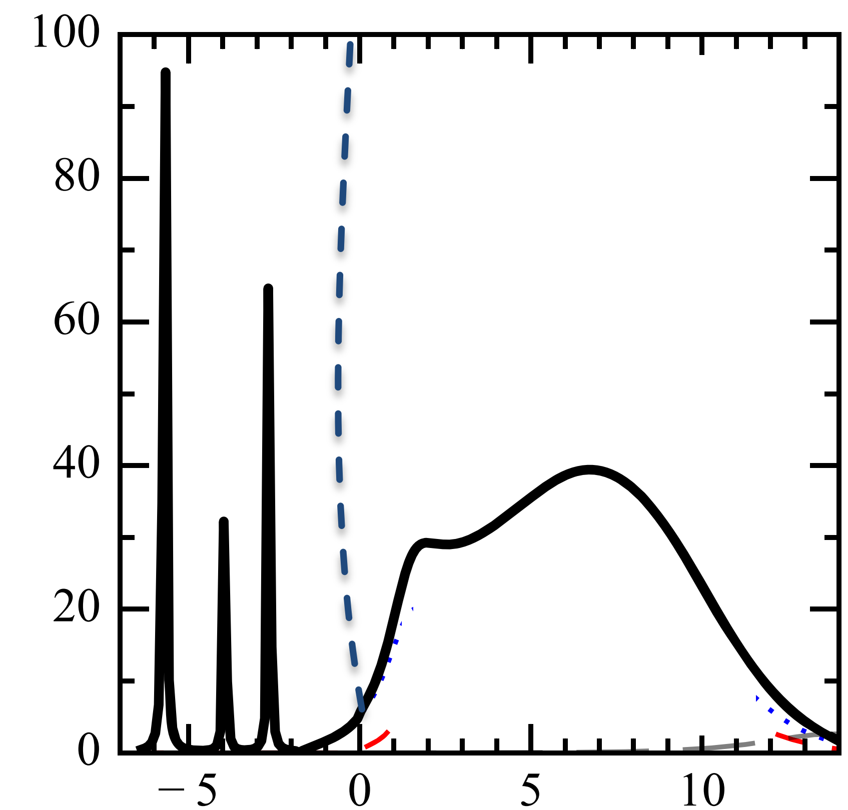

# DWBA vs GFT

$$\sigma_{i0}^{DWBA} \sim |\langle \psi_i | V | \psi_0 \rangle|^2$$

$$\sigma_R^{GFT}(E) \sim \langle G(E)\left(\mathcal{V}(E) + U_b\right)\psi^{HM} | \mathrm{Im}\mathcal{V}(E) | G(E)\left(\mathcal{V}(E) + U_b\right)\psi^{HM} \rangle$$

discrete final states

continuous function of E

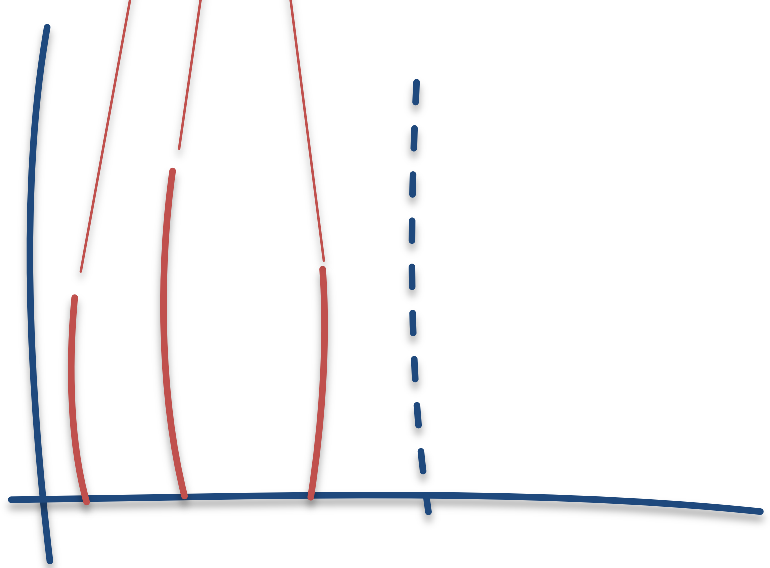

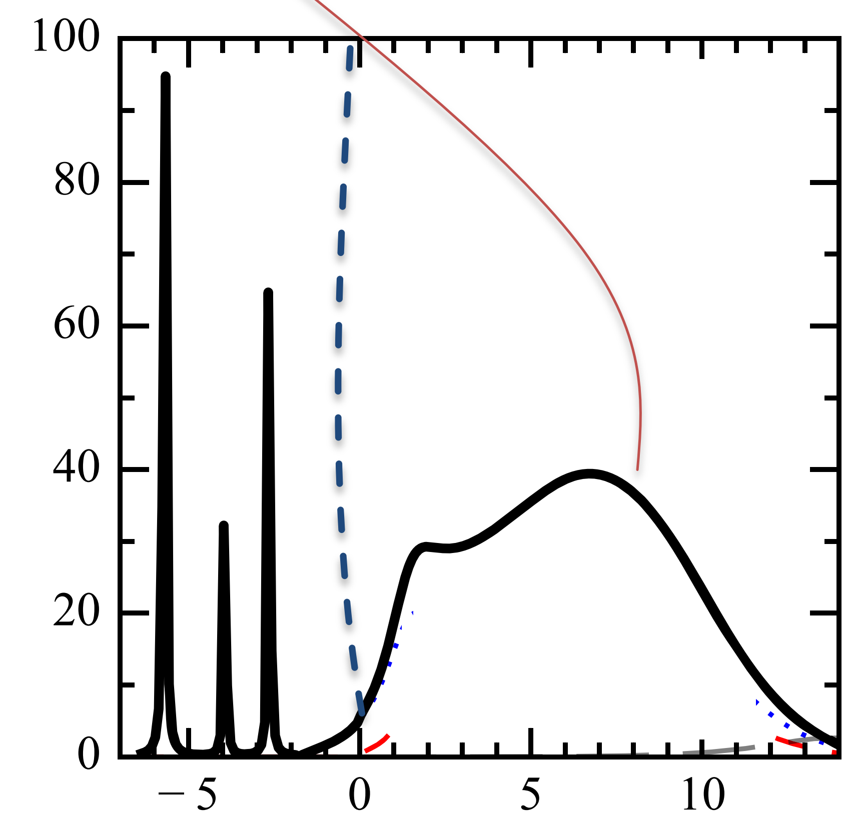

# DWBA vs GFT

$$\sigma_{i0}^{DWBA} \sim |\langle \psi_i | V | \psi_0 \rangle|^2 \qquad \sigma_R^{GFT}(E) \sim \langle G(E)\,(\mathcal{V}(E) + U_b)\,\psi^{HM} | \mathrm{Im}\mathcal{V}(E) | G(E)\,(\mathcal{V}(E) + U_b)\,\psi^{HM} \rangle$$

extracted $S=\sigma_{exp}/\sigma_{th}$

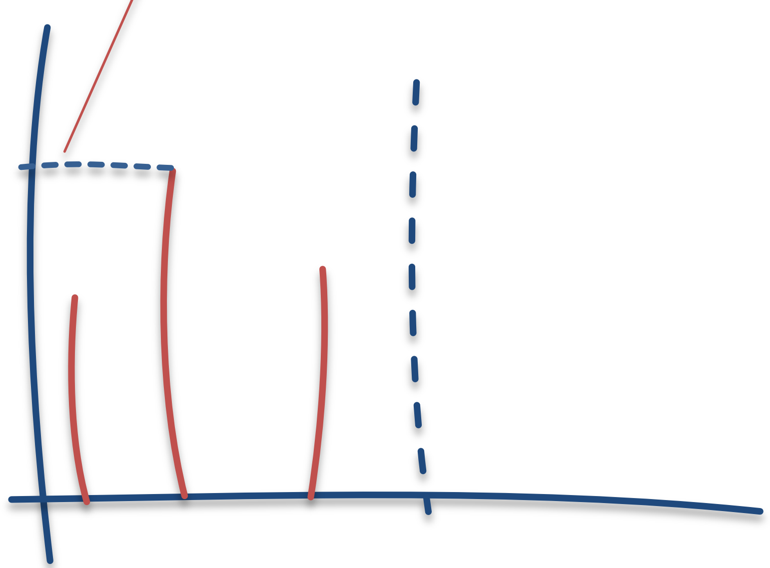

consistent normalization

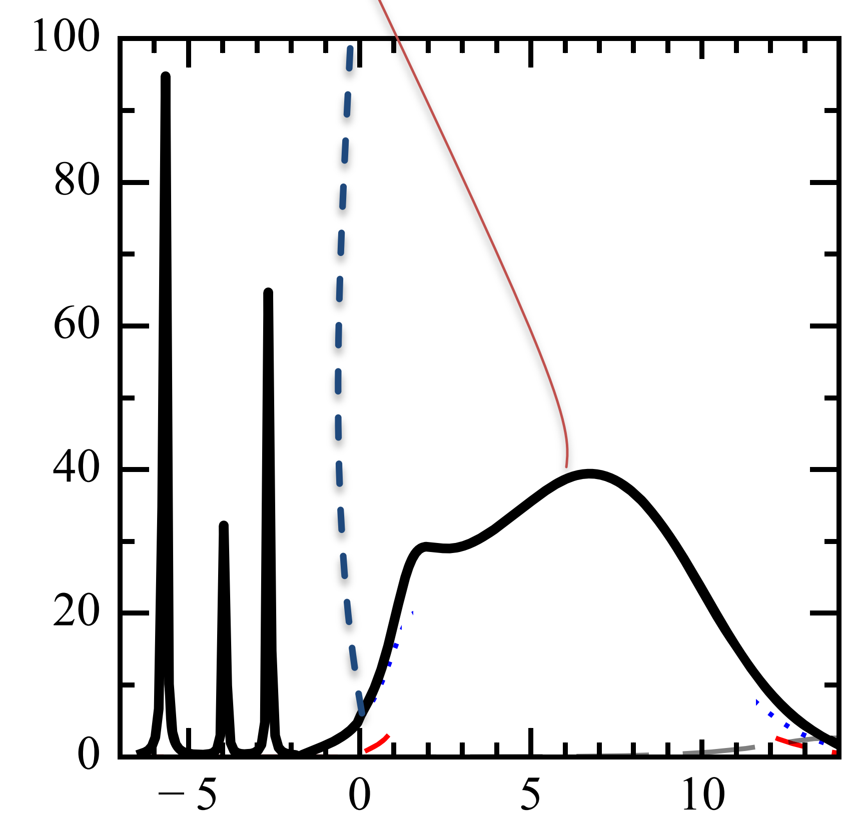

# DWBA vs GFT

$$\sigma_{i0}^{DWBA} \sim |\langle \psi_i | V | \psi_0 \rangle|^2 \qquad \sigma_R^{GFT}(E) \sim \langle G(E)\left(\mathcal{V}(E) + U_b\right)\psi^{HM} | \mathrm{Im}\mathcal{V}(E) | G(E)\left(\mathcal{V}(E) + U_b\right)\psi^{HM} \rangle$$

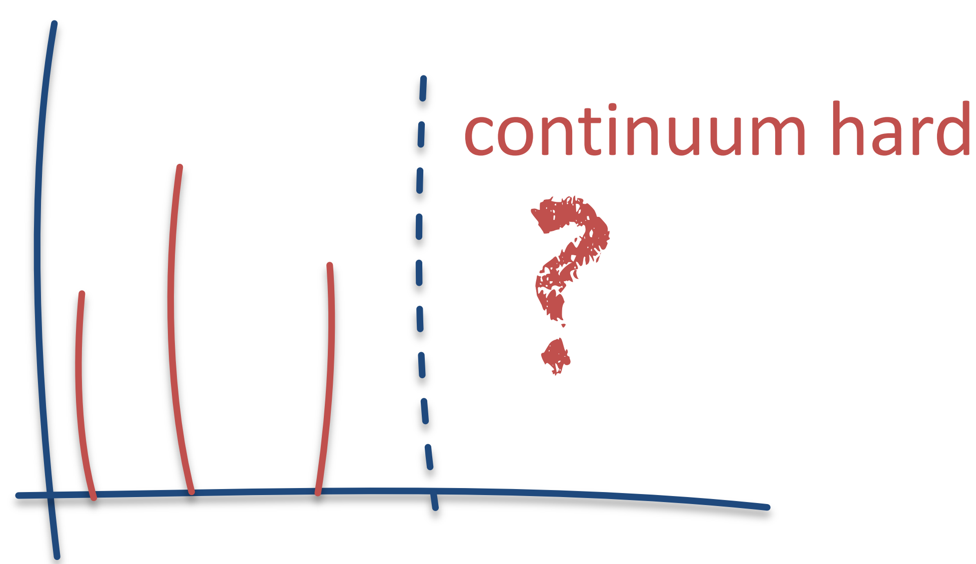


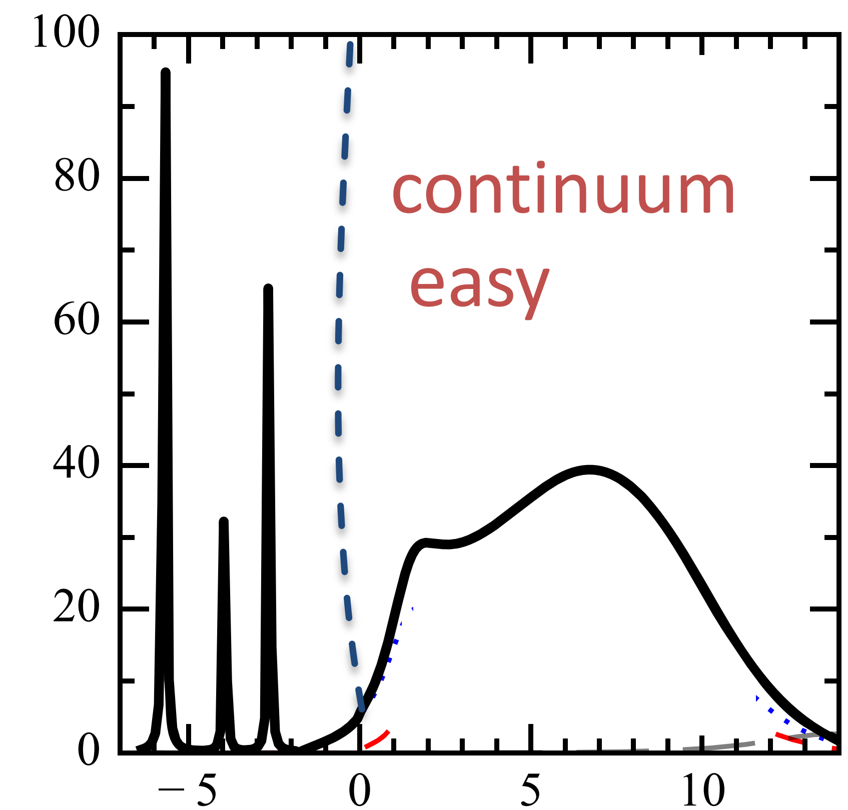

# DWBA vs GFT

$$\sigma_{i0}^{DWBA} \sim |\langle \psi_i | V | \psi_0 \rangle|^2 \qquad \sigma_R^{GFT}(E) \sim \langle G(E)\left(\mathcal{V}(E) + U_b\right)\psi^{HM} | \mathrm{Im}\mathcal{V}(E) | G(E)\left(\mathcal{V}(E) + U_b\right)\psi^{HM} \rangle$$

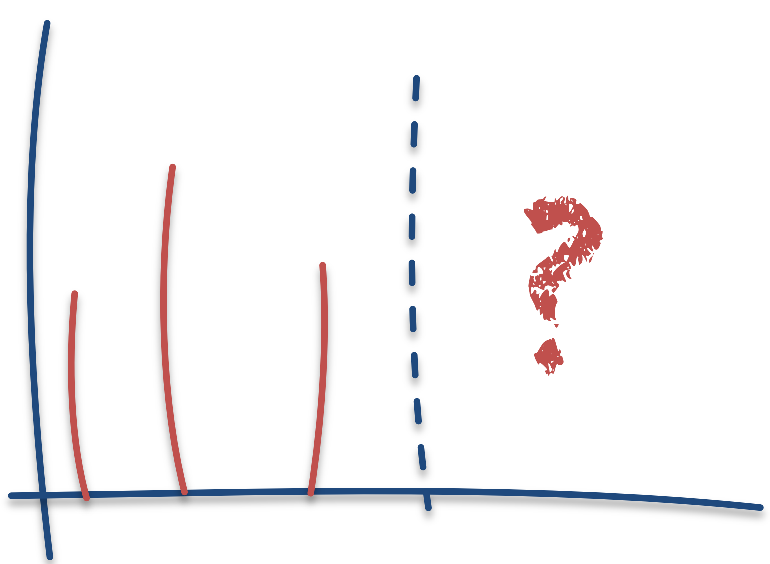


$$G(E) = \left(E - T - \mathcal{V}(E)\right)^{-1}$$

- Consistency between structure and reactions
- Same ingredients as x–A scattering
- Need for tools for inverting Hamiltonians with non-local potentials

# GFT with Nuclear Field Theory (NFT): $^9$Li(d,p)

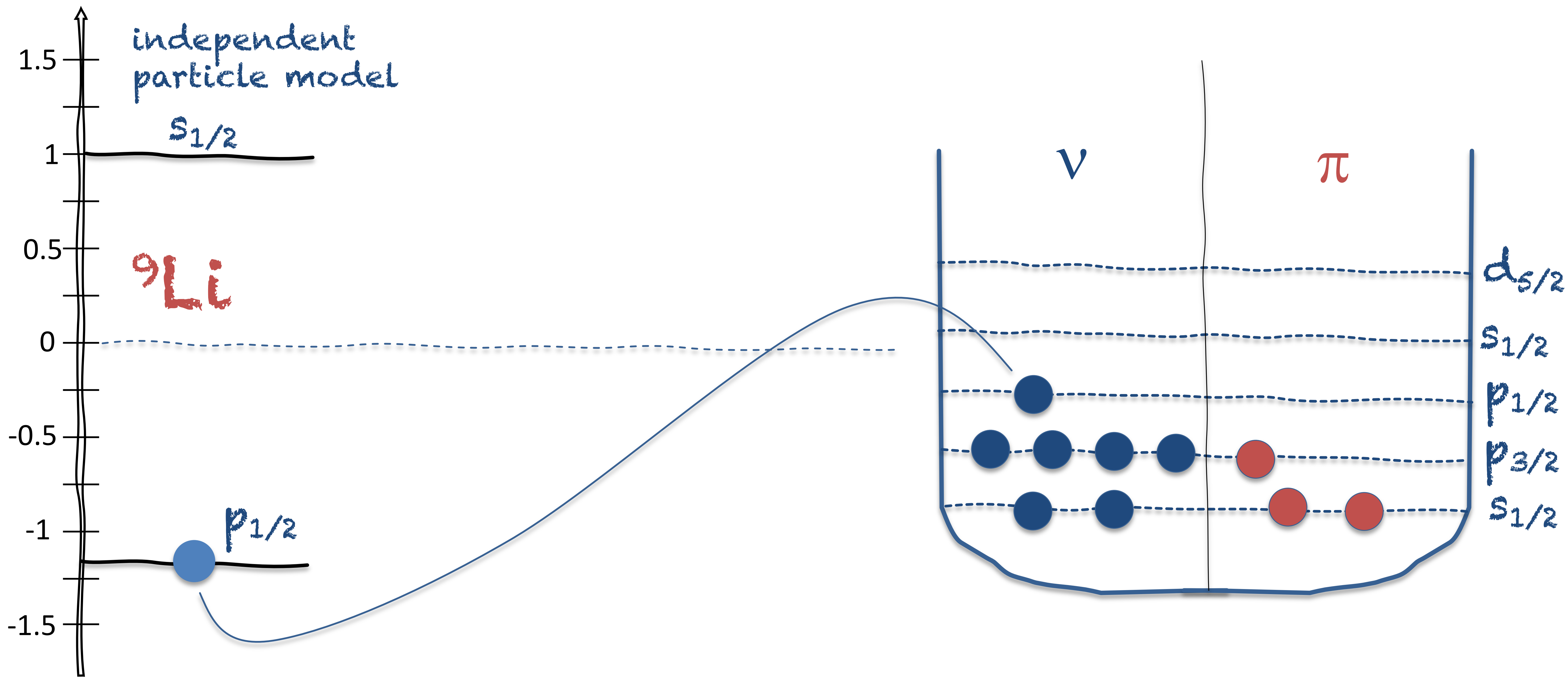

# GFT with Nuclear Field Theory (NFT): $^{9}$Li(d,p)

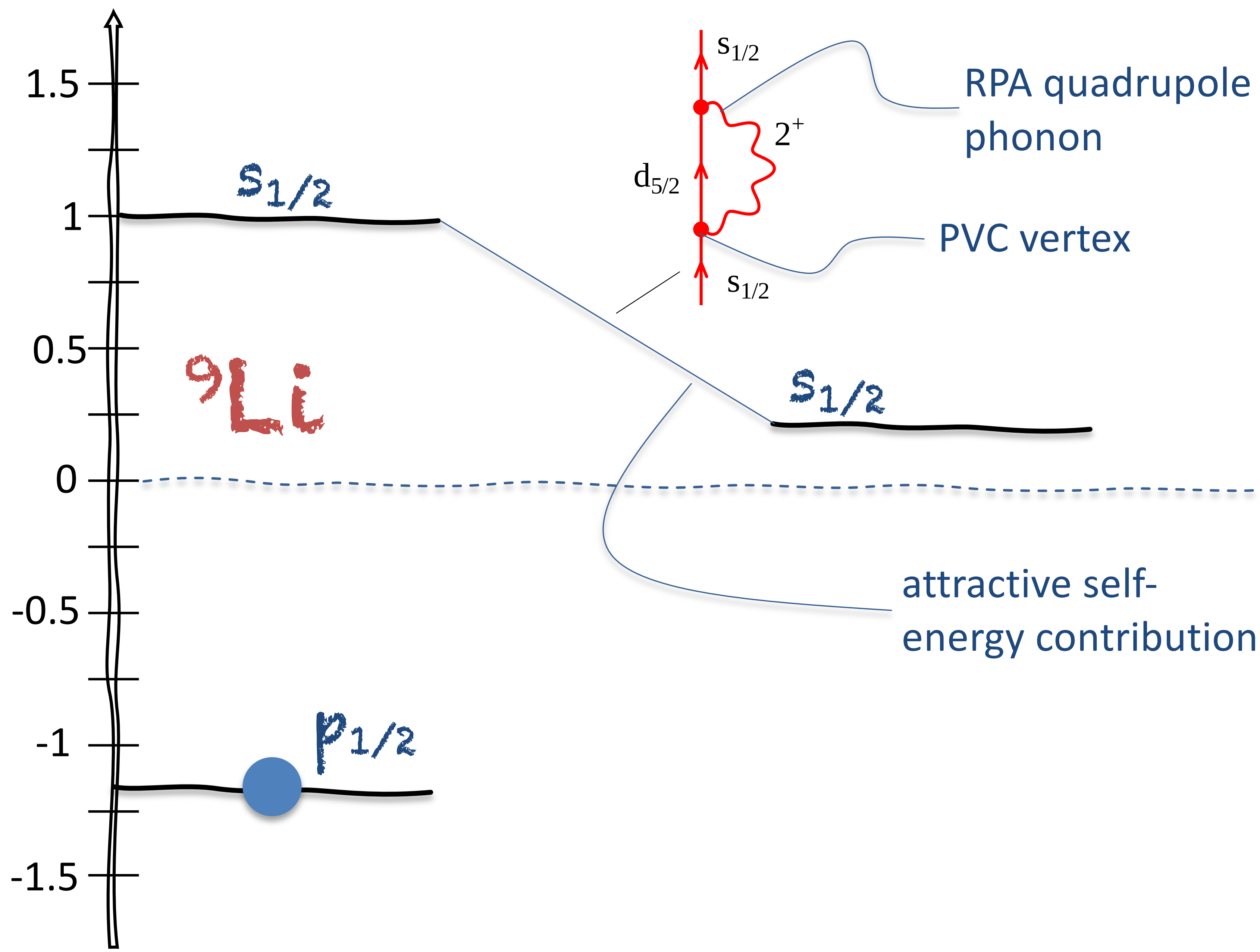

# GFT with Nuclear Field Theory (NFT): $^{9}$Li(d,p)

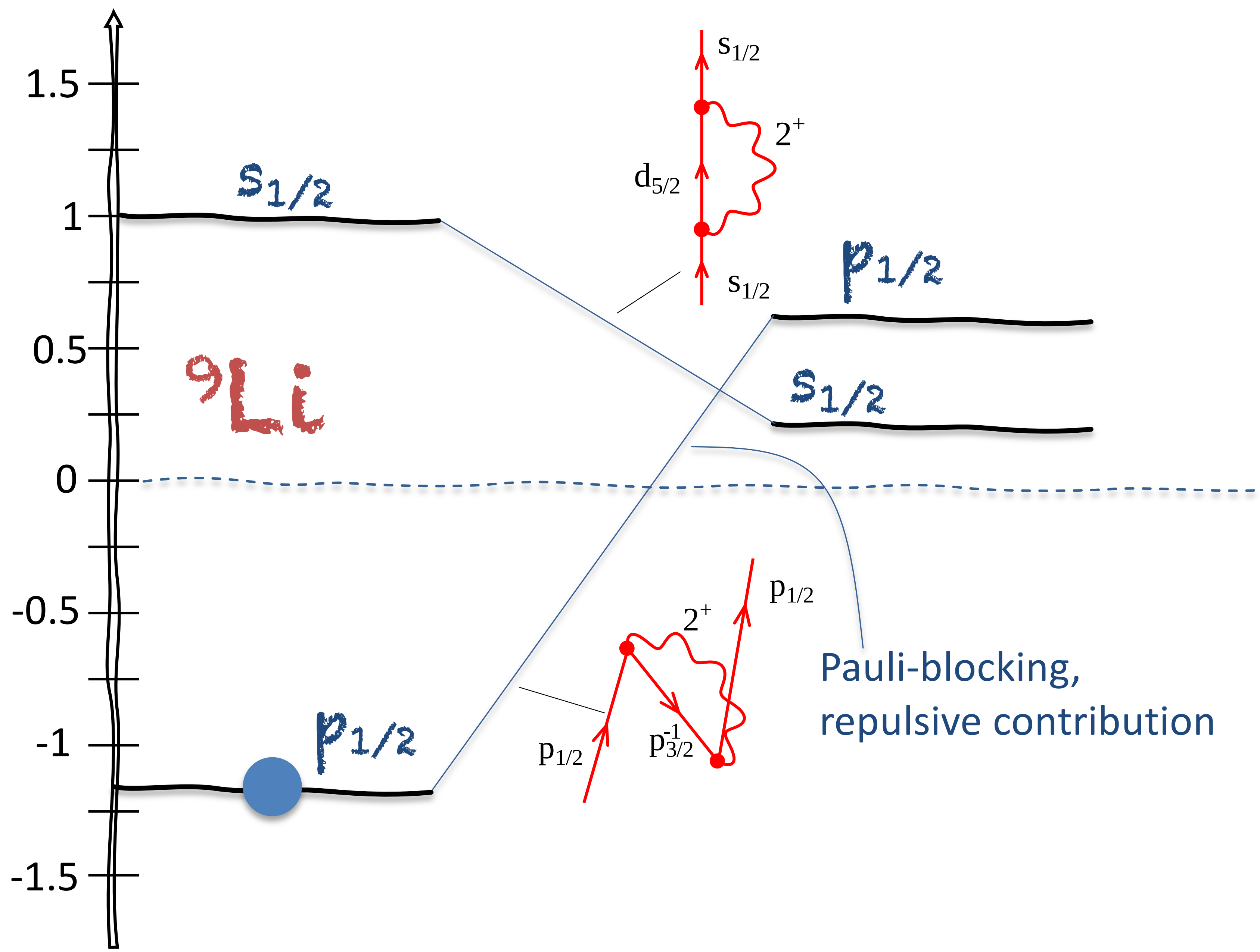

# GFT with Nuclear Field Theory (NFT): $^9$Li(d,p)

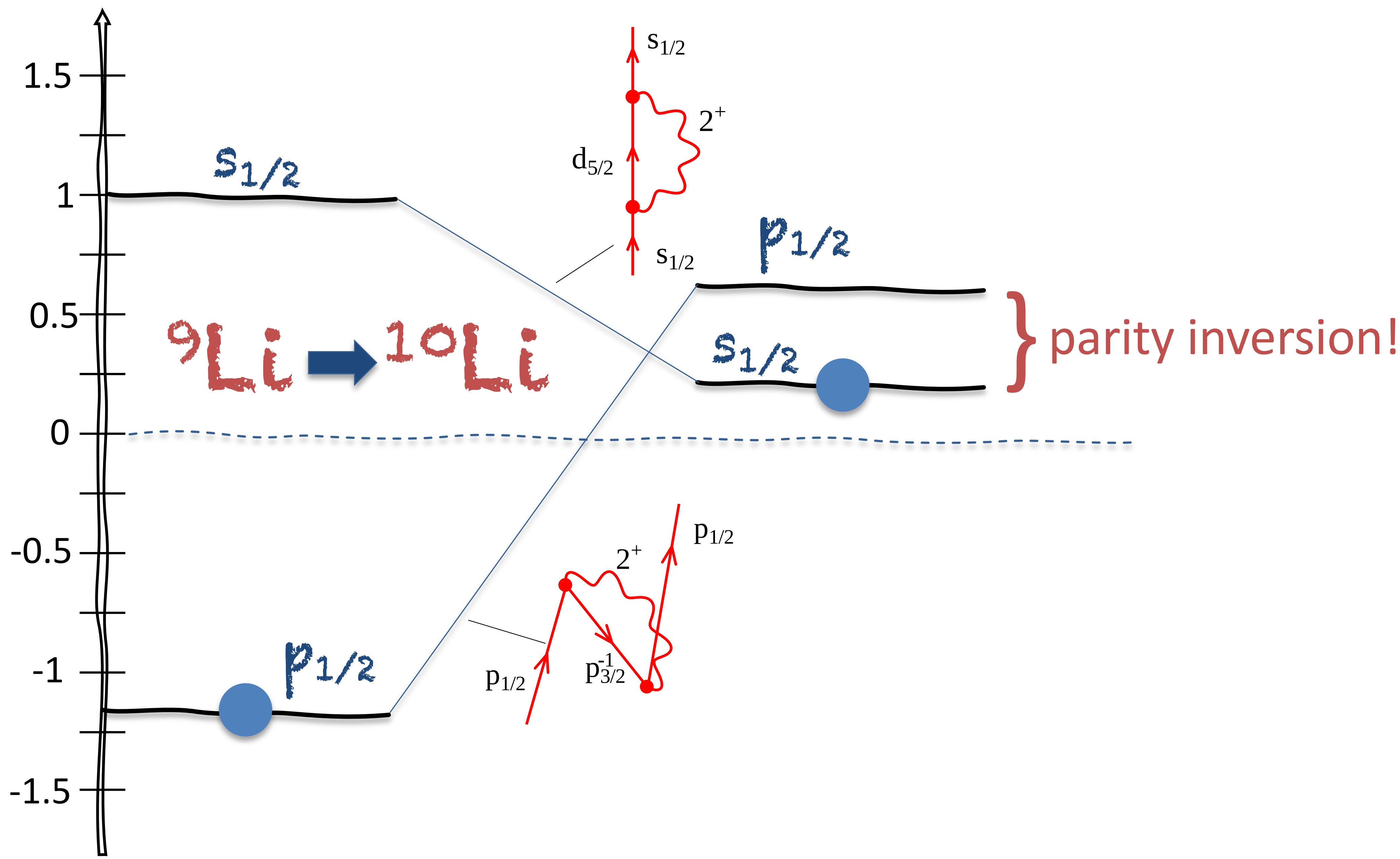

# GFT with Nuclear Field Theory (NFT): $^9$Li(d,p)

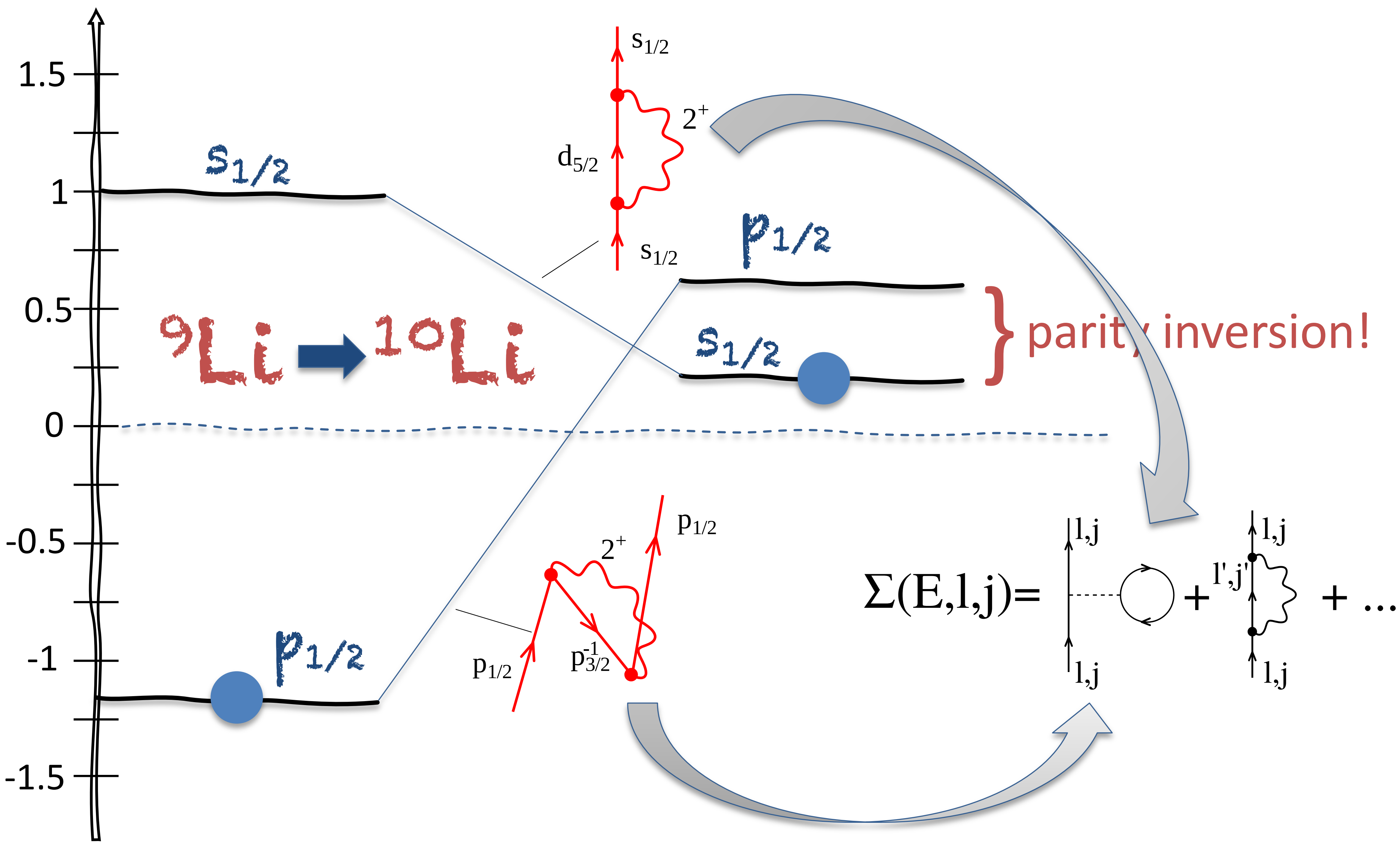

# $^{24}$Mg+n with valence shell model

step 1: $^{25}$Mg shell-model calculation

excitation energy $E_i$, angular momentum, parity, spectroscopic factor $S_i$

| | | | | |
|---|---|---|---|---|
| 0 | 0 | 2 | 1 | 0.584066 |
| 0.701 | 0 | 0 | 1 | -0.716831 |
| 1.169 | 0 | 2 | 1 | 0.488705 |
| 2.033 | 0 | 2 | 1 | -0.288311 |
| 2.529 | 0 | 0 | 1 | 0.318332 |
| 2.701 | 0 | 2 | 1 | 0.542416 |
| 3.859 | 0 | 2 | 1 | 0.0495903 |
| 3.926 | 0 | 1 | -1 | -0.0298132 |
| 4.118 | 0 | 1 | -1 | -0.584623 |
| 4.226 | 0 | 3 | -1 | -0.651056 |
| 4.46 | 0 | 2 | 1 | 0.100777 |
| 4.816 | 0 | 2 | 1 | 0.0975601 |
| 4.945 | 0 | 1 | -1 | 0.516883 |
| 5.065 | 0 | 1 | -1 | -0.0511968 |
| 5.416 | 0 | 0 | 1 | -0.283037 |
| 5.638 | 0 | 3 | -1 | -0.219064 |
| 5.785 | 0 | 2 | 1 | -0.0103979 |
| 5.792 | 0 | 2 | 1 | 0.132477 |
| 5.935 | 0 | 3 | -1 | 0.069005 |
| 5.936 | 0 | 2 | 1 | 0.094658 |
| 6.033 | 0 | 1 | -1 | 0.0353684 |
| 6.12 | 0 | 1 | -1 | -0.159821 |
| 6.243 | 0 | 2 | 1 | -0.174362 |
| 6.35 | 0 | 3 | -1 | 0.122727 |
| 6.385 | 0 | 0 | 1 | 0.182001 |
| 6.417 | 0 | 2 | 1 | 0.115995 |
| 6.609 | 0 | 2 | 1 | 0.100457 |
| 6.739 | 0 | 3 | -1 | 0.157325 |
| 6.771 | 0 | 1 | -1 | 0.419452 |
| 6.801 | 0 | 3 | -1 | 0.160889 |

~600 states from $E_i$=0 to $E_i$=14.6 MeV

Shell model calculations by K. Kravvaris with PSDPF interaction M Bouhelal, *et al.*, Nucl. Phys. A **864** (2011)

# $^{24}$Mg+n with valence shell model

excitation energy $E_i$

angular momentum

parity

spectroscopic factor $S_i$

| | | | | |
|---|---|---|---|---|
| 0 | 0 | 2 | 1 | 0.584066 |
| 0.701 | 0 | 0 | 1 | −0.716831 |
| 1.169 | 0 | 2 | 1 | 0.488705 |
| 2.033 | 0 | 2 | 1 | −0.288311 |
| 2.529 | 0 | 0 | 1 | 0.318332 |
| 2.701 | 0 | 2 | 1 | 0.542416 |
| 3.859 | 0 | 2 | 1 | 0.0495903 |
| 3.926 | 0 | 1 | −1 | −0.0298132 |
| 4.118 | 0 | 1 | −1 | −0.584623 |
| 4.226 | 0 | 3 | −1 | −0.651056 |
| 4.46 | 0 | 2 | 1 | 0.100777 |
| 4.816 | 0 | 2 | 1 | 0.0975601 |
| 4.945 | 0 | 1 | −1 | 0.516883 |
| 5.065 | 0 | 1 | −1 | −0.0511968 |
| 5.416 | 0 | 0 | 1 | −0.283037 |
| 5.638 | 0 | 3 | −1 | −0.219064 |
| 5.785 | 0 | 2 | 1 | −0.0103979 |
| 5.792 | 0 | 2 | 1 | 0.132477 |
| 5.935 | 0 | 3 | −1 | 0.069005 |
| 5.936 | 0 | 2 | 1 | 0.094658 |
| 6.033 | 0 | 1 | −1 | 0.0353684 |
| 6.12 | 0 | 1 | −1 | −0.159821 |
| 6.243 | 0 | 2 | 1 | −0.174362 |
| 6.35 | 0 | 3 | −1 | 0.122727 |
| 6.385 | 0 | 0 | 1 | 0.182001 |
| 6.417 | 0 | 2 | 1 | 0.115995 |
| 6.609 | 0 | 2 | 1 | 0.100457 |
| 6.739 | 0 | 3 | −1 | 0.157325 |
| 6.771 | 0 | 1 | −1 | 0.419452 |
| 6.801 | 0 | 3 | −1 | 0.160889 |

## step 2: Static potential and couplings

$$V(\mathbf{r},\mathbf{r}';E) = U_0(r) + \sum_i U_{0i}(\mathbf{r}) G(E-E_i,\mathbf{r},\mathbf{r}') U_{i0}(\mathbf{r}')$$

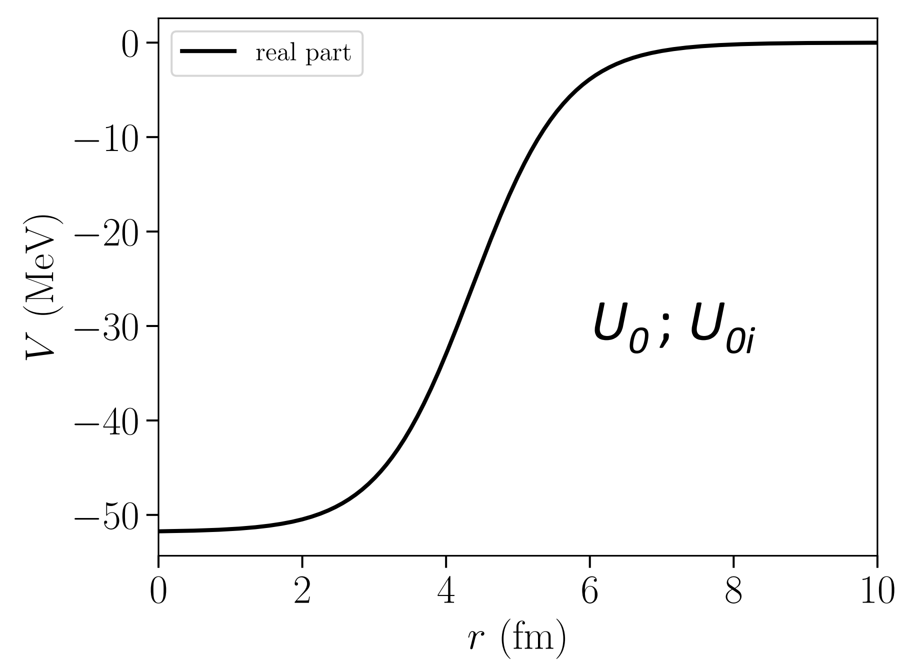


- static potential $U_0$ : real, local Woods-Saxon adjusted to reproduce binding energy of $^{25}$Mg
- couplings $U_{0i}$ : same Woods-Saxon, but adjusted to each $E_i$ and multiplied by spectroscopic factor $S_i$

# $^{24}$Mg+n with valence shell model

excitation energy $E_i$

angular momentum

parity

spectroscopic factor $S_i$

| | | | | |
|---|---|---|---|---|
| 0 | 0 | 2 | 1 | 0.584066 |
| 0.701 | 0 | 0 | 1 | −0.716831 |
| 1.169 | 0 | 2 | 1 | 0.488705 |
| 2.033 | 0 | 2 | 1 | −0.288311 |
| 2.529 | 0 | 0 | 1 | 0.318332 |
| 2.701 | 0 | 2 | 1 | 0.542416 |
| 3.859 | 0 | 2 | 1 | 0.0495903 |
| 3.926 | 0 | 1 | −1 | −0.0298132 |
| 4.118 | 0 | 1 | −1 | −0.584623 |
| 4.226 | 0 | 3 | −1 | −0.651056 |
| 4.46 | 0 | 2 | 1 | 0.100777 |
| 4.816 | 0 | 2 | 1 | 0.0975601 |
| 4.945 | 0 | 1 | −1 | 0.516883 |
| 5.065 | 0 | 1 | −1 | −0.0511968 |
| 5.416 | 0 | 0 | 1 | −0.283037 |
| 5.638 | 0 | 3 | −1 | −0.219064 |
| 5.785 | 0 | 2 | 1 | −0.0103979 |
| 5.792 | 0 | 2 | 1 | 0.132477 |
| 5.935 | 0 | 3 | −1 | 0.069005 |
| 5.936 | 0 | 2 | 1 | 0.094658 |
| 6.033 | 0 | 1 | −1 | 0.0353684 |
| 6.12 | 0 | 1 | −1 | −0.159821 |
| 6.243 | 0 | 2 | 1 | −0.174362 |
| 6.35 | 0 | 3 | −1 | 0.122727 |
| 6.385 | 0 | 0 | 1 | 0.182001 |
| 6.417 | 0 | 2 | 1 | 0.115995 |
| 6.609 | 0 | 2 | 1 | 0.100457 |
| 6.739 | 0 | 3 | −1 | 0.157325 |
| 6.771 | 0 | 1 | −1 | 0.419452 |
| 6.801 | 0 | 3 | −1 | 0.160889 |

## step 2: Static potential and couplings

$$V(\mathbf{r},\mathbf{r}';E) = U_0(r) + \sum_i U_{0i}(\mathbf{r})G(E-E_i,\mathbf{r},\mathbf{r}')U_{i0}(\mathbf{r}')$$

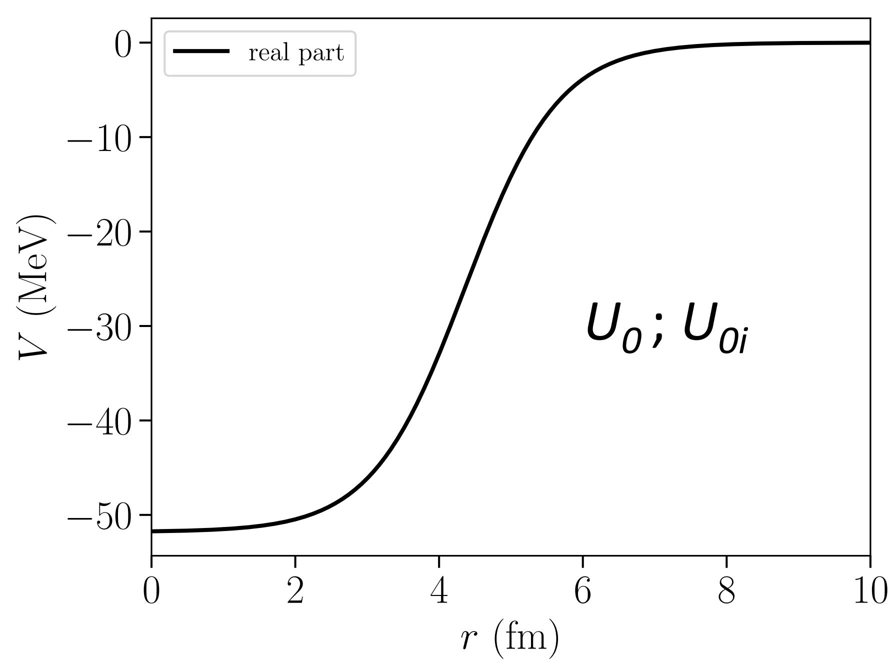


- static potential $U_0$: real, local Woods-Saxon adjusted to reproduce binding energy of $^{25}$Mg
- couplings $U_{0i}$: same Woods-Saxon, but adjusted to each $E_i$ and multiplied by spectroscopic factor $S_i$

can be done better!

# $^{24}$Mg+n with valence shell model

excitation energy $E_i$

angular momentum

parity

spectroscopic factor $S_i$

| | | | | |
|---|---|---|---|---|
| 0 | 0 | 2 | 1 | 0.584066 |
| 0.701 | 0 | 0 | 1 | -0.716831 |
| 1.169 | 0 | 2 | 1 | 0.488705 |
| 2.033 | 0 | 2 | 1 | -0.288311 |
| 2.529 | 0 | 0 | 1 | 0.318332 |
| 2.701 | 0 | 2 | 1 | 0.542416 |
| 3.859 | 0 | 2 | 1 | 0.0495903 |
| 3.926 | 0 | 1 | -1 | -0.0298132 |
| 4.118 | 0 | 1 | -1 | -0.584623 |
| 4.226 | 0 | 3 | -1 | -0.651056 |
| 4.46 | 0 | 2 | 1 | 0.100777 |
| 4.816 | 0 | 2 | 1 | 0.0975601 |
| 4.945 | 0 | 1 | -1 | 0.516883 |
| 5.065 | 0 | 1 | -1 | -0.0511968 |
| 5.416 | 0 | 0 | 1 | -0.283037 |
| 5.638 | 0 | 3 | -1 | -0.219064 |
| 5.785 | 0 | 2 | 1 | -0.0103979 |
| 5.792 | 0 | 2 | 1 | 0.132477 |
| 5.935 | 0 | 3 | -1 | 0.069005 |
| 5.936 | 0 | 2 | 1 | 0.094658 |
| 6.033 | 0 | 1 | -1 | 0.0353684 |
| 6.12 | 0 | 1 | -1 | -0.159821 |
| 6.243 | 0 | 2 | 1 | -0.174362 |
| 6.35 | 0 | 3 | -1 | 0.122727 |
| 6.385 | 0 | 0 | 1 | 0.182001 |
| 6.417 | 0 | 2 | 1 | 0.115995 |
| 6.609 | 0 | 2 | 1 | 0.100457 |
| 6.739 | 0 | 3 | -1 | 0.157325 |
| 6.771 | 0 | 1 | -1 | 0.419452 |
| 6.801 | 0 | 3 | -1 | 0.160889 |

## step 3: Iterative procedure

$$V(\mathbf{r},\mathbf{r}';E) = U_0(r) + \sum_i U_{0i}(\mathbf{r}) G(E-E_i,\mathbf{r},\mathbf{r}') U_{i0}(\mathbf{r}')$$

$$G(\mathbf{r},\mathbf{r}',E) = (E - T - V(\mathbf{r},\mathbf{r}';E))^{-1}$$

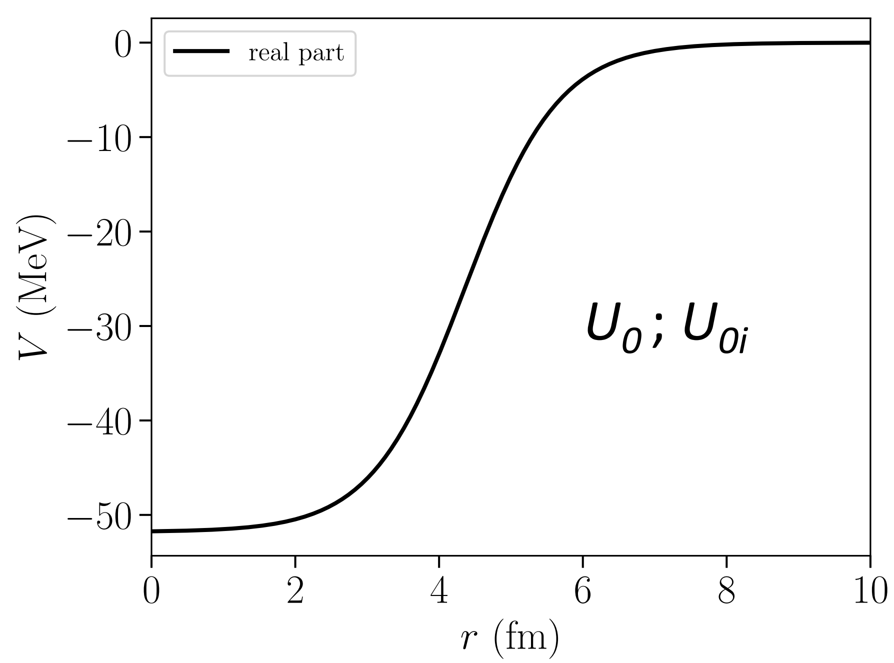


- Iterate until convergence is achieved
- Consistency between potential and Green's function is achieved, as expressed by Dyson's equation:

$$G(\mathbf{r},\mathbf{r}';E) = G_0(\mathbf{r},\mathbf{r}';E) + G_0(\mathbf{r},\mathbf{r}';E)V(\mathbf{r},\mathbf{r}';E)G(\mathbf{r},\mathbf{r}';E)$$

$$G_0(\mathbf{r},\mathbf{r}';E) = (E - T - U_0(r))^{-1}$$

**As a bonus, we obtain the Green's function**

# The dynamical polarization potential is complex, energy-dependent, dispersive, and non-local

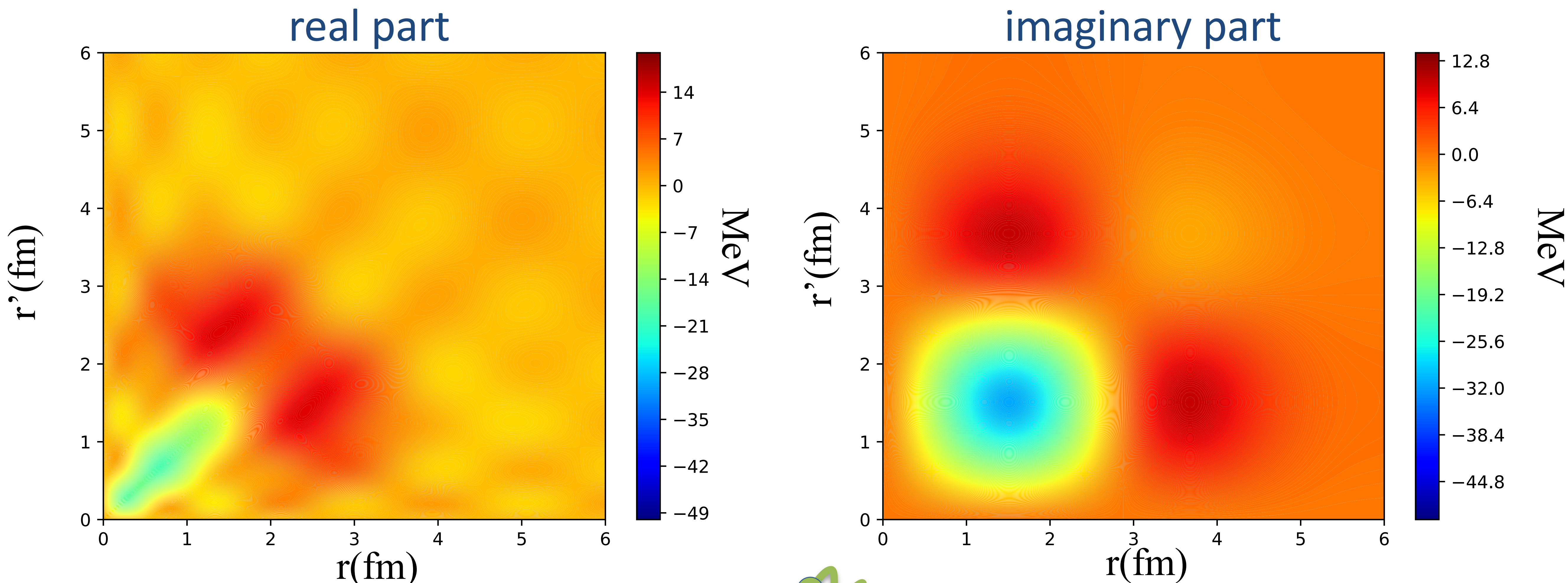


$V_{pol}(r,r';E)=\sum_i$ 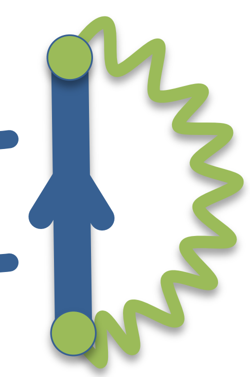 $i$ ; for $E$=1MeV

# Our $^{24}$Mg calculation compares well with experiment

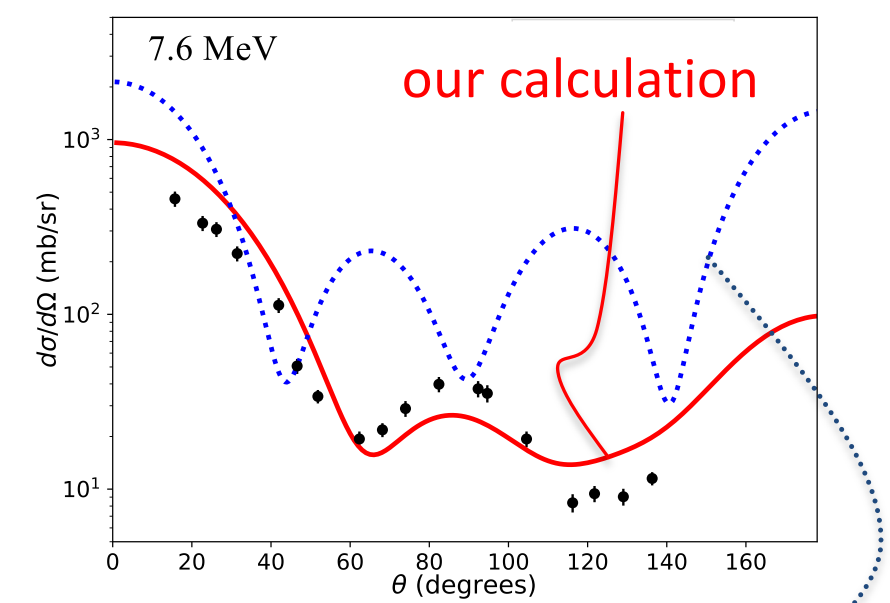


not surprisingly, the static potential alone gives a very wrong result!

# Our $^{24}$Mg calculation compares well with experiment

we check for convergence by looking at the volume integrals as a function of the iteration

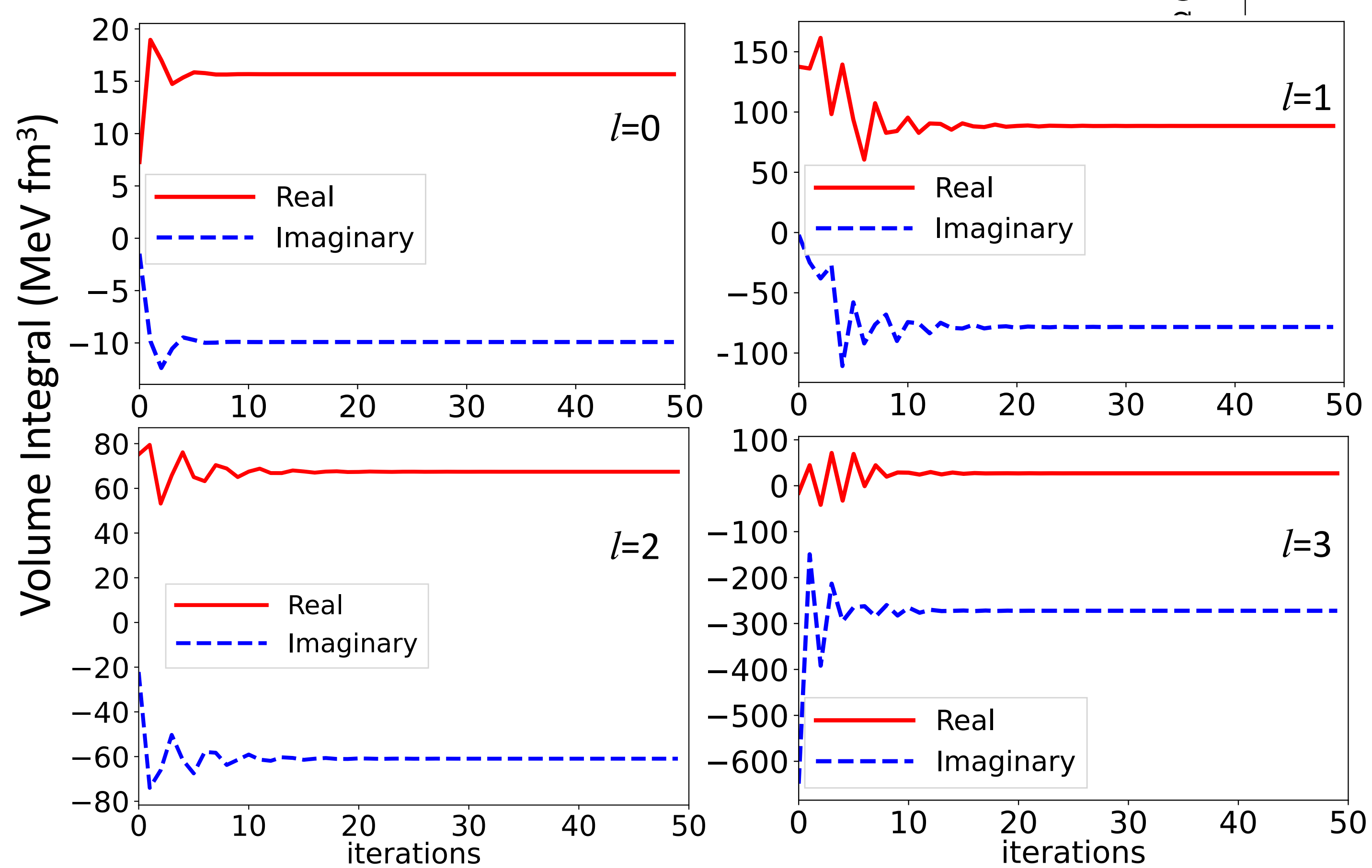


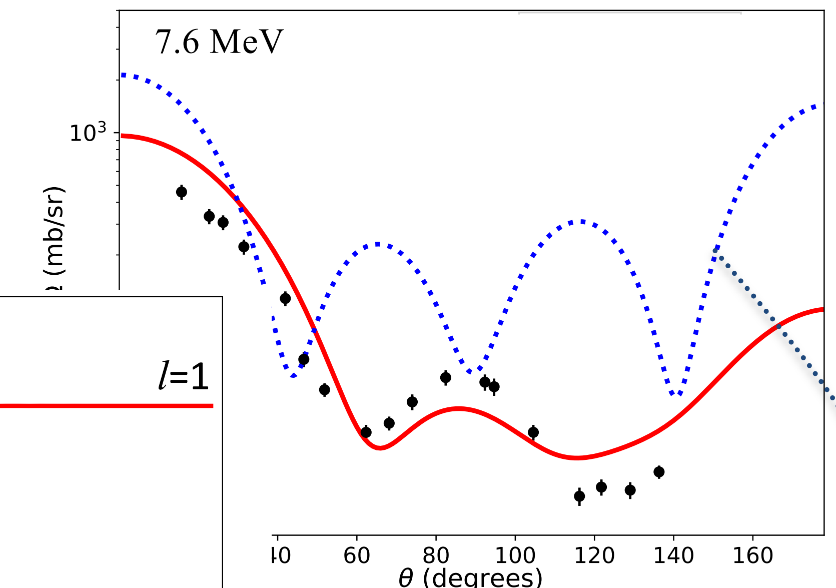


not surprisingly, the static potential alone gives a very wrong result!

# Our $^{24}$Mg calculation compares well with experiment

Koning-Delaroche

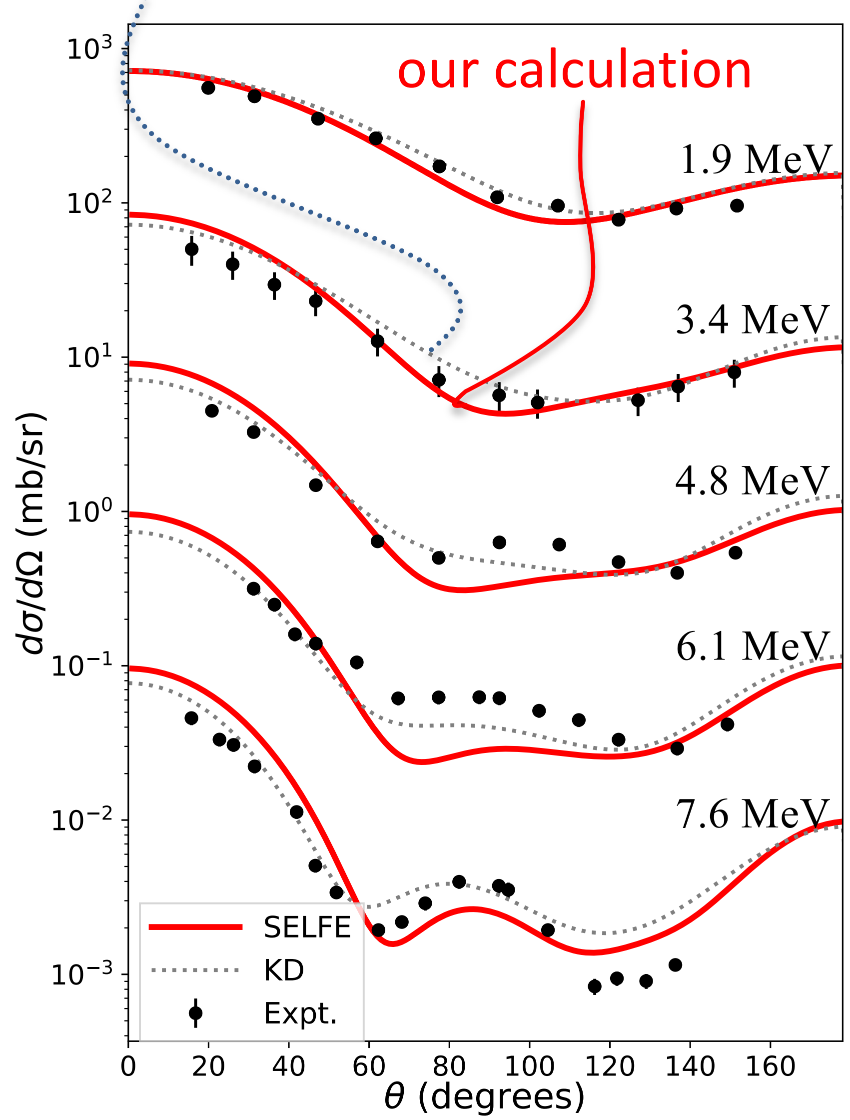


we check for convergence by looking at the volume integrals as a function of the iteration

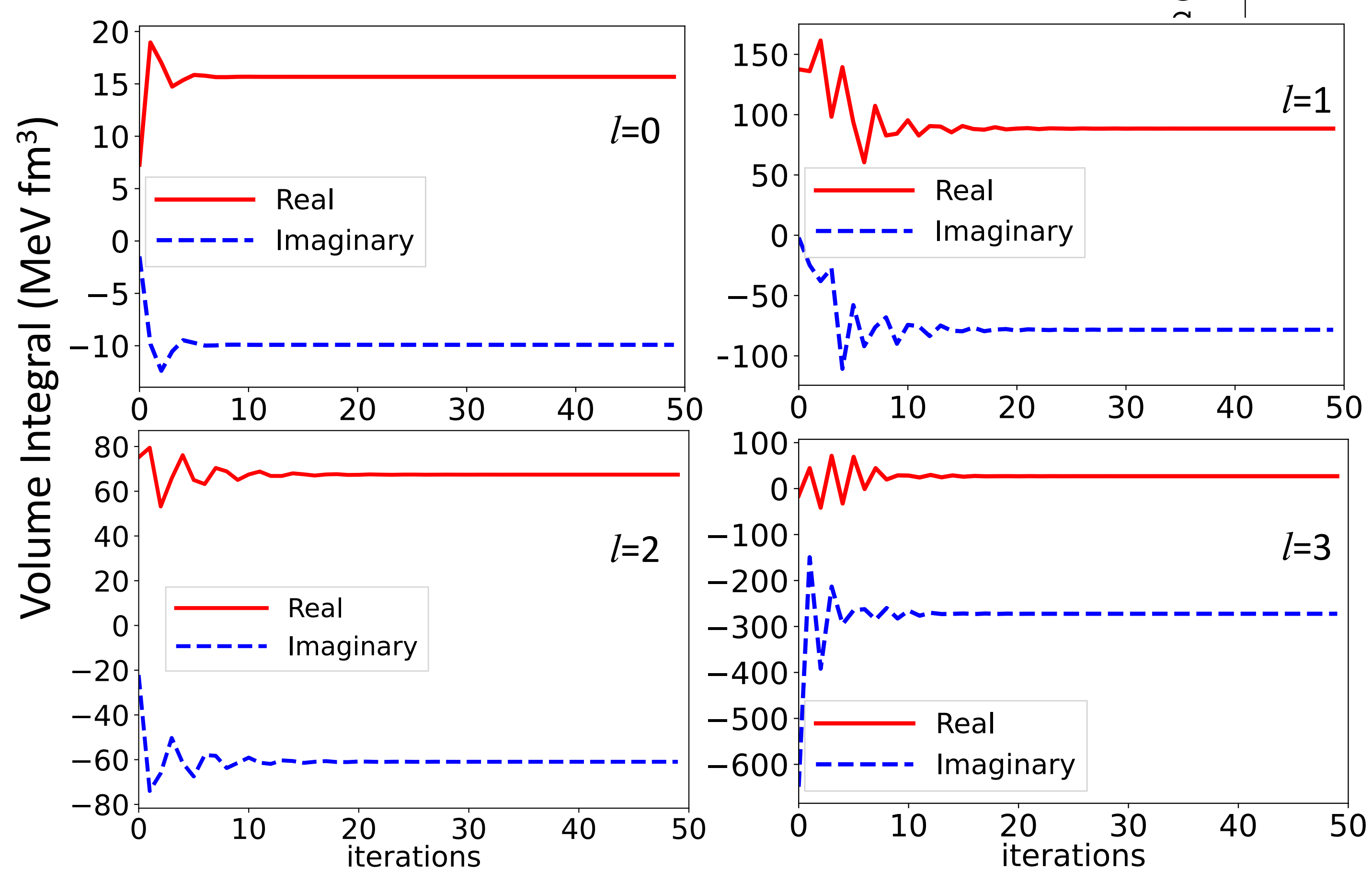


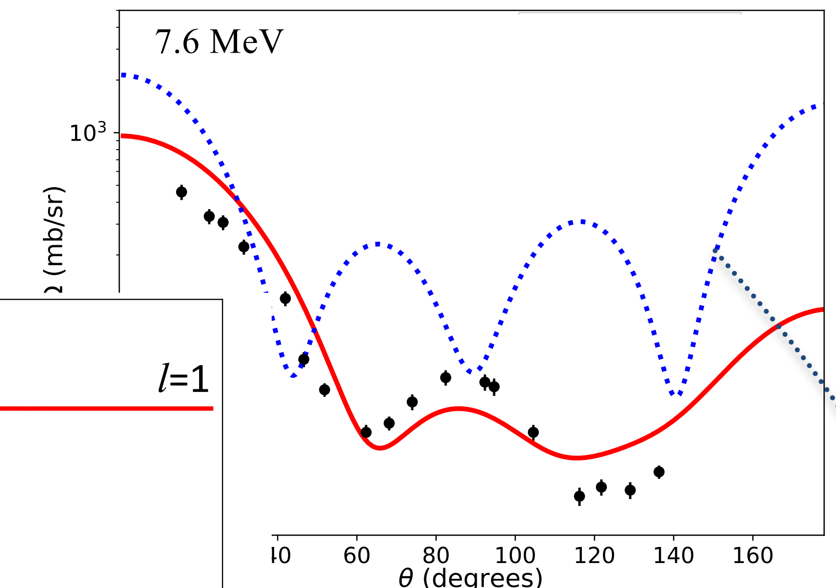


not surprisingly, the static potential alone gives a very wrong result!

**Sargsyan**, GP, Kravvaris, Escher; ArXiv (2024)

# The Optical Potential is a projection of the many-body Hamiltonian on the elastic channel

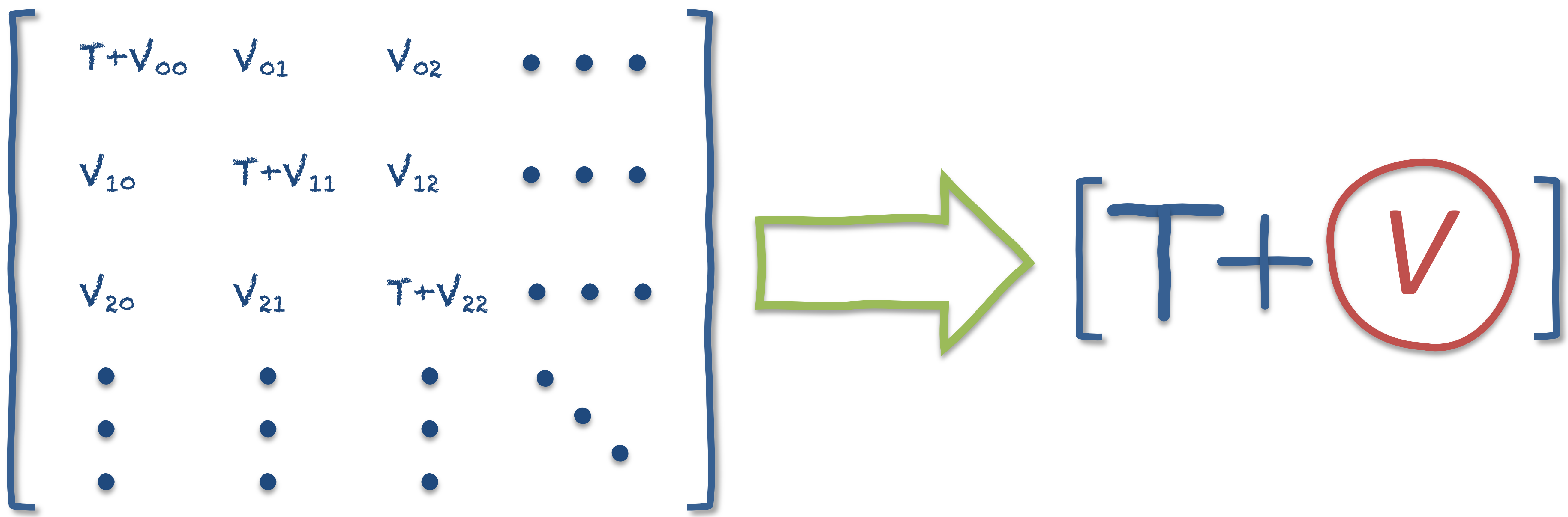


- The “optical reduction” transforms a many-body operator into a one-body operator
- It is a well-defined, in principle exact, mathematical operation

# The OP accounts for the composite nature of the target nucleus

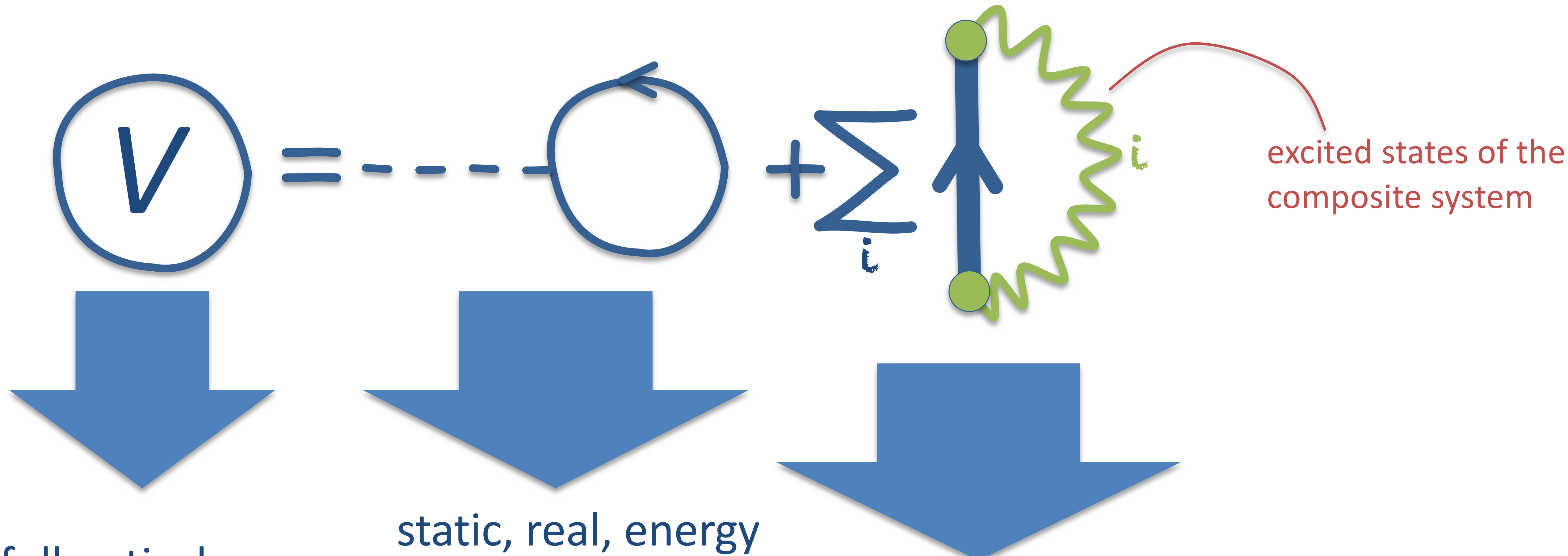


full optical potential (OP)

static, real, energy independent (mean field) potential

energy-dependent, complex, dynamical polarization potential